Studies on triphenylmethane, azo dye and latex rubber biodegradation by actinomycetes

by
Melissa Dalcina Chengalroyen

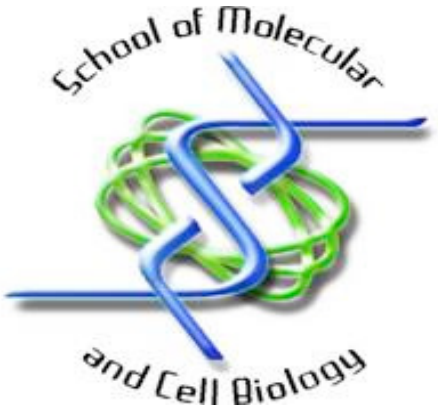

Schoool of Molecular and Cellular Biology

Faculty of Science University

of Witwatersrand South

Africa

2011

I. Declaration

I declare that this research is my own unaided work unless otherwise specified. It is being submitted to the University of the Witwatersrand, Johannesburg for the degree of Doctor of Philosophy. It has not previously been submitted for any other degree or examination in this or any other university.

_____

Melissa Dalcina Chengalroyen

1st day of June 2011

II. Acknowledgements

I am grateful to my family who have made numerous sacrifices. I would like to thank Prof. E.R. Dabbs for his supervision. I am indebted to my lab colleagues for all their assistance. I would also like to acknowledge the National Research Foundation for financial support. The following were kindly provided for this research: pNV18 and pNV19 by J. Ishikawa, LATZ by the rubber research institute of Malaysia and Streptomycete strains by the John Innes Institute.

This study comprises seven components and for clarity has been presented in separate chapters. This is the overall format of the thesis:

Chapter I: Identification and characterization of a gene responsible for amido black decolorization isolated from *A. orientalis*

Chapter II: Identification and characterization of genetic elements from *Amycolatopsis* species contributing to triphenylmethane decolorization

Chapter III: Characterization of rubber degrading isolates and the cloning of DNA conferring an apparent latex degrading ability

Chapter IV: Preliminary characterization of *A. orientlis* phytase activity

Chapter V: Screening for antimicrobial compounds from soil isolates

METHOD DEVELOPMENT

Chapter VI: Construction of broad host range positive selection vectors

Chapter VII: Adaptation of conventional *Rhodococcus* spp. PEG-mediated transformatin procedure for use with *S. lividans* and the generation of *S. lividans* mutants capable of regenerating in liquid broth

III. Abbreviations

Table I: Abbreviations used

Abbreviation	Meaning
A	secretes rubber degrading enzymes
B	adhesive action; unless otherwise stated the rubber type degraded is vulcanized latex glove
Am	amaranth
AB	amido black
ATCC	American Type Culture Collection
BB	bismarck brown
BF	basic fuchsin
BG	brilliant green
BS	biebrich scarlet
CFU	colony forming units
Chl	chloramphenicol
$CoCl_2$	cobalt chloride
CR	congo red
$CuCl_2$	copper chloride
CV	crystal violet
DSMZ	Deutsche Sammlung für Mikroorganismen und Zelkulturen
EB	eriochrome black T
FG	fast green
h	hour/s
JG	janus green
Kan	kanamycin
Kbp	kilobase pairs
LA	Luria Bertani agar
LB	Luria Bertani broth
LBSG	Luria broth supplemented with sucrose and glycine
MG	malachite green
µl	microlitre
ml	milliliter
Min.	minute/s
No.	number
NTG	N-methyl-N′-nitro-N-nitrosoguanidine
O II	orange II
PS	ponceau S
^{R}	resistance
SDS	sodium dodecyl sulfate
Spp.	species
Ta	tartrazine
Tet	tetracycline
Zn	zinc

IV. Tables

Chapter I

Chapter II

Chapter III

V. Figures

Chapter I

Chapter III

Chapter VI

Chapter VII

VI. Table of contents

Chapter IV

Chapter V

Chapter VI

Main Abstract

The first component of this project looked at the production of secondary metabolites by mycelial actinomycetes which could prove useful in the bioremediation of dyes and rubber. Through the screening of a genomic library relevant genes were identified. The second component focussed on the brief characterization of biotechnologically relevant antimicrobials and phytase. The third component dealt with method development through the improvement of a broad host range selective vector and the regeneration of *Streptomyces* spp. in liquid broth.

Identification and characterization of a gene responsible for amido black decolorization isolated from *A. orientalis*

Chapter I abstract

Investigation into the biodegradative capability of several actinomycetes led to the discovery of many strains possessing an ability to decolorize a variety of azo and triphenylmethane dyes. Of particular interest is an *Amycolatopsis* spp. isolate which displayed the ability to decolorize the azo dye amido black. Through the screening of a DNA library a 4.5 kbp fragment coding for the potential decolorization gene was identified. The sequencing of this gene fragment led to the prediction of seven open reading frames encoding a polyprenyl synthetase, cupin-2 conserved barrel domain, transcriptional regulator, membrane protein, DNA-damage inducible gene and two hypothetical proteins. A protein consisting of 312 amino acids with 77 % similarity to a conserved hypothetical protein in *A. mediterranei* was tentatively identified as the enzyme of interest. This is the first report of an amido black biodegrading gene identified in this species and was hypothesized to be a novel decolorizing gene.

1. Introduction

1.1 The history of dyes

The first use of dye in ancient Egypt can be traced to a red dyed fragment found at the Meidum site from the third or fourth dynasty (Nicholson and Shaw, 2000). The Egyptians commonly dyed cloths, using either plant dyes or ochreous earth. For instance, a blue color could be obtained from indigotin found in the plant *Isatis tinctorum* and red from madder in *Rubia tinctorum* [Fig. 1.1]. They were also quite advanced in their understanding of how to attach dyes to fabrics. In particular the use of madder (which is essentially an anthraquinone dye) requires a metallic salt to allow it to bind to the fiber and it is believed the Egyptians used the salt alum to accomplish this.

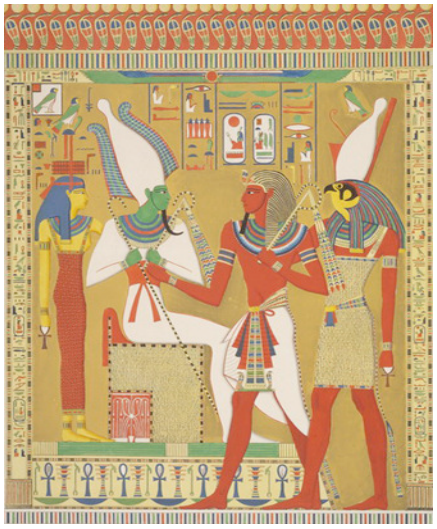

Fig. 1.1: Tomb of Seti I at Thebes. An illustration of the various colored garments worn by the ancient Egyptians (Edublogs.org, 2010).

The majority of dyes used today are synthetic and their origins can be traced back to organic chemists. W.H. Perkin in 1856 discovered the dye mauveine while trying to synthesize the antimalarial drug, quinine. Through oxidation and boiling with ethanol he derived a purple solution, which he found bound to silk more effectively than other natural dyes. After starting up a dye-works factory his discovery allowed him to retire

a wealthy man by age thirty-six, as such he is remembered as the *'father of the dye industry'* (Tyagi and Yadav, 2001).

The synthesis of dyes is a complex process. They are normally manufactured from the primary products obtained through the distillation of coal-tar. This yields aromatic molecules which depending on the dye will undergo reductive, oxidative, condensation, nitration or sulfonation reactions (Tyagi and Yadav, 2001). About half of the dyes used today are obtained by diazotization, a reaction yielding azo dyes. Bismarck brown was the first commercial azo dye.

1.2 Dye treatment

Azo dyes are routinely utilized for coloration in various industrial sectors which include the paper, clothing, food, cosmetic and pharmaceutical industries, making them responsible for the generation of large quantities of dye effluent waste (Rani *et al.*, 2009). In fact, seven hundred thousand tonnes of dyes are produced annually (Stolz, 2001). Colored wastewater discharged into rivers can contain between 10-200mg/l of dye and a mixture of organic and inorganic chemicals, additives, salt, acids and alkali compounds (Doble and Kumar, 2005). Around 90% of dyes are estimated to enter treatment plants and be discharged into rivers chemically unchanged (Molina-Guijarro *et al.*, 2009). The release of colored dyes into rivers affects photosynthesis decreasing oxygen levels and pH in these water bodies, making them harmful to the aquatic ecosystem (Molina-Guijarro *et al.*, 2009). The recalcitrance of these dyes is attributed to the azo groups (-N=N-) which do not occur naturally in nature (Bafana *et al.*, 2008).

Many bacteria, fungi and yeast capable of decolorizing azo dyes have been isolated and their azoreductases and oxidases characterized (Suzuki *et al.*, 2001; Blümel *et al.*, 2002; Kokol *et al.*, 2007). Many bacteria are capable of a non-specific reduction of the azo bond under anaerobic conditions, however this can lead to the unfavorable production of carcinogenic by-products (Grekova-Vasileva *et al.*, n.d.). Within humans several species of anaerobic bacteria known to reside in the intestinal tract have been associated with azoreductase activity (Rafii *et al.*, 1990).

Concern over human health and the environment has necessitated legislation monitoring the use of azo dyes in many countries. Considerable research has been conducted on both the chemical and physical removal of synthetic dyes and currently these are the strategies of choice when treating industrial effluent (Forgacs *et al*., 2004; Robinson *et al*., 2001). Physical and chemical means of removing dyes are expensive; these include adsorption, precipitation, filtration, photolysis and ion pair extraction (Nigam *et al*., 1996; Sani and Banerjee, 1999). There are various advantages and disadvantages associated with the different treatment methods. For instance, membrane technology is fast yet expensive to implement when dealing with high volumes. Adsorption by charcoal is slow, has a high cost and only works well when applied to small volumes (Azmi *et al*., 1998). Coagulation is cheap yet works at a moderate speed.

Table 1.1: Methods for the treatment of dye wastewater

Physical	**Chemical**	**Biological**
Adsorption	Neutralization	Stabilization pond
Sedimentation	Reduction	Aerated lagoon
Floatation	Oxidation	Trickling filter
Flocculation	Electrolysis	Activated sludge
Coagulation	Ion exchange	Anaerobic digestion
Foam fractionation	Wet air oxidation	Bioaugmentation
Polymer flocculation	Ozonation	
Reverse osmosis/ ultrafiltration		
Ionization radiation		
Incineration		

(Azmi *et al*., 1998)

Oxidation using hydrogen peroxide is the most commonly used chemical means of decolorization due to its simplicity (Robinson *et al*., 2001). The photochemical technique relies on the generation of hydroxy radicals, degrading dyes to harmless end products. The obvious disadvantage is the addition of large quantities of

chemicals into the effluent. The adsorption ability of dyes onto organic or inorganic substrates has also been tested. These include wood charcoal, activated carbon, coal and alumina. Cheaper substrates such as clay, corn cobs and rice hulls have also been tested (Robinson *et al*., 2001). While some of these studies have generated good results, they are limited in terms of expense and most have tested the removal of a single dye. Still the adsorption of the dyes onto these supports does not resolve the full problem, since the fate of these attached compounds still needs to be addressed. Microbial decomposition on the other hand offers more promising results. The process is less expensive and complete mineralization would lead to non-toxic end products (Forgacs *et al*., 2004). It is likely however that a combination of either chemical or physical means together with a microbial strategy will be the answer.

1.3 Dye classification

Dyes fall into many classes based on their chemical structural diversity. Over 100 000 exist of which over 2000 are azo dyes, making this the largest class of compounds used (Vijaykumar *et al*., 2007; Stolz, 2001). Some of these classes do not have an equivalent that occurs in the natural environment, these include xanthenes, phenothiazines and sulfur type dyes (Tyagi and Yadav, 2001).

Table 1.2: Types of dyes based on structure

Type of dye
Triphenylmethane
Anthraquinone
Vat
Indigoid
Azo
Polymethine
Aryl carbonium
Nitro
Xanthene
Sulfur
Nitroso
Diphenylmethane
Phthalein
Heterocyclic
Phthalocyamine
Miscellaneous

(Tyagi and Yadav, 2001)

i) Anthraquinone dyes

9,10 Anthraquinone forms the backbone of these dyes and it is the incorporation of amino-, hydroxy-, alkyl-, aryl- or alkoxy- groups which leads to differences. An example includes remazol brilliant blue R [Fig. 1.2].

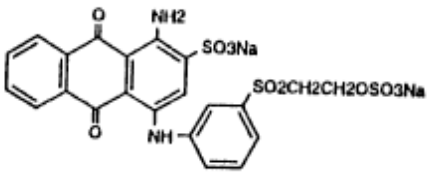

Fig. 1.2: Remazol brilliant blue R structure (Swamy and Ramsay, 1999)

ii) Polymethine dyes

These dyes can be positively or negatively charged, or neutral depending on the atom bound [Fig.1.3]. Examples include CI basic red 12, CI basic blue 41 and oxonol.

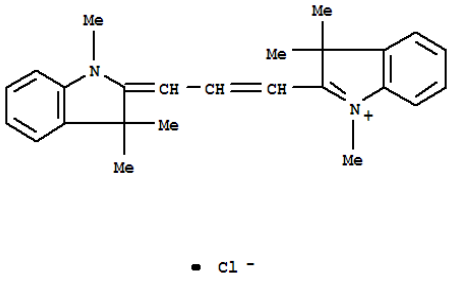

Fig. 1.3: CI basic red 12 structure

iii) Phthalocyamine dyes

This is one of the more recently discovered dyes which consist of metal complexes [Fig.1.4] (Tyagi and Yadav, 2001).

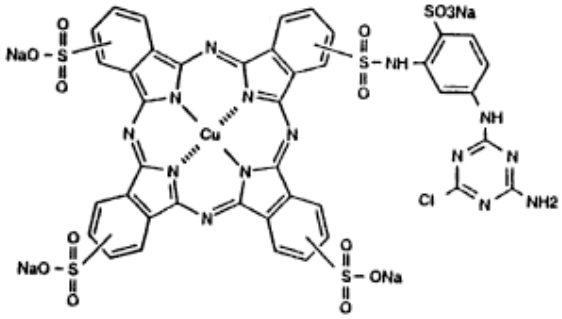

Fig. 1.4: Reactive blue 15 structure (Swamy and Ramsay, 1999)

iv) Azo dyes

The azo dyes are the most extensively studied in addition to being the most commercially important. The basic structure includes an azo bond (-N=N-) which is not found naturally in nature, making them difficult to degrade. Examples include amido black (a diazo dye which contains two azo bonds) and tropaeolin [Fig. 1.5]. Sulfonated azo dyes characterized by the presence of a SO_3H group are commonly

found in industrial effluents.

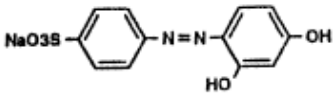

Fig. 1.5: Tropaeolin structure, a mono azo dye (Swamy and Ramsay, 1999)

v) Triphenylmethane dyes

As the name suggests, these contain three phenyl radicals with hydroxyl or NH_2 introduced into the ring (Tyagi and Yadav, 2001). Examples include crystal violet, brilliant green, malachite green and fast green [Fig. 1.6].

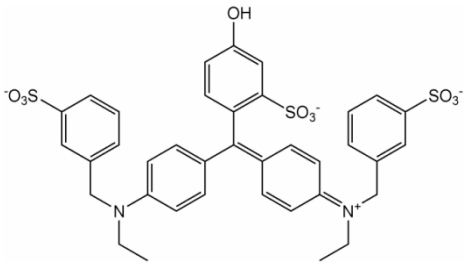

Fig. 1.6: Illustration of fast green

The structural design and electron withdrawing capacity of dyes makes them highly resistant to light, oxidizing agents and microbial oxidases (Rani *et al*., 2009; Grekova-Vasileva *et al*., n.d.). The number of azo bonds, functional group type and arrangement on the compound greatly influence its degradative capacity. Thus, the differences in decolorization by microbes can be attributed to the complex dye structures as well as culture conditions and genetic variations (Rani *et al*., 2009).

1.4 Aerobic and anaerobic mechanism of dye degradation

There are numbers of hypotheses concerning mechanisms of azo dye decolorization by bacteria, employing either intracellular cytosolic enzymes, extracellular enzymes or non-specific extracellular reduction (Doble and Kumar, 2005). Under anaerobic

conditions two mechanisms of azo dye decolorization have been proposed. The generation of ATP during catabolism produces electrons which can be transferred to the azo dye inducing breakage of the azo bond [Fig. 1.7] (Doble and Kumar, 2005). The other mechanism is due to the reducing action of end products such as inorganic compounds produced through catabolic reactions that cleave the dye. Thus, under non-oxygenated conditions many bacteria are capable of decolorization. This process however is documented as a non-specific breaking of the azo bond often resulting in the generation of toxic and carcinogenic products (McMullan *et al*., 2001). To alleviate this problem an anaerobic-aerobic treatment system has been proposed in which the dead-end toxic by-products generated under anoxic conditions can be broken down aerobically. Rajaguru *et al.* (2000) reported on the complete reduction of multiple sulfonated azo dyes by strains using an anaerobic-aerobic system.

Under aerobic conditions electrons move through the electron transport chain to the final electron acceptor, the azo dye which is reduced and thus decolorized and the flavin nucleotide reoxidized (Robinson *et al*., 2001).

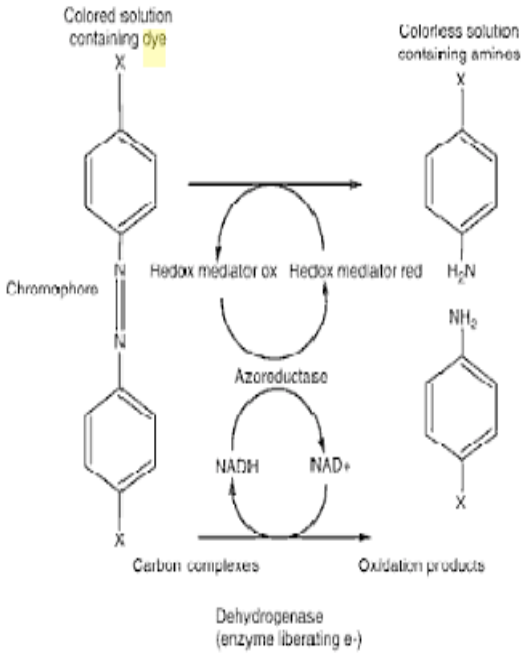

Fig. 1.7: A proposed redox reaction for the degradation of azo dyes under anaerobic conditions by whole bacterial cells (Doble and Kumar, 2005)

If dye reduction occurs intracellularly the molecule must diffuse across the cellular membrane. The presence of sulfonate groups has been linked to a reduced transport of the molecule across the membrane (Doble and Kumar, 2005). Although the relevant transport systems have not been identified yet, it has been suggested that they could be similar to systems which transport other sulfonated substrates such as, p-toluenesulfonate, taurine or alkanesulfonates (Blümel *et al*., 2002).

Mediators are often used to enhance dye break down. In fungi veratryl alcohol is typically used. Azo dye reduction by *Sphingomonas* spp. BN6 was increased in the presence of the redox mediator antraquinonesulfonate (Kudlich *et al*., 1997). Similarly, Liu *et al*. (2009) documented decolorization by *E. coli* spp. which only occurred in the presence of lawsone.

Kudlich *et al*. (1997) found two azoreductases within *Sphingomonas* spp. BN6 [Fig. 1.8]. It was shown that while one remained membrane bound the other was cytoplasmic. Characterization tests verified that these reductases were in fact variable, reacting differently to inhibitors. Similarly, more than one reductase has been isolated from *B. cereus*, *B. subtilis* and *Bacillus* SF (Nachiyar and Rajakumar, 2005).

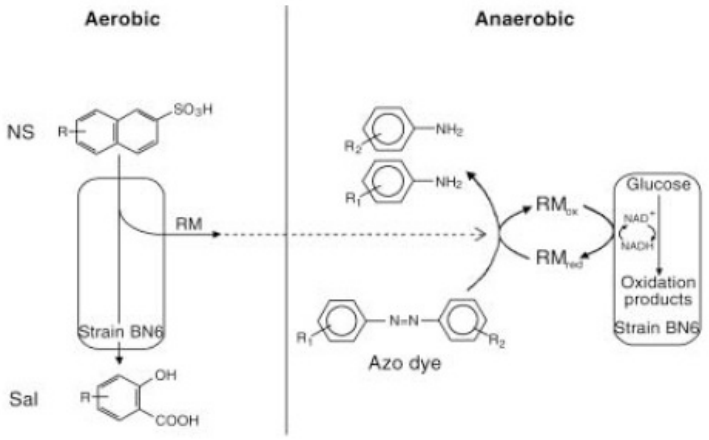

Fig. 1.8: Proposed mechanism for redox mediator (RM) dependent reduction of azo dyes by strain BN6 (McMullan *et al*. 2001)

Goszczynski and coworkers (1994) looked into the concept of developing readily biodegradable dyes. They introduced a lignin type subunit into two sulfonated dyes, making them more accessible to enzymatic oxidative attack and consequently

facilitating the complete breakdown of the compound. The fungal and actinomycete peroxidases tested were able to completely decolorize the dyes in just over two hours. To quote, “Such research could also exemplify how a new generation of less recalcitrant chemicals might be produced in the future” (Goszczynski *et al*., 1994).

Pasti-Grigsby *et al*. (1996) synthesized several dyes in order to analyze the effect of different configurations of chemical groups in relation to the azo bond and the influence thereof on the biodegradability. To summarize their results, they found that a hydroxy group in the *para* position as opposed to the *ortho* position was more favorable for degradation. Furthermore, methyl groups in the *ortho* position in relation to the hydroxy group were broken down more easily. Overall, replacement of the sulfonic groups by carboxylic groups led to the reduction of dyes which prior to this manipulation could not be broken down. In general, manipulations which made the dye structures similar to natural compounds (in this case lignin) greatly enhanced susceptibility by microbial attack [Fig. 1.9].

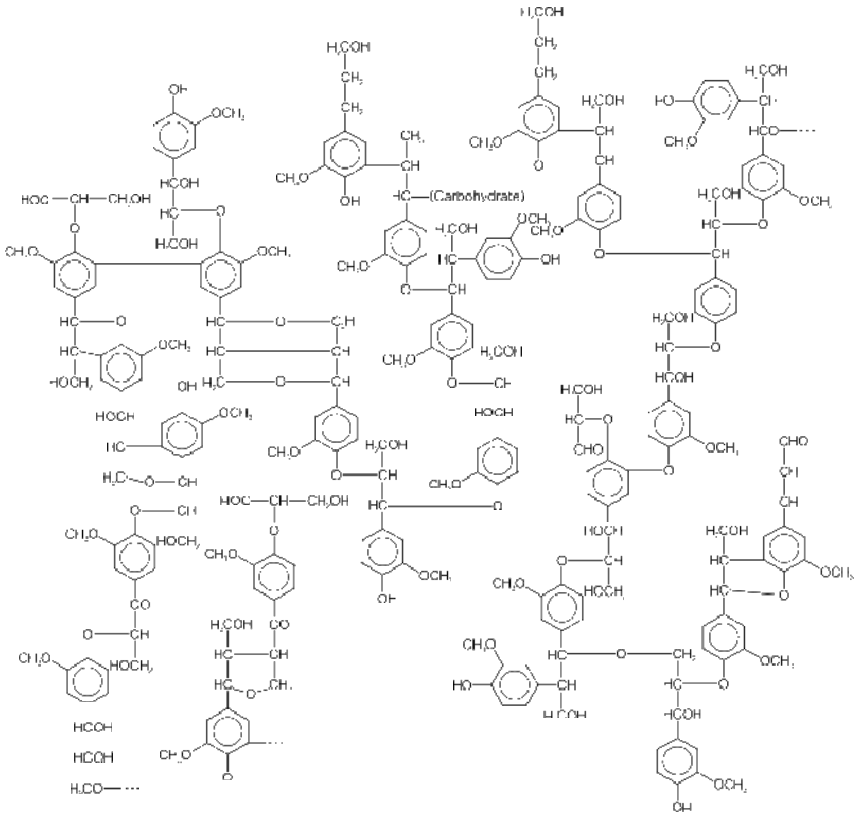

Fig. 1.9: Complex lignin structure

1.5 Bacterial oxidases implicated in dye degradation

Reductases are commonly identified in relation to dye biodegradation. However, there are a few cases in which oxidases have been isolated; Streptomycetes produce peroxidases and laccases which are ligninolytic enzymes. Many publications, particularly with regard to fungi concentrate on oxidases linked to dye decolorization (see section 1.6). Goszczynski and coworkers (1994) identified a *S. chromofuscus* peroxidase capable of degrading sulfonated dyes and where able to elucidate the pathway [Fig. 1.10].

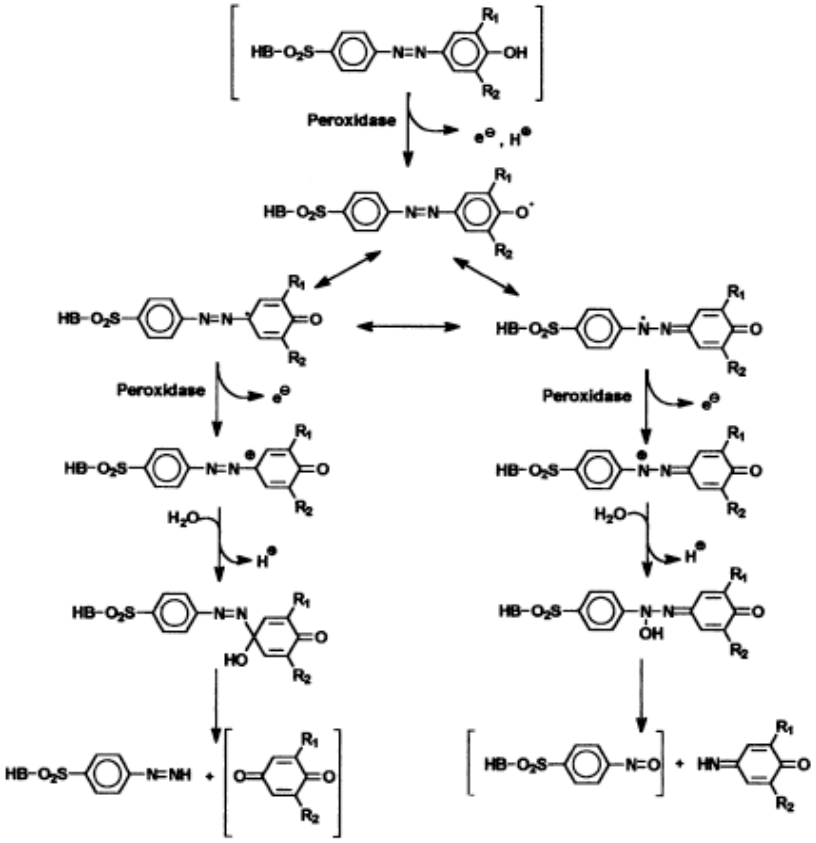

Fig. 1.10: Proposed mechanism for symmetrical and asymmetrical cleaving of sulfonated azo dye by *P. chrysosporium* and *S. chromofuscus* peroxidases (ligninases) (Goszczynski *et al*., 1994). In azo dye 1: R_1=R_2=CH_3 and B=O, in azo dye 2: R_1=H, R_2=OCH_3 and B=NH

Molina-Guijarro and colleagues (2009) isolated a novel halotolerant laccase from *S. ipomoea* that in the presence of a redox mediator was capable of detoxifying 90% of the azo dye orange II. Telke *et al*. (2009) reported on the combined involvement of a phenol oxidase and NADH-DCIP reductase from *Bacillus* spp. ADR on reactive orange.

1.6 Decolorization and degradation of azo dyes by fungi

The first study to report on the biodegradation of dyes by the white rot fungus, *P. chrysosporium* was conducted almost 27 years ago. Since then this species has been recorded as decolorizing amaranth, tropaeolin O, remazol black B, remazol orange, reactive blue, remazol brilliant blue, reactive orange 16 and naphthol blue black (Swamy and Ramsay, 1999; Svobodova *et al*., 2006). *T. versicolor* has also joined the ranks as an effective candidate for dye degradation, decolorizing sulfonated and mono azo dyes as well as reactive dyes (Swamy and Ramsay, 1999).

Fungi, in particular white rot fungi which produce ligninolytic enzymes have been widely studied for their ability to degrade an extensive array of compounds. They are renowned for their possession of manganese peroxidase, lignin peroxidase and laccase which are involved in the breakdown of lignin. In fact, this enzyme system has been found to have a low structural specificity and to act on diversely structured compounds such as synthetic dyes, aromatic hydrocarbons and chlorinated compounds (Rani *et al*., 2009; Pickard *et al.*, 1999. Lignin peroxidase oxidizes non-phenolic compounds and manganese peroxidase oxidizes phenolic compounds. Laccase, by reducing oxygen also oxidizes phenolic compounds (McMullan *et al*., 2001). In general, acidic conditions (pH 4.0-5.0) favor the activity of these enzymes, which is a limitation since textile dyes carry a high pH (Swamy and Ramsay, 1999; Kokol *et al*., 2007). However, the extracellular nature of these enzymes means that the problem of substrate diffusion into the cell is not encountered in fungi (Kaushik and Malik, 2009). High concentrations of nitrogen sources (25-60mM) tend to impede decolorization while in general glucose seems to be the best carbon source supplement (Kaushik and Malik, 2009).

There are numerous studies depicting the multifarious ligninolytic enzyme system in

connection to dye degradation: the white rot fungus, *Phlebia radiata* decolorized 12 synthetic dyes, namely amaranth, chromotrope 2B and 2R, tropaeolin 000, metanil yellow, amido black, congo red, chlorazole black E, trypan blue, chicago blue, procion red HE-7B and procion red M8B, six of which were decolorized completely (Rani *et al*., 2009). Laccase and manganese peroxidase of *Ischnoderma resinosum* led to 80-90% decolorization of four reactive dyes in just twenty four hours (Kokol *et al*., 2007). Promising studies include the use of purified enzymes to mineralize dyes. The laccase isolated from *Pycnoporus cinnabarinus* degraded 70% of chicago sky blue in 1 hour. Similarly, manganese peroxidase from *Trametes versicolor* resulted in 100% decolorization in 1 hour (Kaushik and Malik, 2009).

1.7 Detoxification

It is no longer enough to merely show degradation of azo dyes; in recent years studies have emphasized the need to verify detoxification of the dye as well. Bafana *et al*. (2008) were one of the first to carry out tests verifying the toxicity and mutagenicity reduction of direct red in the presence of *B. velezensis* strain AB.

1.8 Genes /enzymes responsible for azo dye mineralization/ decolorization

Much of azoreductase research has been approached directly from the protein route whereby purification of the enzyme has led straight to its biochemical characterization (Goszczynski, 1994; Grekova-Vasileva *et al*., n.d.; Moosvi *et al.,* 2007)). Unfortunately, this has led to a lack of sequence information of potentially unique enzymes. Suzuki and fellow researchers (2001) opted for the rare approach of DNA screening and designed a probe, screening a *Bacillus* spp. OY1-2 library for the gene responsible for the reduction of methyl red, acid red 88 and reactive black 5. They identified a 20 kDa NADPH-reductase, which they proposed to be a member of a novel family of enzymes due to the highest similarity of just 52.8% to a sequence in the database. A few years later, these researchers also isolated the homolog of this gene from *B. subtilis* ATCC6633, *B. subtilis* ISW1214 and *G. stearothermophilus* (Sugiura *et al*., 2006). Using the same strategy, Blümel and colleagues (2002) identified a 30kDa enzyme from *Xenophilus azovorans* KF46F involved in carboxy-orange II reduction. Peculiarly, the gene sequence did not have a significant match to

other sequences in the public database and shared no significant similarity to the reductase identified in *Bacillus* spp. OY1-2, even though both strains are β-proteobacteria. Notably, sequence information revealed that both enzymes were simple polypeptides containing no enzyme cofactors or metal ions (Blümel *et al*., 2002). The sequences of these genes are under the following accession numbers: *B. subtilis* ATCC6633 (AB071366), *B. subtilis* ISW1214 (AB071368), *G. stearothermophilus* (AB071367), *X. azovorans* KF46F (AF466104), *Bacillus* spp. OY1-2 (AB002631), *E. faecalis* (AY422207) and *R. sphaeroides* (AY150311) [Fig. 1.11].

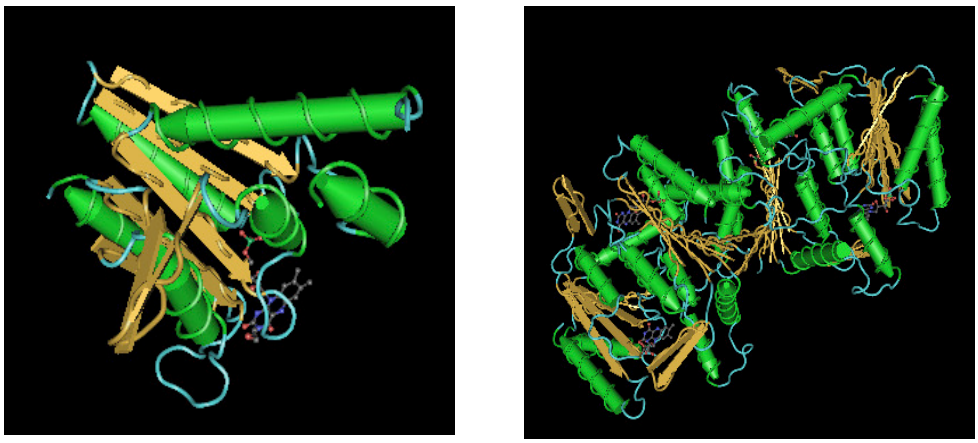

Fig. 1.11: Structure of *E. coli* azoreductase (left) and *E. faecalis* FMN-dependent azoreductase (right) from PubMed database

1.9 Classification of bacterial azoreductases

Azoreductases are first classified broadly based on their oxygen requirement, being either active in the presence or absence of oxygen (Bafana and Chakrabarti, 2008).

Due to the existence of a low level of similarity based on the nucleotide and amino acid sequence of these enzymes, classification is based primarily on the secondary and tertiary structure. These enzymes are further classified along the basis of function, being either flavin dependent or independent. Flavin dependent reductases are further characterized based on their requirement for NADH, NADPH or both coenzymes (Punj and John, 2009). Bürger and Stolz (2010) have just recently proposed a three group classification system based on preferential cofactor usage. The first group encompasses FMN dependent enzymes that preferentially use NADH, the second

group consists of NADPH utilizing enzymes and the third group are flavin-free reductases.

Based on the nucleotide and primary amino acid level, azoreductases show a low level of similarity which caused researchers to conclude that these reductases arose independently in different bacterial strains. Abraham and John (2007) however dispute this, showing that similarities do exist on the tertiary structural level. Correspondingly, they were able to develop a classification system based on this. Their simple yet profound study compared the azoreductases of four *Bacillus* species, *R. sphaeroides* and *E. faecalis*.

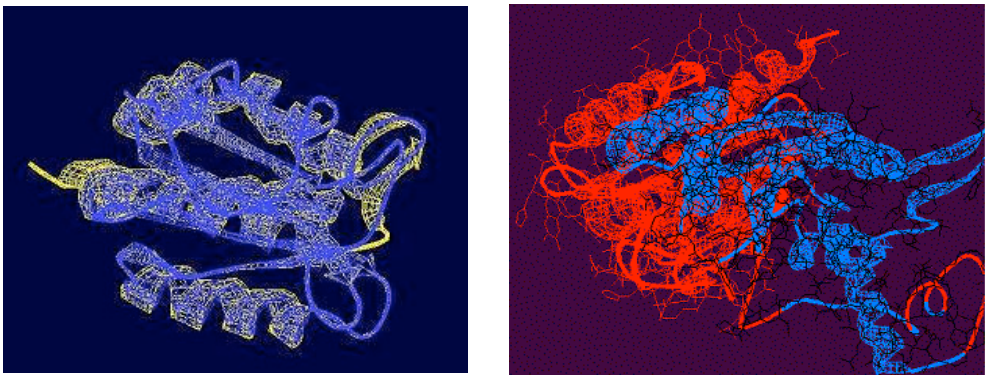

Fig. 1.12: (Left) superimposed images of amino acid sequences generating a tertiary structure (3D) of *Bacillus subtilis* (yellow) and *Rhodobacter sphaeroides* (blue) and (right) superimposed images of amino acid sequences generating a tertiary structure (3D) of *B. subtilis* (red) and *Enterococcus faecalis* (blue) (Abraham and John, 2007)

By superimposing the 3D structures of the azoreductases they were able to conclude that the four *Bacillus* spp. and *R. sphaeroides* could be classified as one family while *E. faecalis* could be placed under a separate family [Fig. 1.12]. Although quite diverse in structures it was also found that *E. faecalis* and *Bacillus* spp. were capable of degrading methyl red to different extents.

Most reductases identified thus far, are monomers, the exceptions being the homodimers of *E. coli* and *E. faecalis* and unusual tetramer of *S. aureus* (Bafana and Chakrabarti, 2008). The optimal pH for many bacterial azoreductases seems to lie within a range of 6 to 8 with a temperature range between 25^{o}C to 45^{o}C. To name a

few, previous reports include the 21.5 kDa reductase of *B. cereus* with an optimal activity at 40^{o}C and a pH of 7.0 (Pricelius *et al*., 2007), a *P. aeruginosa* reductase active at pH 7.0 and 35^{o}C (Nachiyar and Rajakumar, 2005) and *A. hydrophila* with optimal activity at pH 5.0-10.0 and 25-37°C (Chen *et al.,* 2003).

Table1.3: Bacterial strains and associated enzymes implicated in dye decolorization

Bacterial strain	**Type of reductase/ oxidase**	**O_2 sensitive (S)/ O_2 in-sensitive (I)**	**Dye/s degraded**	**Enzyme class-ification**	**Reference**
Enterococcus faecalis ATCC 27274	Azoreductase (AzoA)	I	Methyl red	FMN dependent NAD(P)H reductase	Punj and John (2009)
Streptomyces chromofuscus	Peroxidase	I	3,5-dimethyl-4-hydroxy-azobenzene-4'-sulfonic acid (I), 3-methoxy-4-hydroxyazobenzene-4'-sulfonamide (II)	-	Goszcz-ynski (1994)
Pseudomonas spp. AZO29	-	S	Amaranth	-	Grekova-Vasileva et al. (n.d.)
***Bacillus velezensis* AB**	Azoreductase	I	Congo red	NADH reductase	Bafana et al. (2008)
***Streptomyces ipomoea* CECT 3341**	Laccase oxidoreductase (SilA)	I	Orange II	-	Molina-Guijarro et al. (2009)
Kerstersia spp.	Azoreductase	I	Amaranth, fast red E, congo red, ponceau S, orange II, acid red 151, acid orange 12	FMN dependent NADH reductase	Vijay-kumar et al. (2007)

Bacterial strain	**Type of reductase/ oxidase**	**O_2 sensitive (S) /O_2 insensitive (I)**	**Dye/s degraded**	**Enzyme classification**	**Reference**
Sphingomonas spp. BN6	Azoreductases	Both S	Amaranth	FAD reductase; cofactor independent reductase	Kudlich et al. (1997)
Gracilibacillus spp. GTY	Azoreductase	I	Acid red B	NADH reductase	Uddin et al. (2007)
Bacillus cereus	Azoreductase	S	Indigo carmine, flame orange, ruby red	NADH reductase and an unclassified reductase	Pricelius et al. (2007)
Pseudomonas aeruginosa	Azoreductase	I	Navitan fast blue S5R, amaranth, eriochrome blue black, atul acid black, orange G, tropaeolin	NADH reductase	Nachiyar and Rajakumar (2005)
***Bacillus* spp. OY1-2**	Azoreductase	I	Methyl red, acid red 88, reactive black 5	Flavin free reductase	Suzuki et al. (2001)
Xenophilus azovorans KF46F	Azoreductase	I	1-(4′-carboxyphenylazo)-2-naphthol (carboxy-orange II)	Flavin free reductase	Blümel et al. (2002)
Alcaligenes faecalis and *Commamonas acidovorans* consortium	-	S	Cibarcron red C-2G and orange CG, remazol-navy blue GG, -red RB,-golden yellow RNL, -blue B, -turquoise G 133,-black B and hisperse navy D2GR	-	Nigam et al. (1996)
Paenibacillus polymyxa, Micrococcus luteus and ***Micrococcus* spp.** consortium	-	Active with and without O_2	Ponceau red GR, procion golden, yellow HR, reactive navy, blue HER, reactive black B, reactive violet 5R, red HE8B, procion red H7B, reactive yellow FG, yellow HR	-	Moosvi et al. (2007)

Bacterial strain	**Type of reductase/ oxidase**	**O_2 sensitive (S)/ O_2 in-sensitive (I)**	**Dye/s degraded**	**Enzyme class-ification**	**Reference**
***Bacillus* spp. ADR**	Oxidoreductaes (phenol oxidase and NADH-DCIP reductase)	Active with and without O_2	C.I. reactive orange 16	NADH reductase	Telke et al. (2009)
***Bacillus subtilis* ATCC6633, *Bacillus subtilis* ISW1214** and ***Geobacillus stearotherophilus* IFO13737**	Azoreductases	I	Acid red 88, methyl red, mordant orange 1, reactive black 5, reactive orange 16, reactive red 180 and reactive red 22	NADPH reductase	Sugiura et al. (2006)
Escherichia coli and *Pseudomonas* spp.	-	S	Congo red, direct black 38	-	Isik and Sponza (2003)
Pseudomonas luteola	Azoreductase	S	Red G and three other azo dyes	-	Hu (1994)
Aeromonas hydrophila	-	S	24 dyes which include monoazo, diazo, polyazo, antraquinone and indigoid dyes	-	Chen et al. (2003)
Pseudomonas spp. SU-EBT	Laccase	S	Congo red and textile effluent	-	Telke et al. (2009)
Pseudomonas desmolyticum NICM 2112	Laccase, tyrosinase and lignin peroxidase	S	Direct blue-6	-	Kalme et al. (2007)
Pseudomonas spp. 1-10 and a white rot fungus consortium	-	Cells immobilized – creating anoxic interior and oxygenated exterior	Direct fast scarlet 4BS	-	He et al. (2004)
***Staphylococcus aureus* ATCC 25923**	Azoreductase (Azo1)	I	Orange II, amaranth, ponceau BS and ponceau S	FMN dependent NADPH reductase	Chen et al. (2005)
Shewanella oneidensis	Azoreductase	I	Orange II, direct blue 15	FMN dependent reductase	Mugerfeld et al. (2009)

Bacterial strain	Type of reductase/ oxidase	O_2 sensitive (S)/ O_2 in-sensitive (I)	Dye/s degraded	Enzyme class-ification	Reference
***Paenibacillus azoreducens* spp. nov. CM1**	-	S	Remazol black B	-	Meehan et al. (2001)
Pseudomonas desmolyticum NCIM 2112	laccase	S	Direct blue 6, C.I. reactive green 19A, C.I. reactive red 141	-	Kalme et al. (2009)

Gram postives organisms are highlighted in bold

1.10 Evolution of azoreductases

Due to the high sequence variability amongst azoreductases it was first assumed that they evolved independently. A commendable paper by Bafana and Chakrabarti (2008) however suggested otherwise. They detailed the phylogeny of azoreductases from selected eukaryotes and prokaryotes. Using the sequence information derived from nine bacteria, four mammals and one yeast strain they constructed trees depicting the relation of reductases in different species. They were able to infer a pattern of lateral gene transfer between diverse organisms. Hence, they put forth several noteworthy hypotheses, represented in Fig. 1.13. Grouping of reductase genes of a firmicute with an α-proteobacterium was indicative of a lateral transferal from one to the other. Similarly, a transferal from the γ-proteobacterium, *E. coli* to a firmicute was evident and could be explained by inhabitation of the same niche as both are intestinal microflora. Thus, azoreductases are proposed to be monophyletic. The close grouping of yeast with prokaryotic strains as opposed to with eukaryotes showed that yeast obtained the gene from bacteria. This allowed them to propose that azoreductases initially evolved in prokaryotes and were laterally transferred to the ancestors of yeast. Significantly, they found that β-proteobacteria azoreductases, *P. kullae* and *X. azovorans* were related. While the original researchers who had isolated the genes from these species were able to find no connection due to high sequence dissimilarity, the phylogenetic analysis conducted by Bafana and Chakrabarti (2008) found these reductases fell within the same cluster. However, the researchers claimed that this was not easy to detect possibly due to several mutational insertions in the *P. kullae* gene and a supposed rapid divergence of the genes.

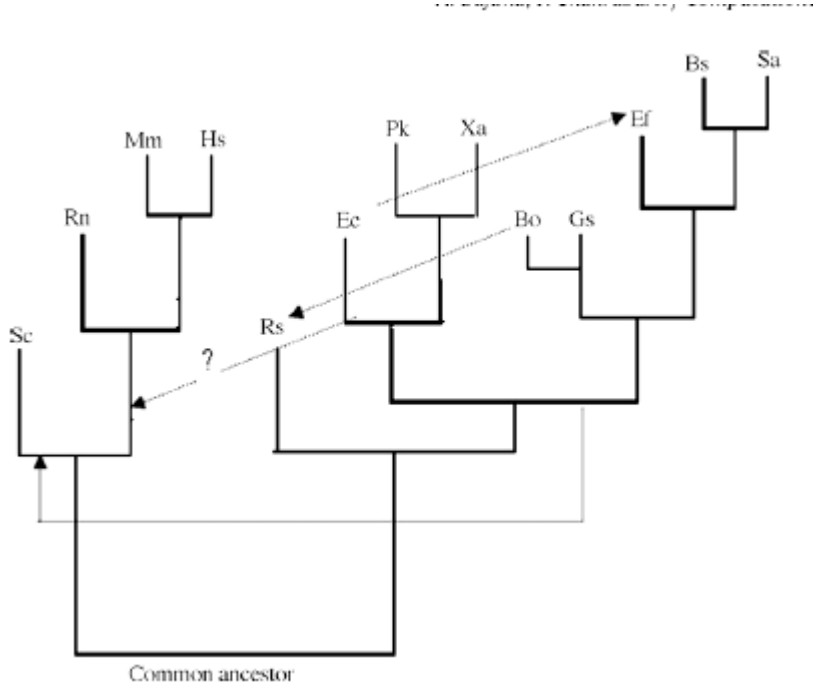

Fig. 1.13: Scheme for evolution of azoreductase gene, shown within the frame of small subunit rRNA-based phylogeny of organisms. Solid lines indicate the small subunit rRNA based phylogeny of organisms, while dotted arrows indicate the lateral transfer of the azoreductase gene. The abbreviations of organisms: Gs – *G. stearothermophilus*, Bs – *B. subtilis*, Sa – *S. aureus*, Ef – *E. faecalis*, Pk – *P. kullae*, Rs – *R. sphaeroides*, Xa – *X. azovorans*, Bo – *Bacillus* spp. OY1-2, Ec – *E. coli* (Bafana and Chakrabarti, 2008)

1.11 Bacterial consortiums

Moosvi *et al*. (2007) identified three isolates from a contaminated site as *Micrococcus luteus*, *Micrococcus* spp. and *P. polymyxa*. Together these isolates were able to decolorize nine dyes, however individually showed no capacity for decolorization. Similar results were reported by Nigam and coworkers (1996) whereby independent decolorization by strains was not detected yet as a consortium a considerably wide range of dyes were reduced. A consortium consisting of four isolates, *P. putida, B. cereus, P. fluorescence* and *S. acidaminiphila* decolorized C.I. acid red 88 in 24 hours while individual isolates took longer than 60 hours (Khehra *et al.,* 2005).

1.12 Treatment of azo dyes

Fungi have progressively overtaken bacteria in bioreactor-based studies. The non-specific activity of the ligninolytic system of white rot fungi allow them to act on a much wider range of substrates. The breakdown of reactive orange 16 in the presence of the white rot fungus, *Irpex lacteus* was compared in a trickle bed and rotating disk reactor (Tavčar *et al*., 2006). Although the highest mineralization (90% in three days) was detected using the trickle bed method, the small scale reactor was completely clogged after a month due to excessive mycelial growth. Other bioreactor systems have also been developed and met with more success, namely the packed-bed bioreactor, fluidized bioreactor and membrane bioreactor (Kaushik and Malik, 2009).

Robinson *et al*. (2001) reviewed literature concerning the chemical, physical and biological methods of dye removal and proposed a combination of methods which they believe would be most applicable on a large scale [Fig. 1.14].

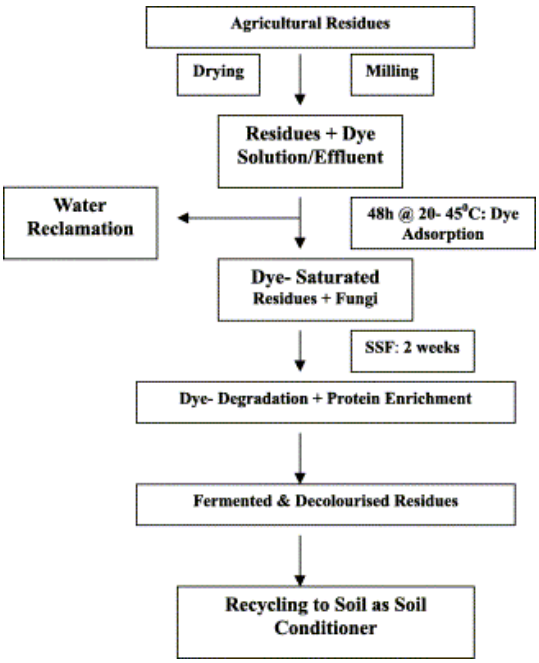

Fig. 1.14: Textile effluent decolorization and dye adsorbed agricultural residue biodegradation (Robinson *et al*. 2001).

Accordingly, they proposed that the dye should be adsorbed onto a cheap waste product (an agricultural residue) which can be treated using solid state fermentation in the presence of white rot fungi. The removal of the dye will be accompanied by the colonization of the substrate. As such, the fermented fungal biomass and residue can be used as a soil fertilizer.

1.13 Project significance

The removal of dyes in wastewater treatment plants still involves physical or chemical processes. Yet numerous studies currently exist on degradation based on the use of microbes - this is in fact a well-studied field. The question is what has prevented progress of the use of biological methods to deal with this environmentally noxious waste? The drawback originates from the types and numbers of dyes; in essence their diverse structures. Isolating a bacterial strain capable of mineralizing dyes within more than one class is rare; yet more than fifteen classes exist, two of which i.e. triphenylmethane and azo dye classes occur predominantly in textile effluent (Yang *et al*., 2009). As such, since wastewater normally contains an array of dye classes (and thus structures) the effective treatment of this wastewater would need to include microbes with the ability to degrade numerous structurally diverse dyes. Thus, the isolation of relevant bacteria and the identification of relevant genes is just the starting point. I looked into the concept of the heterologous expression of functionally relevant genes in an attempt to increase the range of substrate degradation not present in the original host.

1.14 Objectives

i. Screening of environmental isolates and known strains for the ability to decolorize azo and triphenylmethane dyes

ii. Identification of relevant strains by amplification of the 16S rRNA gene

iii. Selection of appropriate decolorizing strain for genetic analysis

iv. Creation of genomic library

~ transformation into intermediate Gram negative host

~ transformation into Gram positive host for the purpose of screening

v. Screening of library for clone displaying phenotypic trait

vi. Sequencing of decolorizing gene fragment

vii. Identification of gene related to decolorization

viii. Characterization of decolorization using whole cell assays, based on the following:

~ pH

~ Temperature

~ Carbon source supplementation

ix. Range of dyes decolorized by *S. lividans* and *R. erythropolis* harboring decolorizing gene fragment

x. Assessment of the percentage of detoxification linked to the decolorizing gene

2. Materials and methods

2.1 Growth and maintenance of strains

2.1.1 *Actinomycetes*

Mycelial actinomycete strains were grown under aerobic conditions in Erlenmeyer flasks containing LB media and glass beads to disperse the cells. These were grown at 30^{o}C for 1-2 days on a 30 rpm shaker. Mycobacterial strains were grown at 37^{o}C in LB media containing 0.05% Tween 80. *Rhodococcus* spp. and *Gordonia* spp. were cultured in LB at 30^{o}C for 2-3 days.

Strains were maintained on non-selective LA plates and appropriate strains streaked onto minimal media plates to induce sporulation.

2.1.2 *Non-actinomycete strains*

Escherichia coli strain MM294-4 was grown on a rotating wheel at 37^{o}C overnight in the presence of 30 μg/ml nalidixic acid. The λ lysogen strain (λ MM294-4) was grown overnight at 30^{o}C to prevent phage induction. *Saccharomyces cerevisiae* was cultured in YPD media at 30^{o}C. *Staphylococcus* spp. and *Bacillus* spp. were grown in LB at 37^{o}C with vigorous shaking to maintain adequate aeration. *Micrococcus* spp., *Pseudomonas* spp. and *Agrobacterium* spp. were cultured in LB at 30^{o}C for 1-3 days till a dense culture was obtained.

2.1.3 *Storage of strains and DNA*

For long term storage of Streptomycete strains, spores or mycelia were stored in 33% glycerol at -70^{o}C. Similarly, non-actinomycete cells were stored in 33% glycerol at -70^{o}C. Plasmid DNA was stored at -20^{o}C in sterile distilled water containing ribonuclease and chromosomal DNA in 4mM Tris-HCl at -20^{o}C.

2.2 Chemicals

List of the dyes used in this study: eriochrome black T, orange II, congo red, crystal violet, amido black, fast green, biebrich scarlet, ponceau S, janus green, bismarck brown Y, brilliant green, tartrazine, amaranth, basic fuchsin, malachite green and indigo.

2.3 Strains and vectors

Table 2.1: Bacterial strains

Species	**Strain**	**Characteristics**	**Source**	**Region and country**
Escherichia coli	MM294-4	*endA1, hsd R17, gyr A*, highly transformable	Dabbs E.R	-
Escherichia coli	λ lysogen	λ lysogen of MM294-4	Dabbs E.R	-
Escherichia coli	GM2929-1	*Dam*$^{-}$ *dcm*$^{-}$	Dabbs E.R	-
Streptomyces lividans	66	tet^{R}, chl^{R}, weak methylation dependent restriction	John Innes Institute	-
Streptomyces lividans	TK23	Highly transformable streptomycete host, amido black decolorizer, non-crystal violet decolorizer, phytase producer	John Innes Institute	-
Streptomyces coelicolor	A3(2)	Latex degrader, phytase producer	John Innes Institute	-
Mycobacterium smegmatis	mc^{2} 155	Highly transformable, crystal violet decolorizer	Durbach S.	-
Rhodococcus erythropolis	SQ1	Highly transformable, crystal violet decolorizer, amido black non-decolorizer	Dabbs *et al.* (1995)	-
Streptomyces tendae	BA1	Latex degrader	Soil	Buenos Aires (Argentina, South America)

Species	Strain	Characteristics	Source	Region and country
Streptomyces aureus strain 3184	Gam	Latex degrader	Soil	Gambia (West Africa)
Streptomyces pseudogriseolus	Reu	Latex degrader	Soil	Reunion
Streptomyces prasinus	Berlin	Latex degrader, antimicrobial activity	Soil	Berlin (Europe)
Streptomyces spp.	Hak	Latex degrader	Soil	Hakone (Japan)
Streptomyces spp.	Cal	Latex degrader	Soil	Caltech (North America)
Streptomyces spp.	Pasa	Latex degrader, antimicrobial activity	Soil	Pasadena (North America)
Streptomyces spp.	Bot1	Latex degrader, antimicrobial activity	Soil	Botswana (Southern Africa)
Streptomyces spp.	Fhome	Latex degrader	Soil	Central Johannesburg (South Africa)
Streptomyces spp.	WitsP	Latex degrader, antimicrobial activity	Soil	Central Johannesburg (South Africa)
Streptomyces spp.	SY3	Latex degrader, antimicrobial activity	Soil	South Johannesburg (South Africa)
Streptomyces spp.	SY5	Latex degrader, antimicrobial activity	Soil	South Johannesburg (South Africa)
Amycolatopsis orientalis	SY6	Amido black and crystal violet decolorizer, latex degrader, phytase producer, antimicrobial activity	Soil	South Johannesburg (South Africa)
Streptomyces spp.	HY	Latex degrader	Soil	Germiston (South Africa)
Streptomyces spp.	WITS	Latex degrader	Soil	Central Johannesburg (South Africa)
Streptomyces spp.	Bedd	Latex degrader, antimicrobial activity	Soil	Beddington (United Kingdom)
Streptomyces spp.	H2	Latex degrader	Soil	Germiston (Gauteng, South Africa)
Streptomyces spp.	H3	Latex degrader, antimicrobial activity	Soil	Germiston (Gauteng, South Africa)
Streptomyces spp.	BotY	Latex degrader, antimicrobial activity	Soil	Botswana (Southern Africa)

Species	Strain	Characteristics	Source	Region and country
Streptomyces spp.	Bot2	Latex degrader	Soil	Botswana (Southern Africa)
Pseudonocardia spp.	Est	Latex degrader	Soil	Estonia (United States)
Streptomyces flavogriseus	Chiba	Latex degrader	Soil	Chiba (Japan)
Streptomyces griseus subsp. *Griseus*	Yeo	Latex degrader	Soil	Central Johannesburg (Gauteng, South Africa)
Streptomyces spp.	Hunt	Latex degrader	Soil	Huntington Garden (North America)
Tsukamurella tyrosinosolvens strain DSM 44234	YeoE	Cholesterol degrader	Soil	Central Johannesburg (South Africa)
Methylibium fulvum	HZ	Latex degrader	Soil	Germiston (South Africa)
Streptomyces spp.	HZBS	Latex degrader, antimicrobial activity	Soil	Germiston (South Africa)
Streptomyces prasinus	HZWS	Latex degrader, antimicrobial activity	Soil	Germiston (South Africa)
Gordonia rubripertincta	25593	Transformable strain	Genetics culture collection	-
Gordonia australis	A554		Genetics culture collection	-
Gordonia desulfuricans	NB4		van Hamme J.	-
Rhodococcus opacus	HLPA1		Genetics culture collection	-
Rhodococcus rhodochrous	RI8		Genetics culture collection	-
Rhodococcus erythropolis	ATCC 4277	Crystal violet decolorizer	Genetics culture collection	-
Pseudomonas aeruginosa	-		Microbiology culture collection	-
Staphylococcus aureus	64-1		Microbiology culture collection	-
Serratia marcescens	-		Microbiology culture collection	-
Micrococcus luteus	-		Microbiology culture collection	-
Micrococcus flavus	-		Microbiology culture collection	-
Agrobacterium	pE 1913		Microbiology culture collection	-
Bacillus subtilis	IA3		Dabbs E.R	-
Saccharomyces cerevisiae	Ray 3A-D		Dabbs E.R	-

Table 2.2: Vectors and associated characteristics

Vector	Characteristics	Source
pLR591	*bla* resistance marker for Gram negatives and tsr resistance marker for Streptomycetes, *Eco*RI endonuclease gene expression regulated by λ promoter, pIJ101 Streptomycete replicon , pMB1 replicon	Hill et al. (1989) and this study
pLR592	Same as pLR591 except pEcoR251 is in opposite orientation	This study
pDA71	*Rhodococcus* replicon, *Eco*RI endonuclease gene expression regulated by λ promoter	Quan and Dabbs (1993)
pNV18	pAL5000 ori, pMB1 replicon, blue-white selection, multiple cloning site	Chiba et al., (2007)
pNV19	Same as pNV18 except the multiple cloning site is in the opposite orientation	Chiba et al., (2007)
pUC18	High copy number, *bla* resistance marker, blue-white selection, pMB1 replicon	Fermentas
pGEM-T Easy	pMB1 replicon, T-A overhangs, blue-white selection, *bla* resistance marker	Promega

2.4 Isolation and culturing of bacteria

See section 3.1 page 162.

2.5 Detection of decolorization on selective plates and in liquid broth

Decolorization was detected on minimal media agar plates supplemented with the relevant dye (10 μg/ml) and an appropriate carbon source (0.25%). Bacteria were spotted onto the plates using a replicator and incubated at 30^{o}C. The plates were monitored continuously over a period of 7 days and viewed above a white light

illuminator. The detection of clear zones surrounding the colonies was recorded as decolorization.

Decolorization experiments in liquid culture were carried out in test tubes containing 5 ml of minimal media broth in addition to the appropriate dye/s (10 µg/ml) and carbon source (0.25%). The inoculum was prepared by growing the strains in complex media till a high cell density was obtained. This was washed three times in sterile distilled water to remove the rich media and an equal volume added to each of the test tubes. Decolorization was monitored spectrophotometrically by reading the decrease in absorbance of the supernatant at the absorbance maxima for each dye. This was done as follows: after the incubation at the appropriate temperature, 1 ml of the culture was microfuged to remove the bacterial pellet and the supernatant added to an absorbance cuvette. Uninoculated controls were included to determine the initial absorbance (A_0) for the optical density reading. All experiments were carried out in duplicate and an average used for the calculation.

The percentage of decolorization was calculated as by Rani *et al.* (2009):

$$\% \text{ decolorization} = \frac{A_0 - A}{A_0} \times 100$$

where, A_0 = initial absorbance and A = absorbance following bacterial inoculation at time t. Bacteria were not preconditioned prior to inoculation for decolorization experiments.

2.6 DNA manipulations

2.6.1 *Salt and ethanol precipitation*

DNA was precipitated by adding 1/10 volume of 1M NaCl and 2 volumes of chilled ethanol to the sample. This was inverted and microfuged (13 000 rpm; 25 min.) at 4^{o}C. The supernatant was discarded and the microfuge tubes blotted onto a paper towel. The pellet was dried in a SpeedVac concentrator for ± 20 min. The DNA was

then resuspended in 4mM Tris-HCl or sterile water to which 1 µl ribonuclease (10 mg/ml) was added.

2.6.2 *DNA digestions*

Restriction enzymes used were purchased from MBI Fermentas or Boehringer Mannheim. 0.5 units of the relevant restriction enzyme and 1.5 µl of complementary buffer was added to 10 µl of DNA and incubated overnight.

Double digestions were performed in a single buffer in which both enzymes exhibited maximal activity.

Partial digestions involved the determination of the enzyme dilution whose activity yielded optimal fragment sizes when analyzed on an agarose gel. A four-fold serial dilution of the restriction enzyme was carried out, added to the DNA and buffer and incubated overnight.

2.6.3 *Phenol-chloroform DNA purification*

The volume of the DNA sample was adjusted with TE buffer to 500 µl. One hundred and seventy µl of phenol was added, inverted and microfuged for 5 min. The upper aqueous phase was transferred to a sterile Eppendorf tube. Two hundred and thirty µl of chloroform was added, inverted and microfuged for 1 min. The upper aqueous phase was transferred to a sterile Eppendorf and precipitated with salt and ethanol.

2.6.4 *DNA ligations*

For ligations a 3:1 ratio of restricted genomic DNA to vector DNA was added to 2 µl 10X ligation buffer and 1 unit of T4 DNA ligase. The total reaction volume was adjusted to 25 µl with sterile water and incubated overnight at 22^{o}C.

2.6.5 *Agarose gel electrophoresis*

DNA was analyzed on agarose gels run in 0.5 TBE (See Appendix for gel preparation). Plasmid DNA and chromosomal DNA were run on 0.8% and 0.4% agarose respectively.

2.6.6 *Photography and visualization of agarose gels*

Gels were viewed under UV light using a Biorad gel doc system and gel images recorded.

2.6.7 *Fragment size determination and DNA quantification*

DNA fragment sizes were determined by comparing their position in relation to that of the DNA molecular weight markers (MBI Fermentas 1kb DNA Plus marker) when run on agarose gels.

DNA was quantified by loading equal volumes of the molecular weight marker and sample onto an agarose gel. The band intensity was compared to that of a selected marker of known concentration using LabWorks 4.5 Image Acquisition and Analysis Software. Alternately, DNA concentration was determined using the Nanodrop 1000 UV spectrophotometer by comparison against an appropriate blank solution.

2.6.8 *Extraction of DNA from agarose gel slice*

This was done using the freeze-squeeze method. The gel slice was placed into an Eppendorf tube and placed at -70^{o}C for 30 min. A metal spatula was heat sterilized and allowed to cool. After 30 min. the Eppendorf tube containing the agarose piece was allowed to thaw at room temperature. Once fully thawed the metal spatula was used to crush the gel slice and the supernatant transferred to a sterile Eppendorf tube. This was subjected to a single phenol-chloroform treatment (section 2.6.3) and precipitated with salt and ethanol (section 2.6.1). The resulting DNA was resuspended in 10-20 µl of sterile water. This was then used for relevant ligations.

2.7 Analysis of 16S rRNA

2.7.1 *Polymerase chain reaction (PCR) of 16S rRNA gene*

The first 500 bp of the 16S rRNA gene was amplified using MicroSeq® 500 primers. The following reagents were added into 0.2 cm thick walled PCR tubes: 5 µl x10 Taq buffer, 1.5 µl 50mM $MgCl_2$, 1 µl 10mM dNTP, 1 µl DMSO, 10 µl sterilized water, 2 µl forward primer, 2 µl reverse primer, 2 µl DNA template (100ng/µl) and 0.5 µl Taq polymerase (5U/µl) giving a total reaction volume of 25 µl. The conditions were as follows: denaturation at 95^{o}C for 30 seconds, annealing at 60^{o}C for 30 seconds and extension at 72^{o}C for 45 seconds set at 30 cycles, using a BioRad MJ Mini TM Gradient Thermal Cycler PCR machine. The PCR product was purified using the Qiagen QIAquick gel extraction kit and cloned into vector pGEM-T Easy. This was transformed into *E. coli* XL-Blue and the recombinant vector selected by means of blue-white screening. Furthermore, the vector was extracted using the GFX™ Micro Plasmid Prep kit and sent to Inqaba for sequencing. A Spectromedix LCC sequencer was used in conjunction with an ABI BigDye Terminator v3.1 sequencing kit. Microbial identification was made by aligning sequences to those in the PubMed public database.

2.8 Extraction of microbial DNA

2.8.1 *Genomic DNA isolation from Gram positive bacteria*

Cells were grown in 100-150 ml of 0.5% LBSG and incubated at 30^{o}C for 2-3 days on a 30rpm shaker. The cells were harvested by centrifugation in a Beckman J2-21 centrifuge (7000 rpm; 10 min.) and resuspended in 10 ml of TE buffer. Lysozyme (1mg ml^{-1}) was added and the tube incubated at 37^{o}C for 30-35 min. 0.5 ml of 10% SDS was added together with proteinase K (0.5 mg ml^{-1}). This was incubated at 55^{o}C for 2 h with occasional inversion. Following the 2 h incubation of DNA in the presence of proteinase K, 0.5 ml of 5M potassium acetate (pH 6.0) was added to the tube, shaken vigorously for 10 seconds and placed on ice for 10 min. This was centrifuged (15 000 rpm; 10 min.) and the viscous supernatant transferred to a 50 Ti tube. This was spun in an angled ultracentrifuge rotor for 45-60 min. at 40 000 rpm. The clear solution was transferred into a sterile tube and 4.4 g cesium chloride added. This was mixed gently by rotating the tube several times till the cesium chloride was completely dissolved. 400 µl of ethidium

bromide (1%) was added and swirled to mix. The refractive index was adjusted to 1.391-1.392 (section 2.8.3.1) and the solution transferred into a quick seal tube using a Pasteur pipette. The tube was sealed and spun in a VTi 65.2 horizontal rotor at 45 000 rpm for 16 h.

2.8.2 *Genomic DNA isolation from Gram negative bacteria*

E. coli MM294-4 was grown in 5 ml LB at 37^{o}C overnight. The following day, 600 µl of cells were transferred to a sterile Eppendorf tube and harvested by microfuging (1 min; 13 000 rpm). The supernatant was discarded and the pellet resuspended in 600 µl of TE buffer to which lysozyme was added. The suspension was incubated at 37^{o}C for 30 min. After the incubation, 120 µl of TE-SDS (10% SDS) was added, inverted and left at room temperature for 10 min. Following the addition of 120 µl 5M potassium acetate (pH 6.0) the tube was mixed vigorously and left on ice for 5 min. The sample was microfuged (13 000 rpm; 5 min.) at 4^{o}C and the supernatant transferred to a sterile Eppendorf tube. Chromosomal DNA was purified by a single phenol-chloroform extraction and precipitated with 1M NaCl and ethanol. The genomic DNA was dried in a SpeedVac and resuspended in 100 µl sterile water.

2.8.3 *Large scale isolation of vector DNA from E. coli utilizing cesium chloride gradient centrifugation (maxi-prep)*

E. coli MM294-4 cells carrying the vector were grown at 37^{o}C in 100 ml of LB supplemented with the appropriate antibiotic. Alternately, λ MM294-4 was grown at 30^{o}C. The culture was transferred to a JA10 centrifuge tube and harvested by pelleting (6000 rpm; 10 min.). The supernatant was then discarded and the cells resuspended in 5ml of solution 1. Thereafter, the mixture was transferred to a JA20 centrifuge tube and 10ml of solution 2 added. This was covered in Parafilm and mixed gently by inversion – causing lysis of the cells. This was left to stand at room temperature for 15 min. In addition, 7.5 ml of solution 3 was added, the tube covered in Parafilm and shaken vigorously for 15-20 sec. This was placed on ice for 10 min. and centrifuged (15 000 rpm; 10 min.) in a pre-chilled rotor. Subsequently, the

supernatant was decanted into a new tube and warmed in a 37^{O}C water bath for 5 min. 12 ml of isopropanol was added, the tube covered in Parafilm, mixed gently by inversion and left to stand at room temperature for 5 min. The DNA was precipitated through centrifugation (15 000 rpm; 10 min.) at room temperature. The resulting pellet was washed with 2ml of ethanol and re-centrifuged (15 000 rpm; 1 min.). The pellet was dried in a SpeedVac for 20 min. and resuspended in 4.1 ml of TE buffer. The tube was then placed in a 30^{O}C rotating water bath for 2 h to allow the DNA to dissolve. Afterwards 4.2 g of cesium chloride was added and dissolved by gentle agitation. This was supplemented with 400 µl of 1% ethidium bromide and the refractive index adjusted to 1.387-1.389 using a refractometer. Using a Pasteur pipette the solution was loaded into a Quickseal tube. This was balanced, sealed and run at 45 000 rpm for 16 h in a L7-55 Beckman ultracentrifuge.

2.8.3.1 *Adjustment of refractive index*

50 µl of the DNA supernatant was spread across the glass plate. Adjustments were made till two phases were clearly distinguishable when viewed under the refractometer. This was adjusted further till the two phases were separated at the intersection of the diagonals. The index number was read off the scale. If the index number was below the expected range, cesium chloride was added (0.1 g of cesium chloride leads to an increase of 1 unit). If the index was too high, TE buffer was added (100 µl of TE buffer leads to a decrease of 1 unit).

2.8.3.2 *Extraction of plasmid band*

The Quickseal tube was secured in place by a metal clamp and pierced at the top with a needle to release the air pressure. A hypodermic needle (1.25 X 38 mm) was inserted just below the second band (plasmid band) and the DNA gently suctioned into the syringe. This was aliquoted into an Eppendorf tube and subjected to a butanol extraction in order to remove the ethidium bromide.

2.8.3.3 *Removal of ethidium bromide following cesium chloride gradient centrifugation*

Ethidium bromide was removed by adding 150 µl of butanol and inverting the tube repeatedly. The red upper aqueous phase (containing ethidium bromide) was discarded by aliquoting. Butanol extraction was repeated 3-4 times until ethidium bromide could no longer be observed in the upper phase. The DNA was precipitated by adding 100 µl of DNA to 200 µl of sterile water and 700 µl of absolute ethanol. This was microfuged for 25 min. at 4^{o}C, the supernatant discarded and resultant pellet dried in a SpeedVac. This was resuspended in sterile water.

2.8.4 *Small scale isolation of vector DNA (miniprep) from Gram negative bacteria*

Bacterial cells carrying the vector were cultivated in 1ml of LB supplemented with the appropriate antibiotic. The cells were harvested by microfuging for 30 sec and resuspended in 80 µl of solution 1. Thereafter, 160µl of solution 2 was added and mixed gently by inversion. This was left to stand at room temperature for 15 min. Afterwards 120 µl of solution 3 was added and mixed vigorously by shaking. This was left to stand on ice for 5 min, microfuged in the cold for 5 min. and the supernatant decanted into a sterile Eppendorf tube. The supernatant was warmed at 42^{o}C for 2-10 min. after which 220 µl of isopropanol was added and gently mixed by inversion. This was left to stand on the bench for 5 min. Plasmid DNA was precipitated by microfuging for 5 min. The supernatant was discarded and the pellet washed with 150 µl of ethanol. This was microfuged for 1 min, the supernatant discarded and carefully blotted onto a paper towel. The pellet was dried in a SpeedVac for 20 min., after which it was resuspended in 100 µl of sterile water.

2.8.5 *Small scale isolation of vector DNA (miniprep) from Gram positive bacteria*

Bacterial cultures were inoculated in 1 ml of LBSG containing the appropriate concentration of glycine and grown for 2-3 days. 300 µl of the cells was transferred to a sterile Eppendorf tube and harvested by microfuging (13 000 rpm; 1 min.) at room temperature. The pellet was resuspended in 300 µl of TE buffer to which lysozyme was added. The suspension was incubated at 37^{o}C for 1 h with regular inversion

every 10 min. Thereafter, 50 µl of TE-SDS (10 %) was added, mixed gently by inversion and left to stand for 10 min. 50 µl of 5M potassium acetate (pH6.0) was added, the tube mixed vigourously and left on ice for 5 min. The sample was microfuged for 5 min. at 4^{o}C and the supernatant transferred to a sterile Eppendorf tube. The DNA was subjected to a single phenol-chloroform extraction (section 2.6.3) and precipitated with 1M NaCl (section 2.6.1). The DNA was then dried using a SpeedVac and resuspended in 50 µl of water.

2.8.6 *Plasmid isolation from Streptomyces spp*.

The plasmid pIJ702 was harvested from *S. lividans* 66, using the protocol of Hopwood *et al.* (1985). The *S. lividans* culture was grown in 500 ml of 0.5% LBSG supplemented with 50 µg/ml of thiostrepton for 2 days and harvested by centrifugation (10 000 rpm; 5 min.). Once the supernatant was discarded, the bacteria were resuspended in 5 ml lysozyme solution. This was incubated for 30 min. at 37^{o}C. After mixing gently with a glass pipette, 2.5 ml of 0.3M alkaline SDS was added. This was immediately mixed by suctioning with a pipette and incubated further for 20 min. at 70^{o}C. When cooled to room temperature, the suspension was mixed by shaking and 800 µl of acid phenol/chloroform added. Following agitation on a vortex to mix the phases, the solution was centrifuged (10 000 rpm; 10 min.), and the supernatant transferred to a new tube. 700 µl of 3M unbuffered sodium acetate and 7 ml isopropanol was then added. This was mixed by inversion, kept at room temperature for 5 min. and centrifuged for 10 min. The supernatant was decanted, the tube re-centrifuged for 20 sec. and all the liquid removed. The pellet was dissolved in 500 µl TE buffer and tapped to mix. 50 µl 3M unbuffered sodium acetate and 250 µl neutral phenol/chloroform was added, vortexed and spun for 5 min. The aqueous phase was transferred to an Eppendorf tube, 500 µl isopropanol added, mixed and centrifuged for 2 min. The supernatant was decanted and the pellet dissolved in 1 ml TE buffer. This was transferred to a centrifuge tube and a further 4 ml TE buffer added together with 250 µl 100mM spermine-HCl. After being mixed, the tube was kept at room temperature for 5 min., centrifuged for 10 min., decanted, re-centrifuged for 20 sec. and all the liquid removed. 0.3M sodium acetate + 10mM $MgCl_2$ and 7 ml ethanol were added to the pellet, tapped and incubated at room temperature for 60 min. Again the solution was centrifuged for 10 min., the supernatant removed and re-

centrifuged for 20 sec. and all the liquid decanted in preparation for cesium-chloride gradient centrifugation as in section 2.8.3.

2.9 Transformations

2.9.1 *E. coli calcium-chloride mediated transformation*

200 µl of a MM294-4 or λ MM294-4 preculture were added to 20 ml of LB containing 0.5% glucose. This was grown with vigorous aeration for 1 h 45 min. at 37°C or alternately 30°C for the λ lysogen. Cells were cooled in an ice water slurry for 5 min. before pelleting (10 000 rpm; 5 min.) in a pre-chilled JA20 Beckman centrifuge. The supernatant was discarded and cells resuspended in half the original volume (10 ml) of transformation buffer. This was left on ice for 15 min. and pelleted (10 000 rpm; 5 min.). The supernatant was again discarded and gently resuspended in one-fifteenth the original volume (1.33 ml) of transformation buffer. This was left on ice for a minimum of 2 h DNA ligations were placed on ice prior to being added to 100 µl of competent *E. coli* cells. This was incubated on ice for 10 min. to facilitate diffusion. The cells were then heat shocked at 44°C for 90 seconds. 0.5 ml pre-warmed LB was added to each tube and incubated for 1 h at 37°C or room temperature for λ lysogen. Cells were then spread onto antibiotic containing plates and incubated overnight at 37°C (MM 294-4) or 30°C (λ MM294-4).

2.9.2 *Rhodococcus spp. polyethylene-glycol (PEG) mediated protoplast transformation*

Rhodococcus erythropolis SQ1 was grown in LBSG liquid media (2% glycine) for 2 days at 30°C. 1 ml of the culture was transferred to an Eppendorf tube and the cells harvested by microfuging for (10 000 rpm; 30 sec.) This was washed in 1 ml B buffer, microfuged for a further 30 seconds, the supernatant decanted and resuspended in 1 ml B buffer containing lysozyme. The mixture was incubated in a 37°C water bath for 1.5 h with inversion every 10 min. Fifteen min. prior to the end of the 1.5 h incubation period, 0.5 g of PEG granules were sterilized under UV for 10 min. and P buffer prepared. The PEG was then dissolved in P buffer by vigorous vortexing. After incubation the protoplast suspension was microfuged for 10 seconds, washed in 1 ml

B buffer and resuspended in 500 µl P buffer. 100 µl of the protoplast suspension was aliquoted into Eppendorf tubes and the appropriate volume of DNA added to each tube. This was left to incubate at room temperature for 10 min. An equal volume of P-PEG buffer was added and the tube contents mixed by bubbling air through to mix the two phases. The contents of the tubes were spotted onto regeneration plates and spread using a glass pipette. The plates were incubated at 30^{o}C for 13 h and underlaid with chloramphenicol (30µg/ml). This was then incubated at 30^{o}C for 5 days.

2.9.2.1 *Antibiotic underlaying*

A metal spatula was heat sterilized over a Bunsen burner flame and allowed to cool. This was used to raise the agar off the base of the plate and 220 µl of a 4mg/ml chloramphenicol stock solution added beneath. The antibiotic was evenly spread by rotating the plate while holding the spatula at the centre of the plate base.

2.9.3 *Streptomyces spp. PEG mediated transformation*

Refer to section 2.2 page 281 for modified *Rhodococcus* spp. transformation protocol.

2.9.4 *Heterologous expression of genes in Rhodococcus spp.*

The gene fragments were ligated into the unique *Bgl*II site of the *Rhodococcus* spp. replicon vector pDA71. The ligation mixture was transformed into *E. coli* MM294-4 using the $CaCl_2$ mediated transformation procedure (section 2.9.1). Random colonies were screened for the presence of inserts. Subsequently, the gene orientation was determined by means of restriction analysis. The appropriate recombinant vectors were transformed into *R. erythropolis* SQ1 via PEG-mediated transformation (section 2.9.2). To confirm the presence of the recombinant vector in the *Rhodococcus* spp. clones (and rule out the possibility of these being antibiotic resistant mutants), random colonies were chosen and the vector DNA reisolated using the Gram positive miniprep protocol (section 2.8.5). This was again transformed into *E. coli* spp., miniprepped, the DNA digested and analyzed on a gel.

2.9.5 *Heterologous expression of genes in Mycobacterium spp.*

The gene fragments were ligated into the unique *Bam*HI site of the *Mycobacterium* spp. replicon vectors, pNV18 and pNV19. The ligation mixture was transformed into *E. coli* MM294-4 using the $CaCl_2$ mediated transformation procedure (section 2.9.1). Random colonies were screened for the presence of inserts. Subsequently, the gene orientation was determined by means of restriction analysis. The appropriate recombinant vectors were transformed into *M. smegmatic* mc^2 155 via electroporation (section 2.1 page 253). To confirm the presence of the recombinant vector in the *Mycobacterium* spp. clones, random colonies were chosen and the vector DNA reisolated using the Gram positive miniprep protocol (section 2.8.5). This was again transformed into *E. coli* spp., miniprepped, the DNA digested and analyzed on a gel.

2.10 Genomic libraries

2.10.1 *Construction and screening of genomic libraries*

Genomic DNA was extracted as described in section 2.8.1. This was digested with several restriction enzymes namely: *Hind*III, *Pst*I, *Bgl*II, *Bam*HI, *Bsp*1431 (*Sau*3A), *Psu*I (*Xho*II), *Kpn*I, *Xba*I and *Mph*1103I (*Nsi*I). Those enzymes which cut the DNA optimally (when viewed on an agarose gel) were selected for library construction. Bacterial DNA was digested with *Bgl*II and the genomic fragments ligated into the vector pLR591 (section 2.6.4) and transformed into *E. coli* MM294-4. Transformants were selected on ampicillin plates (100µg/ml) and at this stage a rudimentary statistical analysis done to determine the number of clones required to constitute a complete genomic library (section 2.10.4). The clones were then pooled as in section 2.10.2. Recombinant vector DNA was isolated using the cesium chloride gradient centrifugation procedure (section 2.8.3) and transformed into *S. lividans* TK23 using PEG mediated transformation (section 2.9.3). *S. lividans* transformants were patched onto selective dye agar plates containing 0.1% glucose and 30 µg/ml thiostrepton (section 2.10.3). These plates were incubated at 30°C and routinely analyzed for clear zone formation around colonies.

2.10.2 *Pooling of clones*

Once the recombinant vectors were transformed, transformants were collected by adding 2 ml LB to each plate and running a sterile glass pipette across the plate to loosen the colonies. Once the colonies were resuspended in the LB, this was suctioned and aliquoted into a sterile Schott bottle. The *E. coli* library was stored at -20^{o}C.

2.10.3 *Patching of colonies*

A paper grid block numbered from 1- 100 was placed beneath the screening plate. Using a sterile toothpick, the centre of the colony was stabbed and streaked across a single grid block. This was incubated and the plate monitored daily for any signs of a clear zone surrounding a colony.

2.10.4 *Calculation of number of clones needed to comprise a gene bank*

Ten random colonies were picked from the representative genomic library and grown overnight in the presence of ampicillin. These were miniprepped and digested with the appropriate restriction enzyme to release the insert. In addition, this was run on an agarose gel and the insert size estimated in relation to the standard molecular weight marker. The number of clones carrying inserts was also noted. Calculations were based on the following standard formula: N =ln (1-p) / ln (1- a/b), with the probability of finding a clone taken as 95% and the genome size as 8.7 Mbp. The size used was based on the sequencing of the entire genome of *S. coelicolor* A3(2) which yielded a chromosome length of 8.7 million base pairs.

N: number of clones required to represent a complete genomic library
p: probability
a: average insert size (total insert sizes / no. of clones tested)
b: genome size

2.11 Strain characterization

2.11.1 *Gram staining*

Strains were grown in LB and harvested for use in gram staining once they had reached exponential phase. A drop of the culture was placed onto a slide and air dried. The bacteria were fixed to the slide by passing it once through a flame. This was flooded with crystal violet and left to stand for 1 min. This was followed by gentle rinsing under tap water. Iodine was added and again left to stand for 1 min. This was again rinsed with tap water. A few drops of decolorizer was added and immediately rinsed. The slide was flooded with the counter-stain safranin and left for a minute. This was rinsed and the slide examined under a microscope.

2.11.2 *Light microscopy*

Slides of gram stained cells were examined using 400X magnification and the images recorded with a digital camera.

2.12 Monitoring of azoreductase activity using liquid assays

2.12.1 *The effect of pH on dye decolorization*

This was examined in the pH range 6-8 in a 0.1M potassium phosphate buffer (Table 5.4.1 page 315). The dye (10 µg/ml) was added to 5 ml of the appropriate phosphate buffer with no additional carbon source and incubated for a week. The decolorization percentage was determined as described in section 2.5.

2.12.2 *The effect of temperature on dye decolorization*

This was examined in the range 20-50^{o}C in minimal media broth supplemented with dye (10 µg/ml) and 0.25% glucose. These were incubated for a week and the optical density readings taken as in section 2.5 used to determine the decolorization percentage.

2.12.3 *The effect of carbon and nitrogen sources on dye decolorization*

A range of carbon or nitrogen sources (0.25%) were added to 5 ml of minimal media with dye (10 µg/ml) and incubated for 2 h and 48 h for crystal violet and amido black decolorization experiments respectively. The nitrogen sources tested include; yeast extract, peptone and a combination of both and carbon sources include: glucose, glycerol and starch.

2.12.4 *Acclimatization*

The strain was incubated in minimal media containing 10 µg/ml of the dye. Once decolorization occurred the culture was pelleted and transferred into 20 µg/ml of dye with fresh media. This process was repeated using 10 µg/ml increments till the strain could no longer decolorize the dye efficiently.

2.12.5 *Bioabsorption study*

The cells were grown in LB till a dense culture was obtained. The mycelia were washed in sterile water and autoclaved at 120^{o}C for 20 min. in order to kill the bacteria. The mycelial mass was used as organic material source to test for bioabsorption of the dyes to the bacterial cellular wall.

2.12.6 *Detoxification*

The decolorized supernatant was transferred to Eppendorf tubes and microfuged in order to pellet the cells. The supernatant was then collected and passed through a sterile 0.25 µm filter. Five ml of this was transferred to a test tube and 5-10 µl of a stationary phase *E. coli* culture added. Similarly, the controls included the use of non-supplemented minimal media and minimal media to which glucose (0.25%) was added. Again an appropriate volume of *E. coli* cells was added to each test tube and all were incubated for 2 h. on a rotating wheel at 37^{o}C. Following the incubation, a serial dilution was carried out and plated onto LA media. This was incubated

overnight and the colony forming units per ml determined the following day using the equation:

CFU/ml = number of colonies x dilution factor / volume spread (ml)

2.13 Assessment of degradative products

2.13.1 *Thin layer chromatography (TLC)*

The decolorized supernatant was separated from the cells by microfuging (10 000 rpm; 30 sec). This was spotted onto the TLC plate (Kieselgel 60 F_{254}) approximately 1.5 cm from the base of the plate. Once dry the plate was placed into a glass chamber containing a solution of 90 isopropanol: 1 glacial acetic acid: 9 water. This was allowed to run till the mobile phase was 1 cm from the plate end. This was dried and the R_f values recorded. R_f was calculated as the distance of the band (mm) divided by the distance traveled by the solvent front (mm).

2.14 Bioinformatics

2.14.1 *Nucleotide and protein sequence matches*

Protein and DNA sequences were matched using the blastx and nucleotide blast facilitates of NCBI PubMed. Default parameters were used in both cases. The partial 16S rRNA PCR products were aligned against those in the database and the highest percentage similarity recorded.

2.14.2 *Phylogenetic tree construction*

Trees were constructed with Blast Tree View using the neighbour-joining method with a maximum sequence difference of 0.85 and Grishin distance.

2.14.3 *Enzyme analysis*

2.14.3.1 Tertiary structures

The NCBI PubMed structure database was used for the structural analysis of the proteins.

3. Results

3.1 Isolation and taxonomic characterization of relevant microorganisms

3.1.1 *Collection of soil samples*

Sixteen soil samples collected from regions in America, Europe and Africa were originally screened for the presence of rubber degrading strains (see section 3.1 page 162). Soil samples were collected from various environments; a tyre scrap yard, compost, arid dry soil and soil alongside a riverbank to name but a few. From these twenty-six isolates were purified using an enrichment technique (see section 2.2.1 page 157).

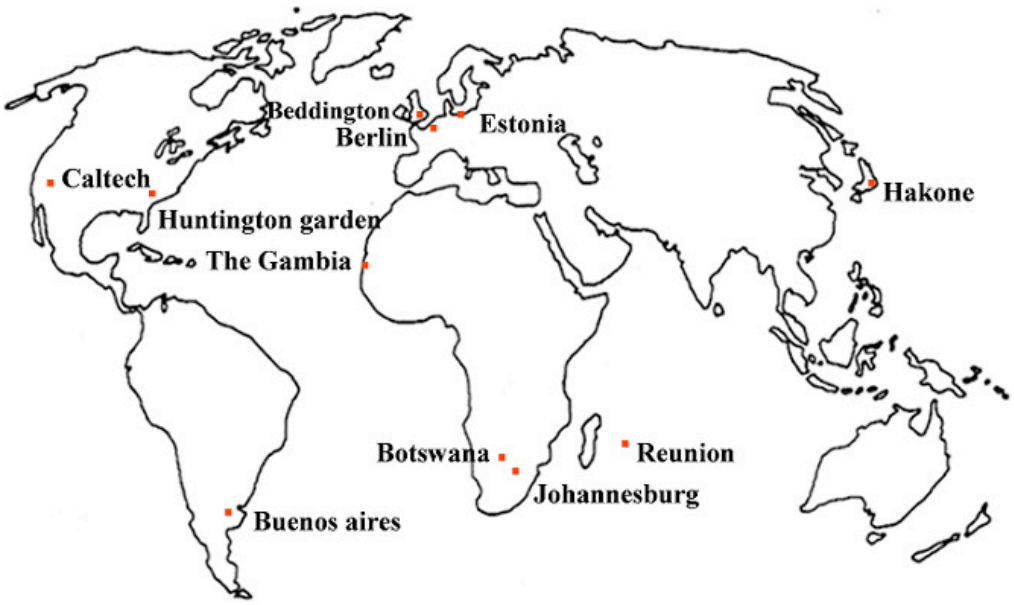

Fig. 3.1: Illustration of regions where soil samples were collected

3.1.2 *Microscopic studies*

Genus identification relied on morphological characteristics observed using Gram staining in conjunction with light microscopy [Fig. 3.2]. All strains were mycelial with the exception of strains YeoE (Gram positive rods) and HZ (Gram negative rods).

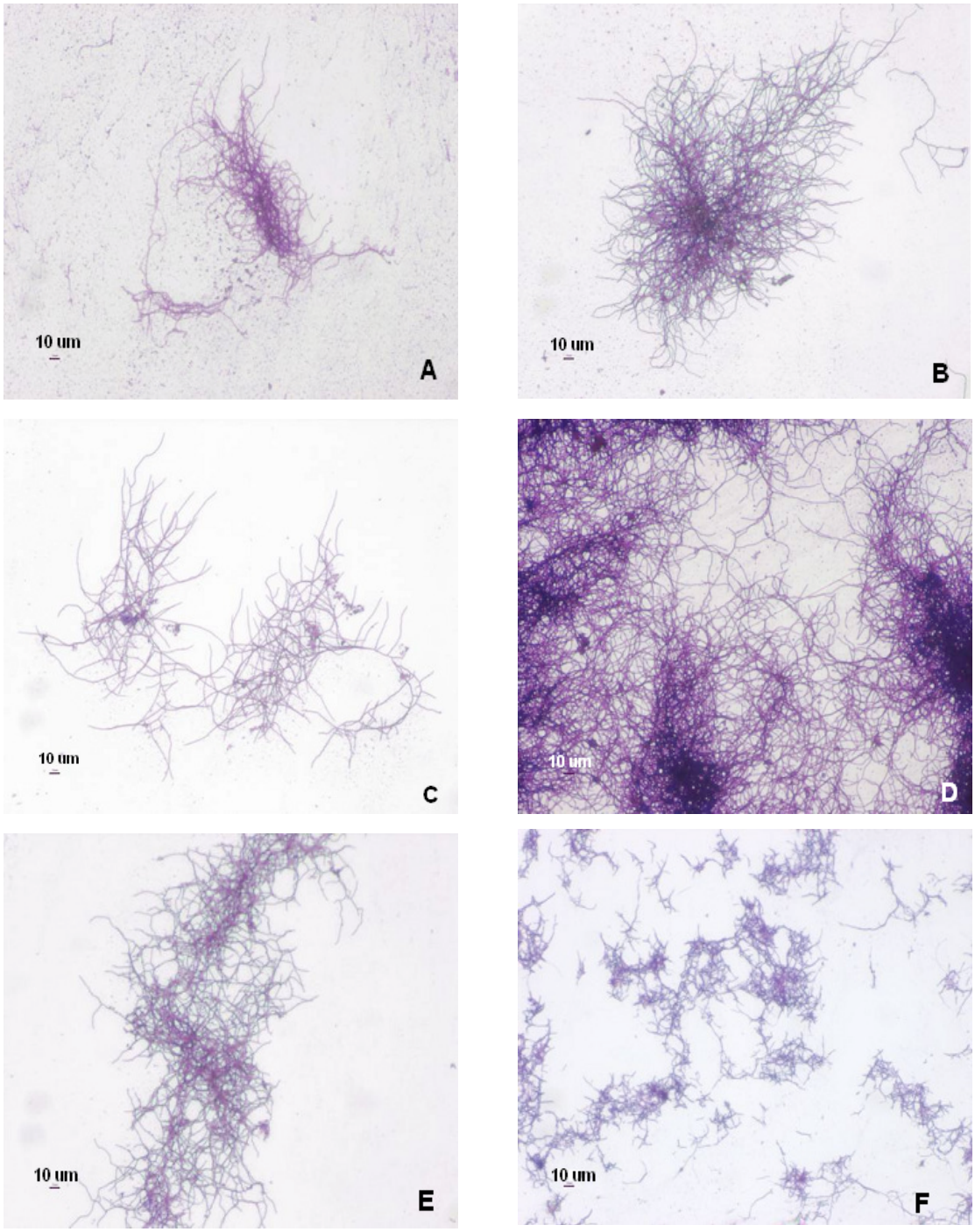

Fig. 3.2: Gram staining of strains (A) BA1, (B) Berlin, (C) Gam, (D) SY5, (E) Reu and (F) SY6

3.1.3 Antibiotic profile of isolated strains

The antibiotic resistance of the isolates was determined as a rapid means to identify *Streptomyces* spp. since they generally carry a low level resistance to ampicillin and are sensitive to thiostrepton and kanamycin. From the mycelial forming bacteria it was immediately evident that the profiles of strains Est and SY6 contrasted with the other strains evidenced by resistance to streptomycin.

Table 3.1: Representation of antibiotic resistance of selected strains

	Antibiotics (μg/ml)							
	Streptomycin 10	**Ampicillin 10**	**Chloroamphenicol 10**	**Kanamycin 10**	**Thiostrepton 10**	**Rifampicin 10**	**Ciprofloxacin 100**	**Nystatin 100**
Strains								
BA1	-	+	-	-	-	-	-	+
Est	+	+	+	-	-	-	-	+
Gam	-	+	-	-	-	-	-	+
Reu	-	+	+	-	-	-	-	+
Berlin	-	+	+	-	-	-	-	+
Hak	-	-	-	-	-	-	-	+
Cal	-	-	-	-	-	-	-	+
Pasa	-	-	+	-	-	-	-	+
Bot1	-	+	-	-	-	-	-	+
FHome	-	+	-	-	-	-	-	+
WitsP	-	-	+	-	-	-	-	+
SY3	-	+	-	-	-	-	-	+
SY5	-	+	-	-	-	-	-	+
SY6	+	-	+	-	+	+	-	+
HY	-	+	-	-	-	+	-	+

	Antibiotics (μg/ml)							
	Streptomycin 10	**Ampicillin 10**	**Chloroamphenicol 10**	**Kanamycin 10**	**Thiostrepton 10**	**Rifampicin 10**	**Ciprofloxacin 100**	**Nystatin 100**
WITS	-	+	-	-	-	-	-	+
Bedd	-	+	-	-	-	-	-	+
H2	-	-	+	-	-	-	-	+
H3	-	+	-	-	-	-	-	+
BotY	-	+	+	-	-	-	-	+
Chiba	-	+	-	-	-	-	-	+
Yeo	-	+	-	-	-	-	-	+
Hunt	-	+	+	-	+	+	-	+
HZ	-	+	-	-	+	+	-	+
Yeo E	+	+	+/-	+	+/-	-	-	+
HZBS	-	+	-	-	-	-	-	+
S. lividans 66	-	+	+	-	-	+	-	+

+ = growth - = no growth +/- = slight inhibition of growth

3.1.4 *Taxonomic identification*

3.1.4.1 *Small scale genomic DNA extraction in preparation for PCR for species identification*

The DNA was digested with various enzymes to determine which restriction enzymes yielded optimal restriction patterns in preparation for the creation of libraries [Fig. 3.3]. The *Bgl*II digestion seemed appropriate in most cases yielding fragment sizes ranging from 10 000 - 1500 bp.

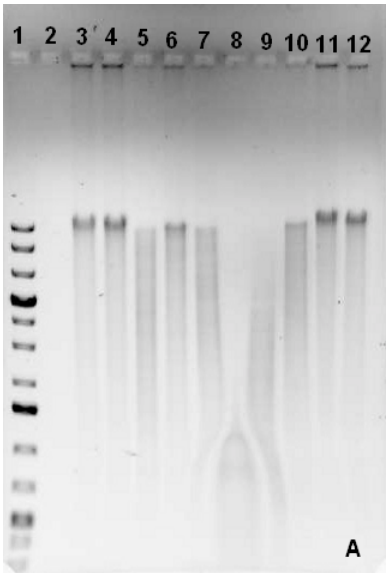

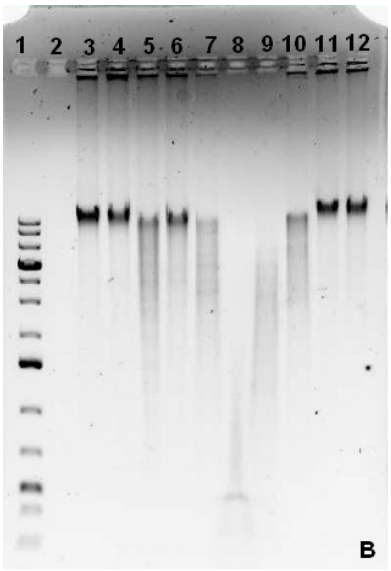

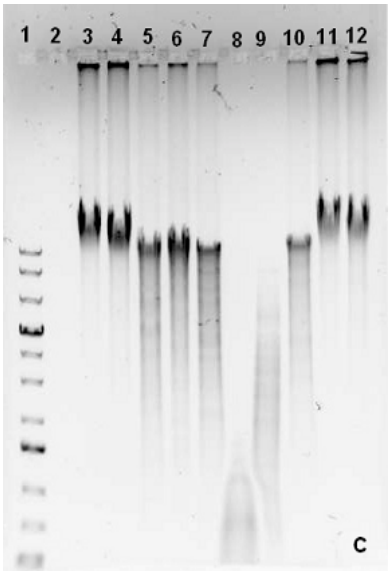

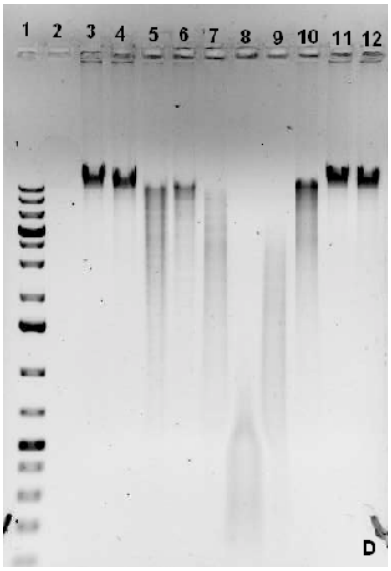

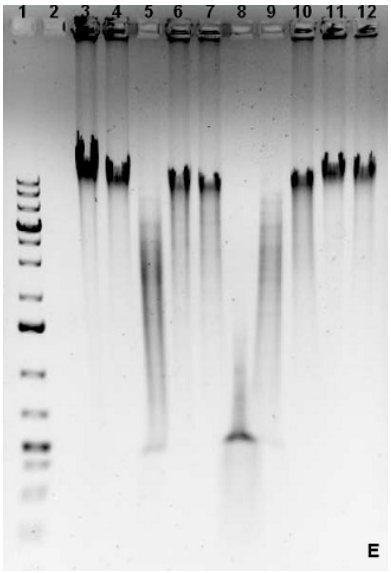

Fig. 3.3: Aliquots of DNA were digested with the following restriction enzymes: Lanes **1**: 1kb GeneRuler DNA Ladder, **3**: uncut DNA, **4**: *Hind*III, **5**: *Pst*I, **6**: *Bgl*II, **7**: *Bam*HI, **8**: *Bsp*1431 (*Sau*3A), **9**: *Psu*I (*Xho*II), **10**: *Kpn*I, **11**: *Xba*I and **12**: *Mph*1103I (*Nsi*I). The genomic DNA of the following strains was digested with the above enzymes (A) Gam, (B) Berlin, (C) Chiba, (D) SY6 and (E) HZ

3.1.4.2 *PCR (polymerase chain reaction)*

Further taxonomic identification was carried out by means of PCR amplification of the first 500 bp of the 16S rRNA region using commercial primers [Fig. 3.4]. Thirteen of the isolates were chosen for species identification.

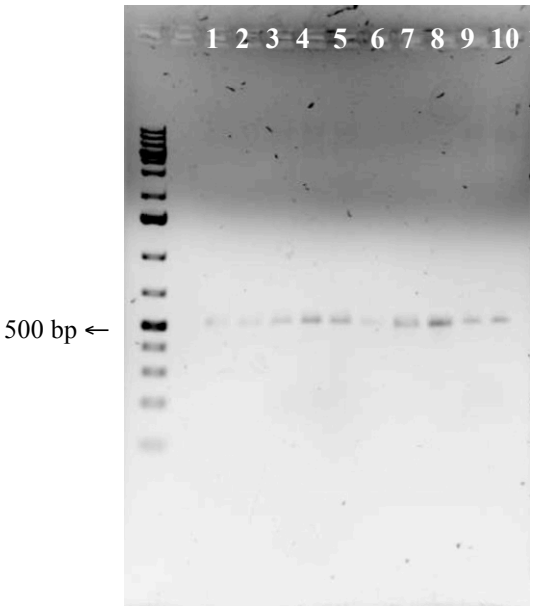

Fig. 3.4: Agarose gel (0.8% w/v) showing the amplification of 16S rRNA from the following strains: Lanes **1**: DNA marker, **3**: *S. lividans* 66, **4**: YeoE, **5**: Gam, **6**: Reu, **7**: Chiba, **8**: Berlin, **9**: Yeo, **10**: SY6, **11**: HZ and **12**: HZWS

The sequencing of the partial 16S rRNA PCR products and alignment to those in the Entrez PubMed Blast Database revealed the following percentage identity:

Table 3.2: Identification of bacteria using partial 16S rRNA sequences

Strain	**Genus and species identification**	**Percentage similarity to identified species**
Gam	*Streptomyces aureus* strain 3184	100
Reu	*Streptomyces pseudogriseolus*	99
Chiba	*Streptomyces flavogriseus*	99
Berlin	*Streptomyces prasinus*	99
Yeo	*Streptomyces griseus* subsp. *griseus*	99
SY6	*Amycolatopsis orientalis*	98
YeoE	*Tsukamurella tyrosinosolvens* strain DSM 44234	100
HZ	*Methylibium fulvum*	98
HZWS	*Streptomyces prasinus*	99
BA1	*Streptomyces tendae*	100
Est	*Pseudonocardia* spp.	98

The other fifteen strains based on morphological characteristics were tentatively identified as members of the genus *Streptomyces*.

3.2 Dyes used in study

Sixteen dyes were chosen, representing two dye classes and six sub-classes. Five triphenylmethane dyes (crystal violet, basic fuchsin, malachite green, fast green and brilliant green), one non-sulfonated azo dye (janus green), three sulfonated diazo dyes (amido black, congo red and biebrich scarlet), six sulfonated mono azo dyes (tartrazine, orange II, eriochrome black T, congo red, ponceau S and amaranth), one diazo dye (bismarck brown Y) and one indigoid (indigo).

Table 3.3: Illustration of different dye structures

Dye	**Visual image of dye in liquid media**	**Dye class**	**Dye structure**
Tartrazine		Sulfonated azo dye	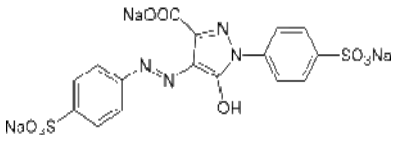
Amaranth		Sulfonated azo dye	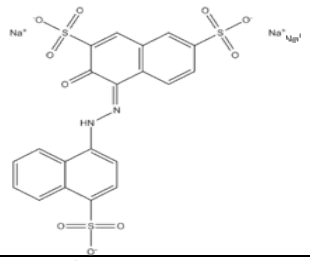
Ponceau S		Sulfonated azo dye	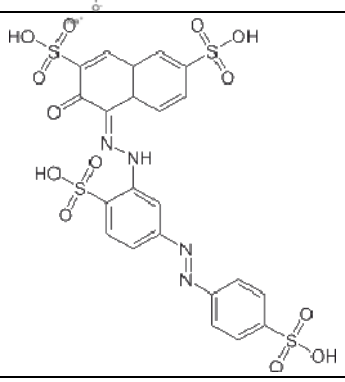
Eriochrome black T		Sulfonated azo dye	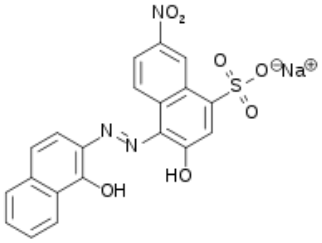

Dye	Visual image of dye in liquid media	Dye class	Dye structure
Orange II		Sulfonated azo dye	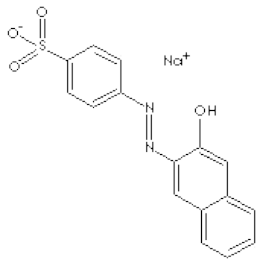
Basic Fuchsin		Triphenyl-methane	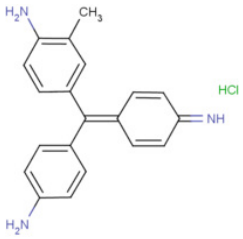
Crystal violet		Triphenyl-methane	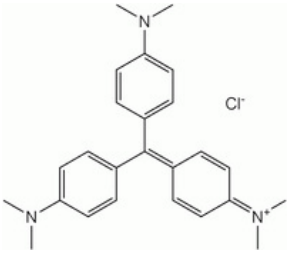
Brilliant green		Triphenyl-methane	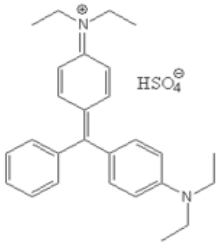

Dye	Visual image of dye in liquid media	Dye class	Dye structure
Malachite green		Triphenyl-methane	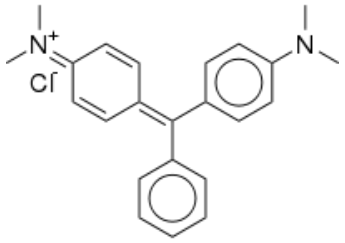
Fast green		Triphenyl-methane	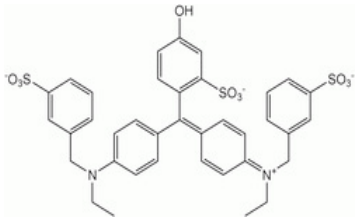
Amido black		Sulfonated diazo dye	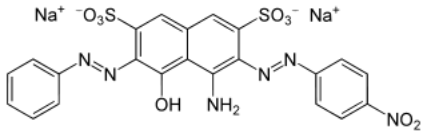
Janus green		Azo dye	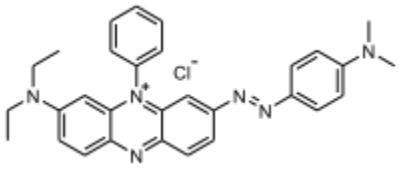

Dye	Visual image of dye in liquid media	Dye class	Dye structure
Congo red		Sulfonated diazo dye	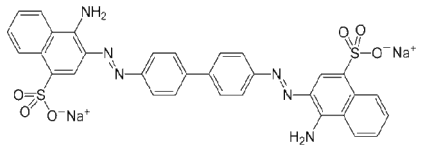
Biebrich scarlet		Sulfonated diazo dye	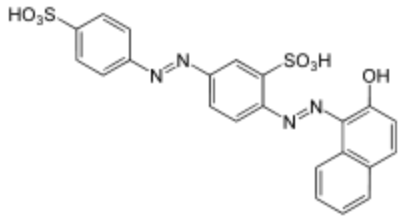
Bismarck brown Y		Diazo dye	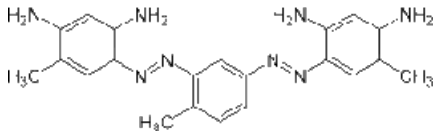
Indigo	Dye precipitates in minimal media	Indigoid	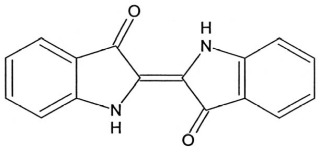

3.3 Screening of decolorizing bacteria on dye supplemented agar plates

All twenty-six strains isolated from the soil were tested alongside fifteen other known strains from the bacterial culture collection. Four carbon supplementations (0.5%) were chosen to work with; glucose, succinate, tween 20 and tween 80. Colonies

around which zones of clearing were apparent were recorded as dye decolorizers. See Table 6.2 page 295 for table specifying the dyes decolorized by each strain. Tartrazine, amaranth and fast green could not be decolorized by any of the strains tested, even in the presence of additional carbon sources. The dyes orange II, eriochrome T, amido black, biebrich scarlet and bismarck brown could only be decolorized by certain strains once carbon sources were present [Fig. 3.5].

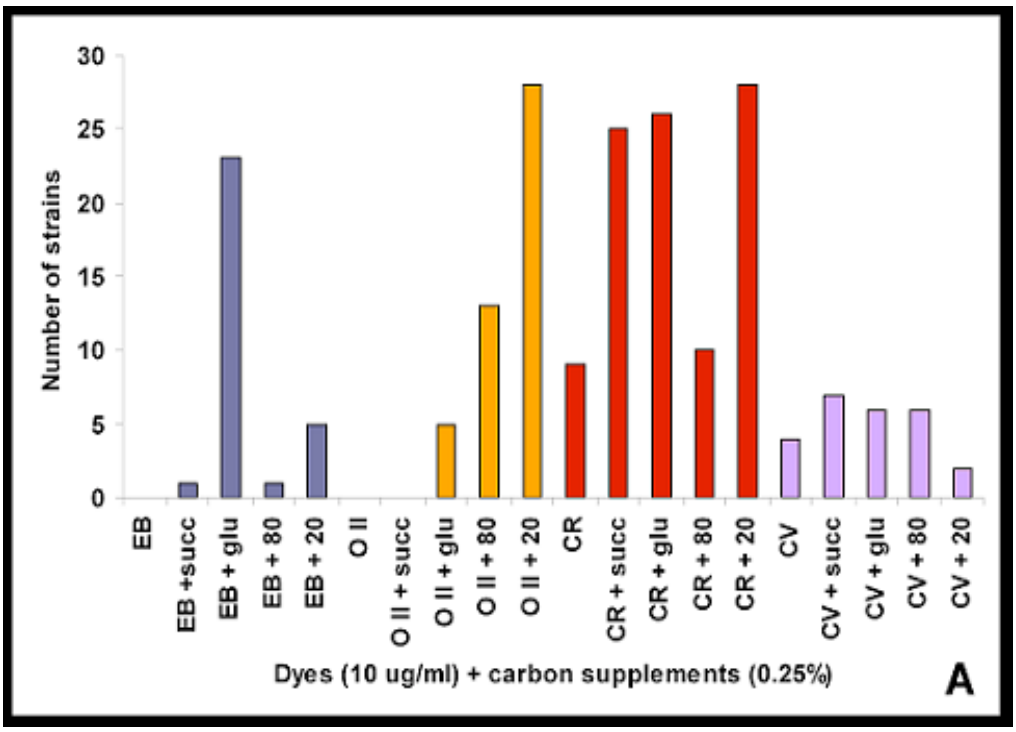

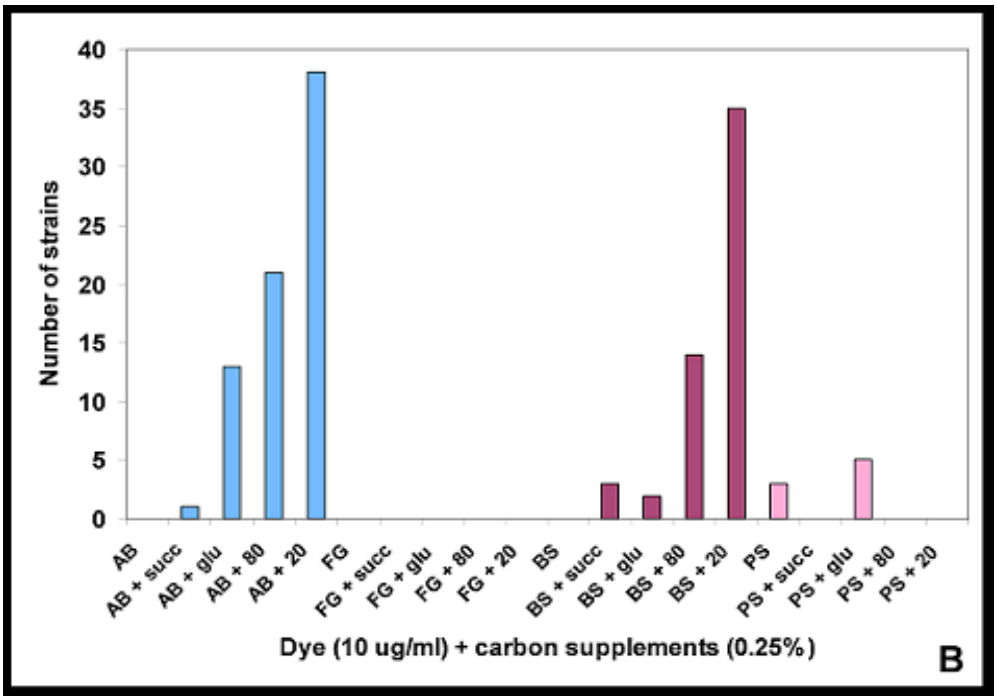

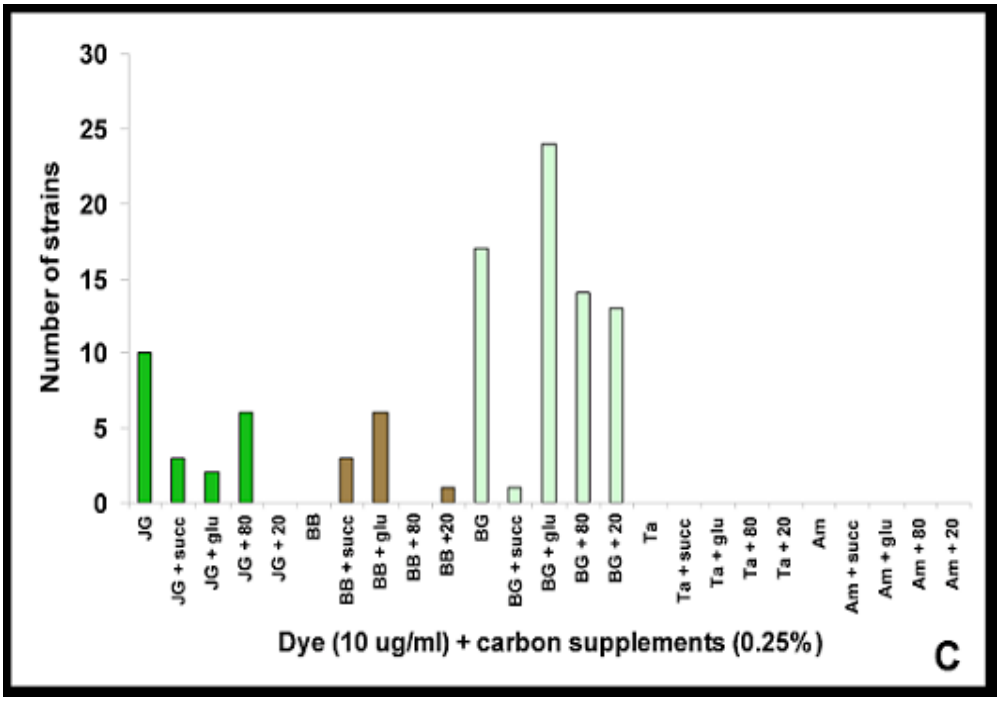

Fig. 3.5: Strains capable of decolorizing specific dyes with supplemented carbon sources. Each colour represents a specific dye. For visual clarity these results are represented in three different figures. Notably, no change in the dye only + carbon source control was noted.

Overall, including succinate in the dye media offered little improvement over the non-supplemented media. Predictably, the inclusion of glucose greatly improved

decolorization. Unexpectedly, the addition of tween 20 augmented the range of dyes decolorized. This was especially noticeable in relation to amido black, orange II and biebrich scarlet; in which a three to four fold increase was apparent [Fig. 3.6 and Fig. 3.7].

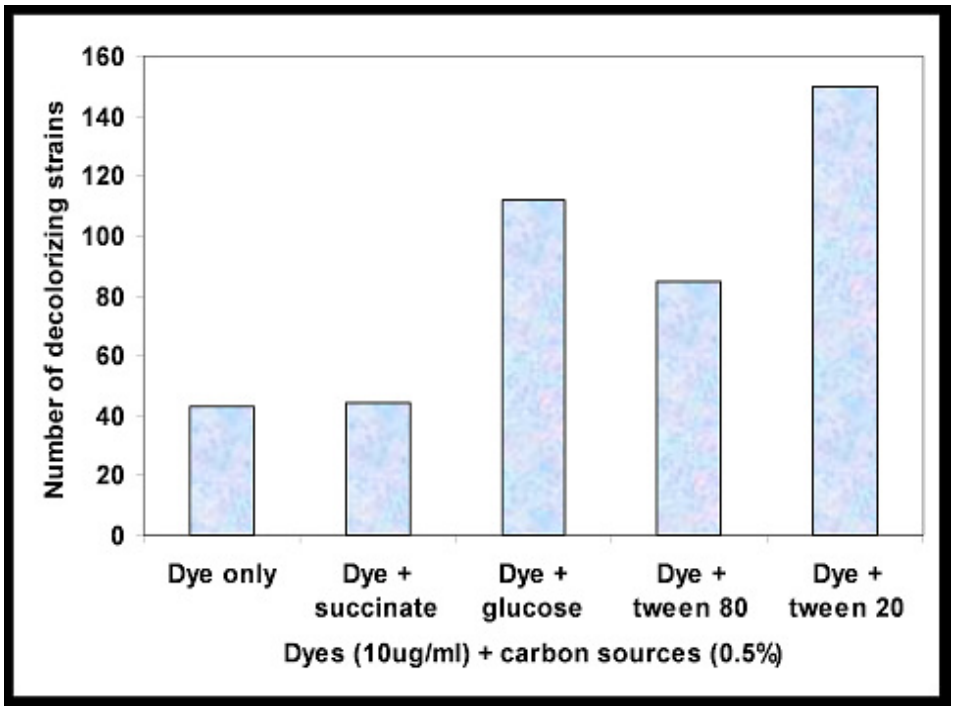

Fig. 3.6: Total number of strains capable of decolorization in the presence of additional carbon sources

Below is a visual representation of the vast difference encountered when adding surfactants into the agar media [Fig 3.7].

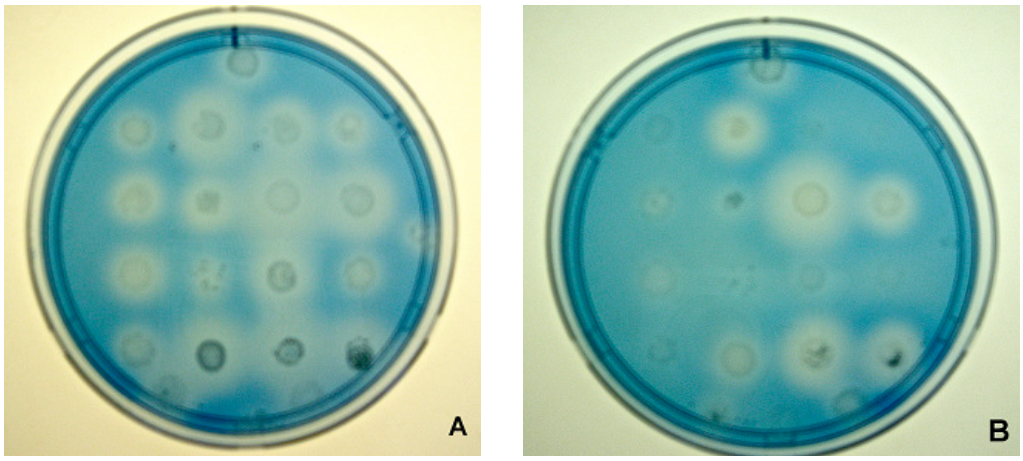

Fig. 3.7: Decolorization observed on (A) tween 20 and (B) tween 80 supplemented amido black replicated plates

A single zone of clearing was observed around bacteria capable of decolorizing specific dyes. An exception was strain HZ which produced two zones; a condensed inner zone and clear outer zone similar to the other bacteria [Fig. 3.8]. Although the isolate did not degrade the dye, evident by adsorption to the bacterial cell wall, I looked for a possible explanation for two zones.

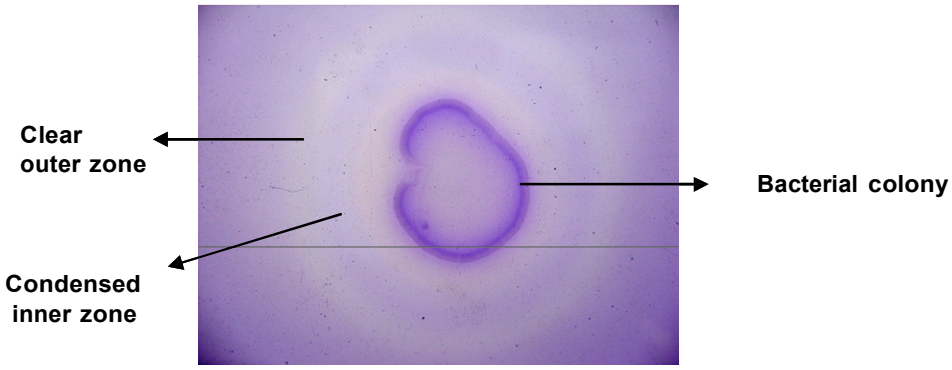

Fig. 3.8: Inner and outer zone around bacterial colony HZ

Of the forty three isolates tested, strain SY6 was chosen for further characterization studies based on its ability to decolorize crystal violet, amido black, brilliant green, janus green as well as orange II and biebrich scarlet in the presence of surfactants.

3.4 Decolorization study in liquid culture by strain SY6

The addition of tween 20 in liquid media in stark contrast to its effect on agar media reduced decolorization. The reason for this is unclear. Thus, for all liquid culture studies glucose (0.25%) was added. A decision was made to focus on the azo dye, amido black. Prolonged incubation (just under two days) of strain SY6 in liquid minimal media containing amido black led to a distinct color change from blue to violet [Fig. 3.9 (A) and (B)]. Comparatively, brilliant green was decolorized to colorless derivatives in under an hour [Fig. 3.9 (C) and (D)].

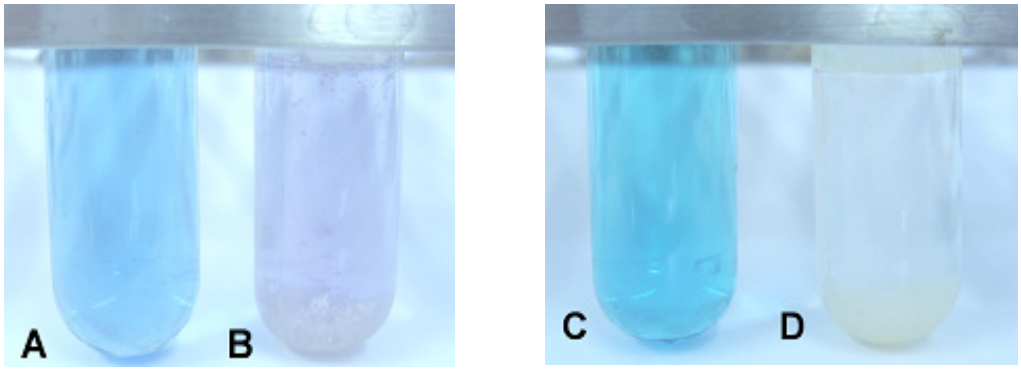

Fig. 3.9: Decolorization of dyes (10 µg/ml) (A) amido black, (B) amido black decolorized by strain SY6, (C) brilliant green and (D) brilliant green decolorized by strain SY6

3.5 Creation of a genomic library

In order to isolate the gene/s responsible, a genomic library was created. Genomic DNA was isolated using cesium-chloride gradient centrifugation. Aliquots of this DNA were incubated with the following enzymes: *Hind*III, *Pst*I, *Bgl*II, *Bam*HI, *Bsp*1431 (*Sau*3A), *Psu*I (*Xho*II), *Kpn*I, *Xba*I and *Mph*1103I (*Nsi*I) and run on 0.4% agarose gels to determine which restriction enzyme yielded an optimal fragment size range. The digestion of *A. orientalis* SY6 DNA with *Bgl*II yielded an average DNA fragment size of 3830 bp [Fig 3.10]. Calculations estimated that less than 7000 clones were needed to ensure a high probability of containing the gene of interest.

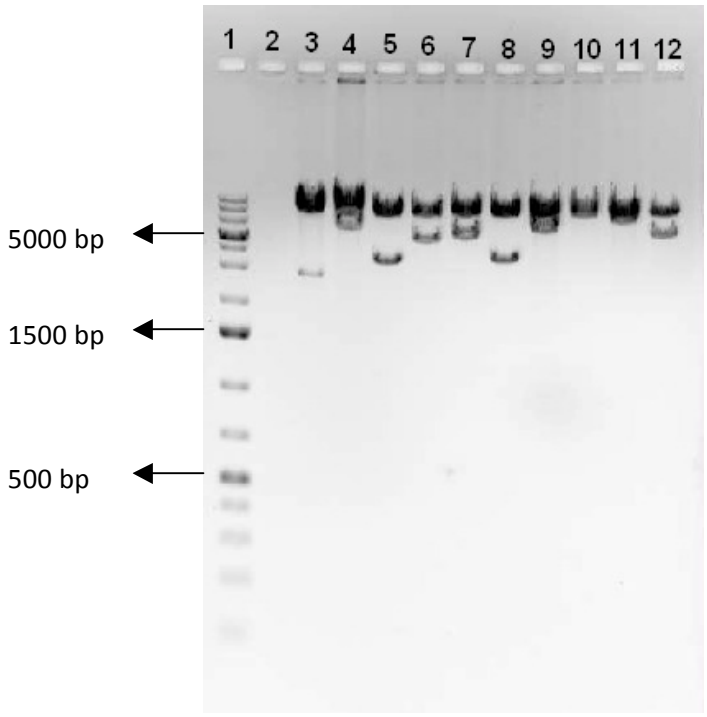

Fig 3.10: Inserts released from clones of *A. orientalis* SY6 library. Calculations were based on the following standard formula: No. of clones =ln (1-p) / ln (1- a/b), with the probability of finding a clone taken as 95% and the genome size as 8.7 Mbp. The size used was based on the sequencing of the entire genome of *S. coelicolor* A3(2) which had a length of 8.7 million base pairs, about twice the size of many other bacterial genomes (Redenbach *et al.*, 1996).

Once the actinomycete DNA was digested with the appropriate restriction enzyme and ligated to vector pLR591 (*Streptomyces* spp. replicon vector), the DNA was transformed into an intermediate *E. coli* host using calcium chloride mediated transformation to concentrate and purify the DNA. See section 2.1 page 281 for construction of vector pLR591.

Recombinant vector DNA was re-isolated from the *E. coli* pooled library consisting of approximately 40 000 clones by means of a large scale maxi-prep and transformed into *S. lividans* TK23 using PEG mediated transformation, for the purpose of screening. Unfortunately, a *Streptomyces* spp. host strain lacking the ability to decolorize amido black was not available to us. However, it was evident that strain TK23 was only capable of azo dye decolorization when at a high cell density. Since patching of the clones entails the transfer of a small bacterial inoculum onto the screening media, expression of the native gene was not detected.

3.6 Screening for the azo dye decolorizing gene on amido black plates

Approximately 5000 clones carrying *A. orientalis* SY6 DNA were patched onto selective dye media. A single clone displaying a zone of clearing was detected [Fig. 3.11].

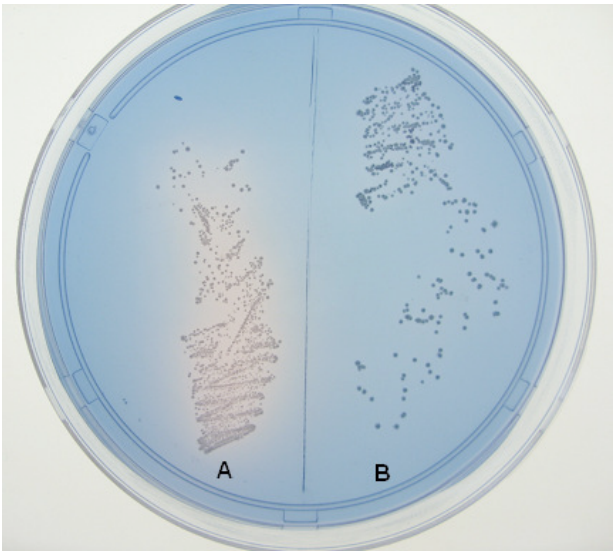

Fig. 3.11: (A) *S. lividans* TK23 clone carrying azo dye decolorizing gene fragment and (B) *S. lividans* TK23

3.7 Isolation and restriction analysis of amido black decolorizing gene fragment

The recombinant plasmid was extracted from the *Streptomyces* spp. host and restricted in order to determine the size of the fragment [Fig. 3.12].

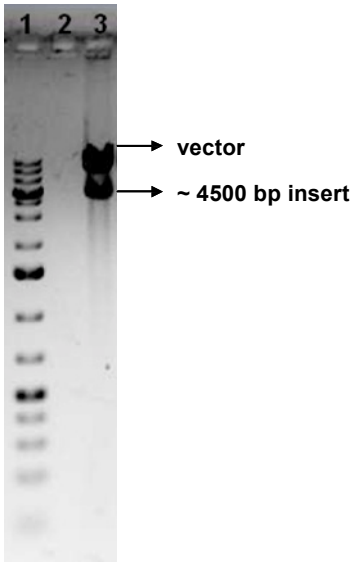

Fig. 3.12: Release of the insert from plasmid pLR591 using *Bgl*II

The recombinant vector harboured a 4500 bp insert. A restriction profile was mapped using the enzymes seen in the diagram for the purpose of subcloning and subsequent testing of the minimal DNA required for phenotypic expression [Fig. 3.13]. The recombinant vector was named pAM1 and the clone SlivAM1. Cloning of the *Xho*II fragments revealed that the larger 2800 bp region harbored the decolorization gene. A parallel cloning experiment revealed that 1600 bp of the aforementioned region was not required for amido black break down. Reasonably, the gene of interest was mapped to a 1200 bp region.

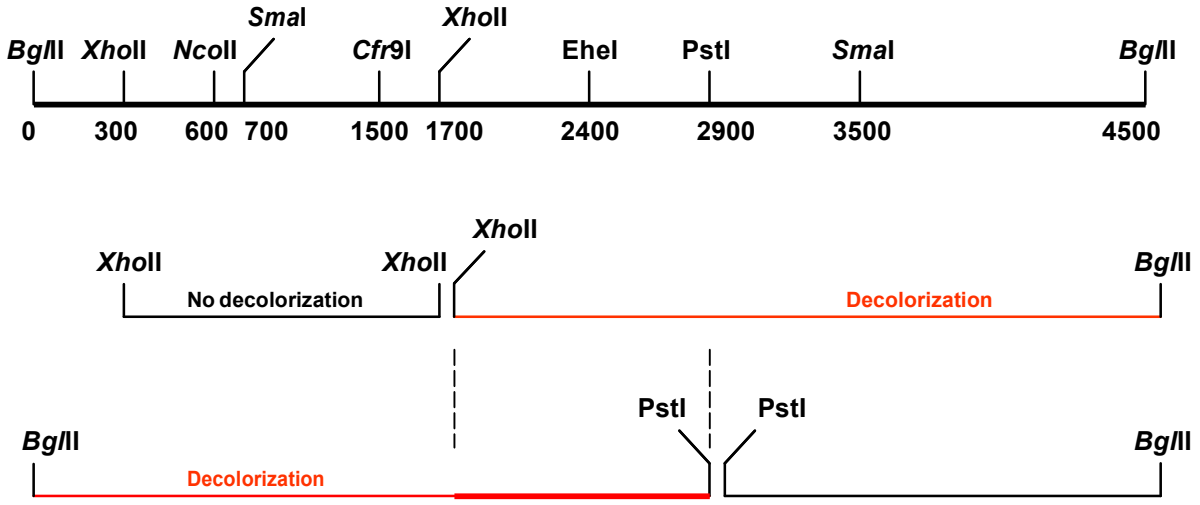

Fig. 3.13: Restriction analysis of the 4500 bp insert. Region within the dashed lines was predicted to carry the decolorization gene

3.8 Sequencing of pAM1 insert

Sequencing of the 4500 bp gene fragment revealed seven open reading frames [Fig. 3.14]. From the subcloning results three of the predicted proteins (within the first 1700 bp) were eliminated. Thus, four potential protein candidates remained namely ORF's D, E, F and G. Subsequently, further subcloning revealed ORF's E, F, and G were non-essential. Thus, ORF D encoding a conserved hypothetical protein was believed to be the gene responsible for decolorization.

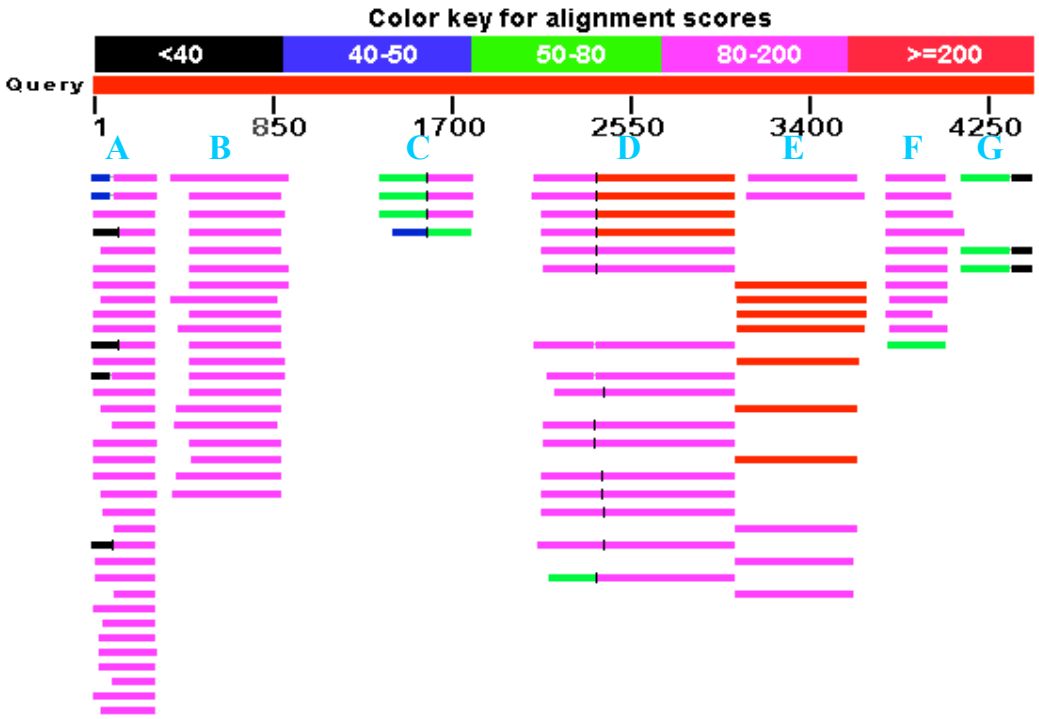

Fig. 3.14: Predicted open reading frames of pAM1 insert

Table 3.4: Summary of identified homologues of open reading frame prediction of pAM1 insert using Entrez PubMed blastx

Open reading frame	**Description**	**Species***	**Maximum identity (%)****	**E value**
A	Conserved hypothetical protein of DinB family	*Amycolatopsis mediterranei* U32	75	9e-21
B	Integral membrane protein	*Stackebrandtia nassauensis* DSM 44728	42	2e-26
C	Hypothetical protein AMED 7643	*Amycolatopsis mediterranei* U32	67	8e-30
D	Conserved hypothetical protein AMED 2278	*Amycolatopsis mediterranei* U32	77	6e-104
E	Transcriptional regulator, TetR family	*Nakamurella multipartita* DSM 44233	54	8e-41
F	Cupin 2 conserved barrel domain protein	*Amycolatopsis mediterranei* U32	82	2e-40
G	Polyprenyl synthetase	*Micromonospora* sp. ATCC 39149	55	8e-14

* - identified homologues of ORFs in pAM1 inserts
** - identified by Blastx search using NCBI database

3.9 Functional determination of conserved hypothetical protein

3.9.1 *Phylogenetic analysis of hypothetical protein*

The hypothetical protein from *A. mediterranei* U32 that was identified as a homologue of ORF D of *A. orientalis* SY6 has a significant similarity to the DsbD cytochrome biogenesis protein transmembrane region in *Streptosporangium roseum* DSM 43021. ORF D showed a 60 % sequence identity match to the DsbD gene of *S. roseum*. A phylogenetic tree was constructed to infer the relationship between ORF D in *A. orientalis* and homologues within other species. ORF D is closely related to DsbD homologues of *A. mediterranei* and *C. acidiphila* (a mycelia actinomycete) forming a cluster, but only distantly related to those in other species.

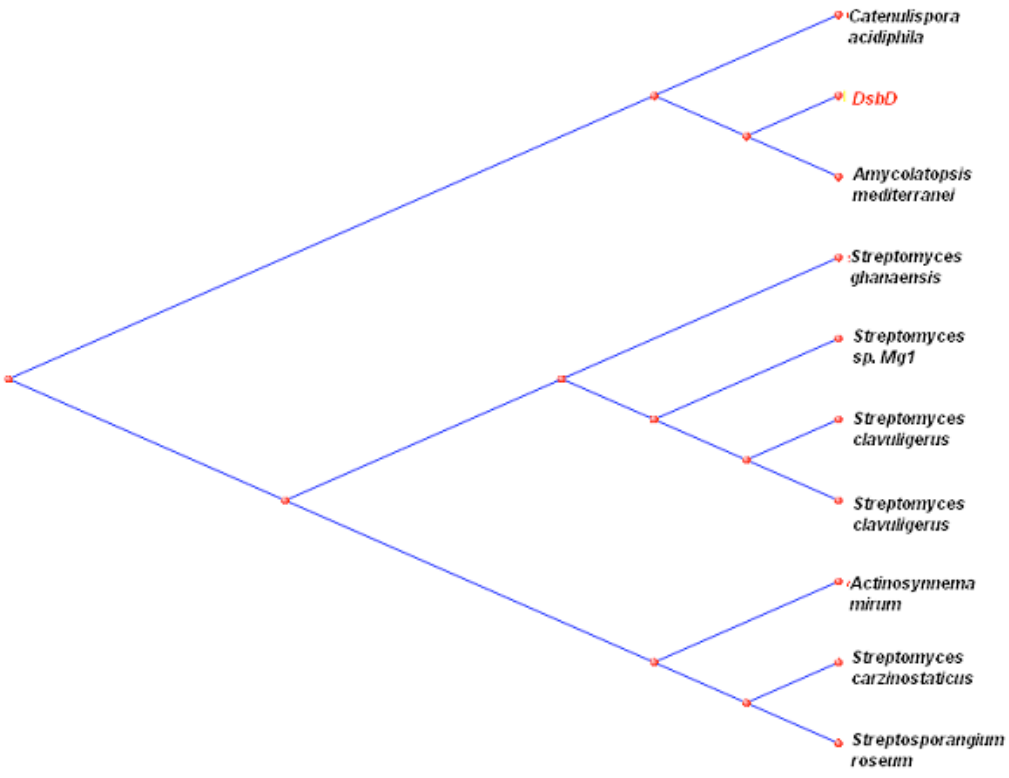

Fig. 3.15: A phylogenetic tree of DsbD homologues related to *A. orientalis* SY6 (represented in red)

3.10 Characterization of optimal pH, temperature and carbon source utilization of enzyme

Whole cell assays were conducted to determine the optimal parameters of activity for this enzyme. A temperature of 37^{o}C led to the highest decolorization dropping rapidly with either a 10^{o}C increment or decrease [Fig. 3.16]. The lack of activity at 50^{o}C potentially suggests weak thermostability. Notably, since the host strain possessed a native ability to decolorize the dye this activity could not be separated from the activity of the cloned pAM1 gene. In all graphs error bars represent standard deviation from experiments carried out via. inter-experimental duplication.

3.10.1 *Liquid assay determining optimal temperature profile*

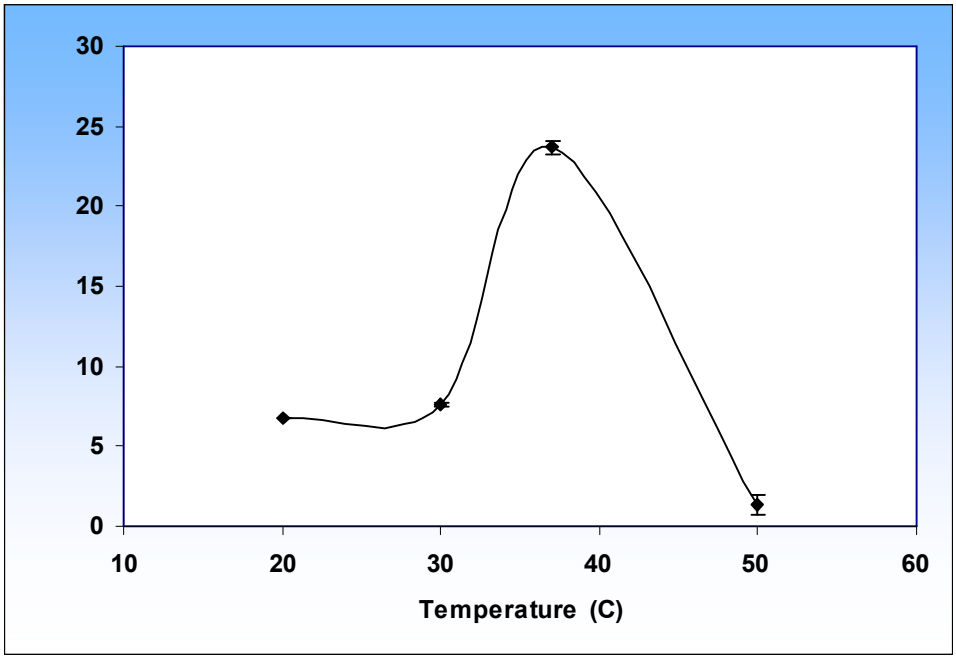

Fig. 3.16: Decolorization at different temperatures

3.10.2 *Liquid assay determining optimal pH profile*

Optimal activity occurred at a pH of 6.5. Moderate activity occurred at an acidic pH and was repressed at an alkaline pH [Fig. 3.17].

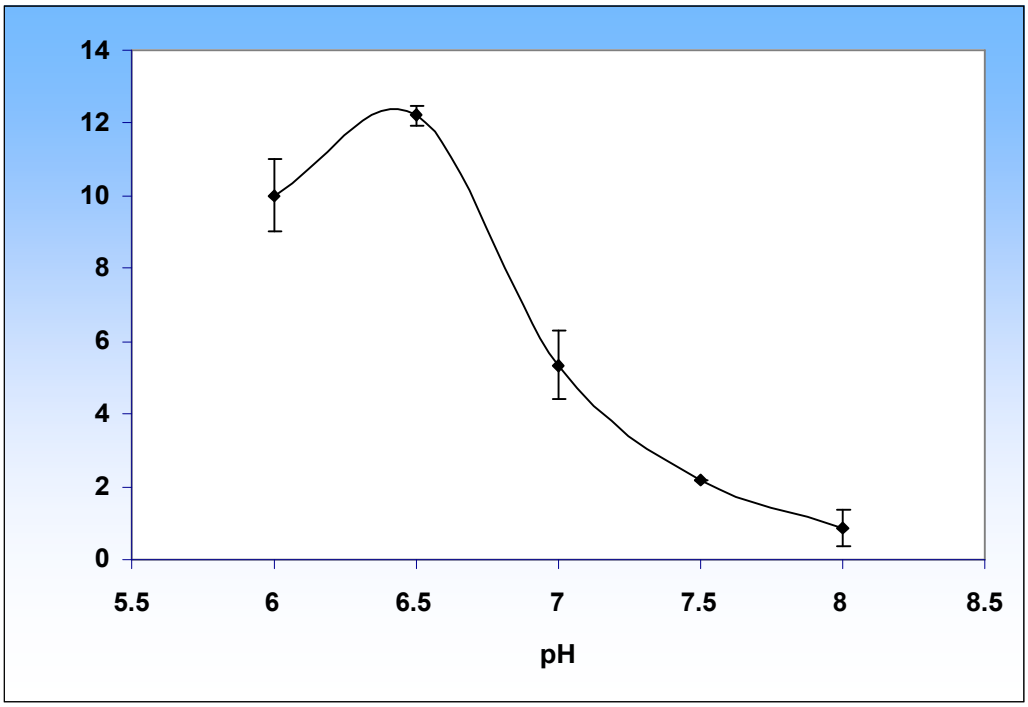

Fig. 3.17: Representation of decolorization at different pH values

3.10.3 *Liquid assay determining carbon source utilization*

Early studies showed that a carbon source was required for efficient decolorization. Correspondingly, various carbon sources were tested to establish which would be most efficient. Glucose was the best supplement resulting in 45 % decolorization and increased cell biomass [Fig. 3.18].

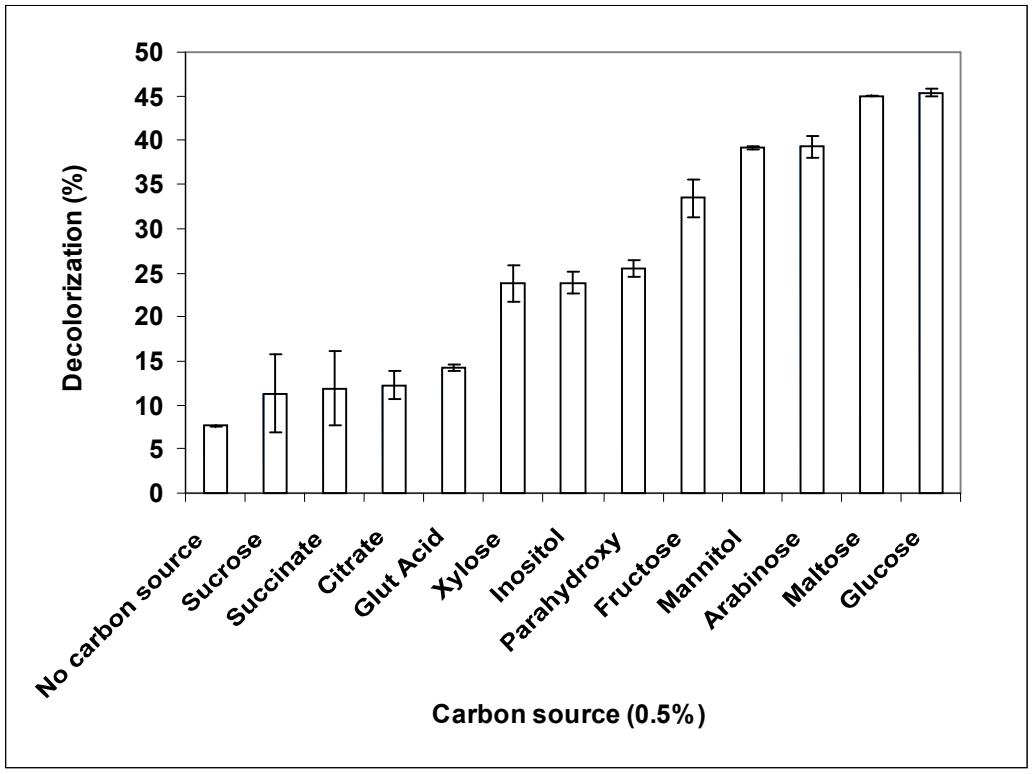

Fig 3.18: Decolorization in the prescence of various carbon sources

3.10.4 *Effect of carbon and nitrogen sources on decolorization of SlivAM1*

Carbon sources, glycerol and glucose positively influenced decolorization by SlivAM1 leading to a greater than 40 % decolorization. The addition of the nitrogen source peptone was equally effective. Both yeast extract and starch caused a non-significant decrease of approximately 2% [Fig. 3.19].

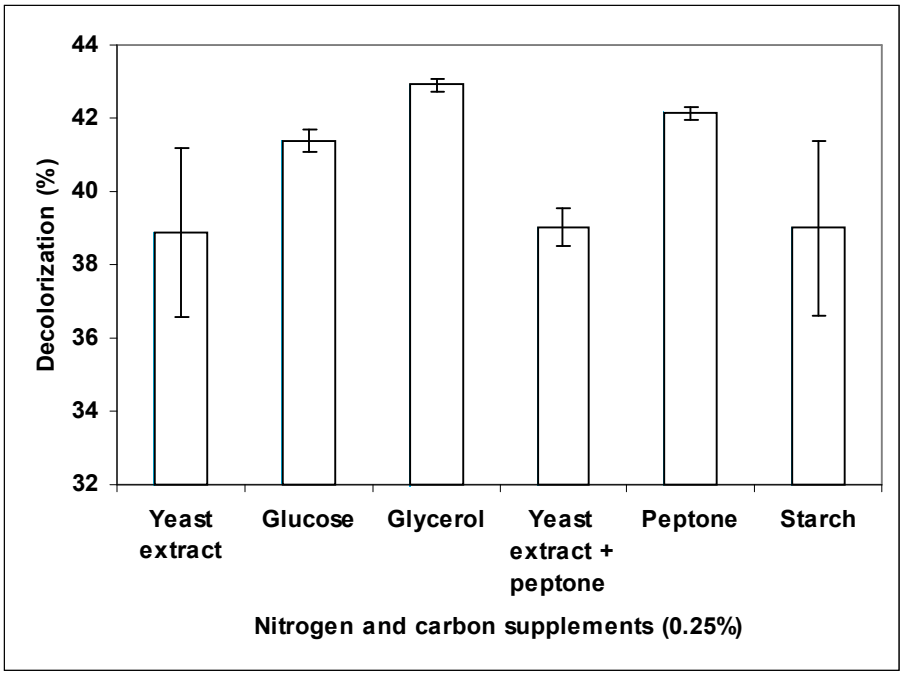

Fig. 3.19: Representation of the addition of nitrogen and carbon sources

3.11 Range of dyes decolorized by clone SlivAM1

Further analysis was conducted to determine whether pAM1 would have an affect on other dyes. Results indicated that its activity was highly restricted to amido black [Table 3.6].

Table 3.6: Comparison of *S. lividans* dye degrading capacity against clone SlivAM1

Dyes	**SlivAM1**	***S. lividans* TK23**
Brilliant green	+	+
Tartrazine	-	-
Basic fuchsin	-	-
Crystal violet	-	-
Amido black	+	+
Orange II	-	-
Janus green	+	+
Malachite green	+	+
Ponceau	-	-

Dyes	SlivAM1	*S. lividans* TK23
Biebrich scarlet	-	-
Indigo	-	-
Bismarck brown	-	-
Congo red	-	-
Eriochrome T	-	-
Amaranth	-	-
Fast green	-	-

Since the liquid assays were conducted using a high cell density the decolorization of amido black by *S. lividans* TK23 was observed in the above experiment. However, the choice to use *Streptomyces* spp. as the host for screening purposes was due to the ease of detection of the phenotype since the mycelia extend beyond the immediate periphery of the colony.

3.12 Expression of pAM1 in *R. erythropolis* SQ1

R. erythropolis SQ1 does not have the ability to degrade amido black hence the expression of the gene fragment in this background host proved pAM1 habored a biodegradative ability. Hence, vector pAM1 was transformed into *Rhodococcus* spp. (clone SQ1AM1) and the decolorization of various dyes monitored. It was found once again that its expression did not have an affect on other dyes [Table 3.7].

Table 3.7: Comparison of *R. erythropolis* SQ1 dye degrading capacity against clone SQ1AM1 to establish the activity of pAM1 on other dyes

Dyes	SQ1	SQ1AM1
Brilliant green	+	+
Tartrazine	-	-
Basic fuchsin	+	+
Crystal violet	+	+
Amido black	-	+
Orange II	-	-
Janus green	+	+
Malachite green	+	+
Ponceau	-	-
Biebrich scarlet	-	-

Dyes	SQ1	SQ1AM1
Indigo	-	-
Bismarck brown	-	-
Congo red	-	-
Eriochrome T	-	-
Amaranth	-	-
Fast green	-	-

3.13 Detoxification study

E. coli was added to the decolorized supernatant of SlivAM1 and incubated against controls. A two-fold decrease in colony forming units was detected when compared to the glucose supplemented control, indicating inhibition thus suggesting partial detoxification of the dye [Fig. 3.20]. Additionally, the morphology of *E. coli* when incubated in the presence of the decolorized dye was viewed under a light microscope. No dramatic change in structure was noted.

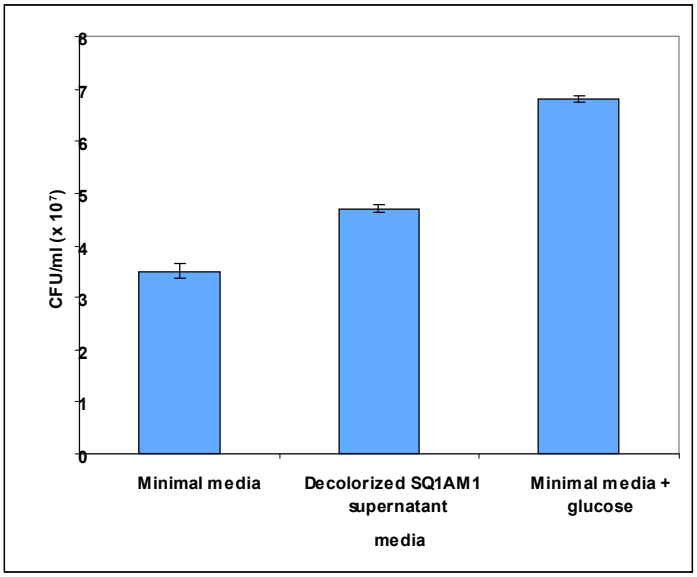

Fig. 3.20: Effect of decolorized supernatant on the growth of *E. coli*

3.14 Influence of bioabsorption on decolorization

This experiment was conducted in line with Robinson and coworkers (2001) suggestion that the adsorption of dyes onto an organic substrate and microbial treatment thereafter would be a good bioremediation strategy. Thus, live *A. orientalis* SY6 cells were incubated with live *S. coelicolor* A3(2) or dead *S. coelicolor* A3(2) cells. The SY6 and A3(2) strains consortium led to the additional breakdown of Amaranth and Orange II. The incubation of strain SY6 with dead A3(2) cells led to the removal of Scarlet from the media. No dye however was removed due to bioabosorption onto the dead mycelial mass. The adsorption was anticipated to occur due to the interaction of the charge on the cell wall and dye.

Table 3.8: Decolorization by mixed cultures of strain SY6 and live or dead strain A3(2)

Dyes	**SY6**	**A3 (2)**	**SY6 + live A3(2)**	**SY6 + dead A3(2)**
Brilliant green	+	+	+	+
Tartrazine	-	-	-	-
Basic fuchsin	+	+	+	+
Crystal violet	+	-	+	+
Amido black	+	+	+	+
Orange II	-	-	+	-
Janus green	+	+	+	+
Malachite green	+	+	+	+
Ponceau	-	-	-	-
Scarlet	-	-	-	+
Indigo	-	-	-	-
Brown	-	-	-	-
Congo red	-	-	-	-
Eriochrome T	-	-	-	-
Amaranth	-	-	+	-
Fast green	-	-	-	-

4. Discussion

Interest in the family of nocardioform actinomycetes lies in the extraordinary primary and secondary metabolism possessed by this group, with members involved in the ability to synthesize antibiotics or antimicrobial peptides, break down rubber, mineralize dyes and produce phytases (Goszczynski, 1994; Jendrossek *et al.*, 1997a; Walsh, 2003). This family remains an untapped fountain of valuable genes, enzymes and pathways (Gurung *et al.*, 2009). Studies have continuously demonstrated that this group possess exceptional attributes; focus was placed on one of the lesser acknowledged features of actinomycetes; in particular azo dye decolorization.

Soil samples were collected from geographically and environmentally diverse regions covering five of the seven continents. This was done with the expectation of isolating novel strains and subsequently novel genes and compounds (Gurung *et al.*, 2009). The original enrichment for these strains was through the use of latex rubber which led to the isolation of twenty-nine strains, and the biased selectivity of twenty-two *Streptomyces* spp. The identification of nine of these in contrast to what was expected gave high percentages of similarity to known species. Studies conducted on *Streptomyces* spp. for their ability to break down dyes are surprisingly limited (McMullan et al., 2001). This encouraged the screening of these strains on sixteen dyes.

The results of the plate decolorization assays showed that many strains were restricted in their capacity to decolorize either the triphenylmethane or azo dyes. The inability of any of the tested strains to decolorize the triphenylmethane dye, fast green and sulfonated dye, tartrazine was not unexpected. To the best of my knowledge, literature on the bacterial break down of fast green is non-existent and with regard to tartrazine very limited. Just one article detailed the reduction of tartrazine by *Proteus vulgaris* by means of a FMN- flavoprotein (Roxon *et al.*, 1967). Their work showed that this dye could only be utilized by older cells due to more lenient cell permeability of the cells at this phase.

The break down of amaranth however is reasonably common in the literature. Azoreductases from a *Kerstersia* spp., *Sphingomonas* spp., *Pseudomonas* spp. and *Staphylococcus* spp. strains have been characterized in the degradation of this dye

(Vijaykumar *et al.*, 2007; Kudlich *et al.*, 1997; Nachiyar and Rajakumar, 2005; Chen *et al.*, 2005). Notably, with the exception of *Staphylococcus aureus*, the other bacterial strains were Gram negative. Nevertheless, this information is not enough to deduce that amaranth biodegradation occurs more frequently in Gram negative bacteria. In this study since just two Gram negative strains were carried (out of forty-three strains tested) it is difficult to make a comparison between the two groups. The failure to detect this ability could simply be attributed to the selection of strains; the majority of which are *Streptomyces* species. To the best of our knowledge no azoreductase has ever been isolated from this genus, however a potential azoreductase has been identified in *S. coelicolor* by means of the genome sequencing project. This reasoning could be applied in parallel to the small number of bacteria capable of mineralizing other azo dyes in this study. Other dyes difficult to degrade included the azo dyes eriochrome T, orange II, amido black, biebrich scarlet, ponceau S and bismarck brown, all of which could not be decolorized unless an additional carbon source was added. In particular, orange II and ponceau S, like amaranth are fairly common in the literature. Alternately, this might be explained by the choice of media used by researchers for the screening of dye decolorization. Notably, minimal media used in much of the literature contains yeast extract, peptone or trace elements (Grekova- Vasileva *et al.*, n.d.; Hu., 1994). The minimal media used within this study contains the most basic components; namely phosphates, a nitrogen source (in the form of ammonium chloride) and the dye serving as the main carbon source.

Glucose reportedly acts as a source of electrons when consumed by microorganisms and was found to favorably increase decolorization and growth of most strains tested. An exception to this was the supplementation of janus green which led to a decrease in the number of strains decolorizing the dye. No evidence in the literature of glucose repressing azo dye decolorization could be found, thus the reason for this occurrence is unclear. Harazono and Nakamura (2005) described an increase in decolorization potential upon the addition of surfactants to a liquid dye mixture containing the fungus *P. sordida*. It was checked whether the same pattern would be manifested with these strains, using tween 80 and 20. Tween 80 is an anionic surfactant derived from an unsaturated fatty acid, while tween 20, a non-ionic surfactant contains saturated fatty acid (Harazono and Nakamura, 2005). The addition of tween 20 onto dye containing plates in this study clearly improved the number of strains capable of

decolorization while the action of tween 80 was less pronounced. The prominent zones surrounding colonies on tween 20 supplemented plates allowed us to tentatively propose an increase in enzyme yield. Reese and Maguire (1968) reported a similar occurrence when conducting a comprehensive study into the ability of surfactants to stimulate enzyme production in fungi. These researchers made several interesting observations, which include a general increase in enzyme production in strains which initially produced small quantities of enzyme, yet insignificant increases for strains which were good enzyme producers. The mode of action was believed to be an interaction with the cell membrane, resulting in a release of the enzymes. A closer monitoring of different enzymes within the same host showed that tween 80 could result in the selective inhibition of some enzymes and enhancement of others, proving that a complex interaction is involved. I hypothesized that the detection of decolorizing strains only observed in the presence of tween 20 yet not with tween 80 could be accredited to superior protein stabilization by the latter providing greater protection to the enzyme/s once released into the media (Chou *et al.*, 2005). This consequence brings a new dimension in this work suggesting that azoreductases are widespread amongst *Streptomyces* species, yet go unnoticed due to their low concentrations.

Noticeably, *Streptomyces* spp. were able to readily decolorize congo red, a structurally complex dye which contains two azo bonds and polyaromatic and sulfonated groups. Yet, the structurally simpler dye, orange II which has a single azo bond and sulfonated group was not cleaved at all. It is obvious from the literature that azoreductase action is variable among strains. For instance *Kerstersia* spp. decolorized dyes carrying sulfonated groups on either side of the azo bond to a higher extent than dyes which carried a single sulfonated group. This is in contrast with decolorization reported by *Sphingomona*s species. Evidently, greater structural complexity of a dye does not signify greater difficulty in its breakdown. Instead it has been found to be dependent on several factors namely, the type, position and number of functional groups. Additionally, the presence of phenolic, amino, acetoamido and 2-methyoxyphenol groups on the ring were found to lead to an increase in biodegradation (Swamy and Ramsay, 1999).

An interesting phenomenon was noticed on the dye supplemented plates carrying *Methylibium fulvum* HZ. Two concentric zones surrounded the colony opposed to a single zone as seen with all the other bacteria. This can be explained by the

electrostatic interaction of the enzyme with the dye. Crystal violet is a basic dye; thus the release of a basic polymer into the media creates a clear zone, however the release of an acidic polymer causes the dye to condense (Nishikawa and Ogawa, 2002). In principle, this suggests that two enzymes are being released into the media by this strain, which from the zones can be interpreted as a low molecular weight basic enzyme (due to its diffusion furthest from the colony) and higher molecular weight acidic enzyme, creating the inner condensed zone.

The range of dyes decolorized by strain SY6 and the detection of strong zones suggesting potent enzyme activity made it apparent that this isolate demanded further attention. Basic characterization tests revealed that this strain was an aerobic, Gram positive, filamentous bacterium which formed a 'crusty' colony on complex media and gave rise to fragmented mycelia in liquid broth. However, its atypical antibiotic profile set it apart from the other *Streptomyces* spp. strains. Its resistance to streptomycin, thiostrepton and rifampicin are not common features of this genus. Sequencing of the 16S rRNA led to 98% identification to both *Amycolatopsis japonica* and *Amycolatopsis orientalis*. These strains are easily distinguishable based on the aerial spore and diffusible pigment color (Tan *et al.*, 2006). *A. japonica* has white aerial spores, releasing a dark olive brown pigment with a deep yellow-brown reverse color, while *A. orientalis* has light blue aerial spores, releases a light olive brown pigment with an orange-yellow reverse color (Tan *et al.*, 2006). Based on this rudimentary assessment strain SY6 was identified as *A. orientalis*.

The majority of strains tested were capable of decolorizing dyes within a single class. *A. orientalis* SY6 was unique in the fact that it crossed this boundary, capable of degrading diazo, azo and triphenylmethane dyes. To our knowledge no *Amycolatopsis* species has ever been implicated in azo dye decolorization and thus encouraged our pursuit of the gene/s involved in this particular strain.

One clone exhibiting a zone of clearing was acquired from a genomic library. Analysis of the insert revealed a match to a conserved hypothetical protein in *A. mediterranei*, which was unhelpful in determining the function of the associated enzyme. The hypothetical protein however, matched a cytochrome c biogenesis transmembrane region (DsbD) in *S. roseum*. The Dsb (disulfide bond formation) family of enzymes serves the same function as the protein disulfide isomerases (PDI)

found in eukaryotes (Missiakas *et al.*, 1995). These enzymes play an important role in the formation and rearrangement of disulfide bonds that is crucial to the stability of many proteins (Missiakas *et al.*, 1995). The pathway within Gram negative bacteria has been deciphered; DsbA is responsible for the introduction of disulfide bonds into synthesized proteins, an action which causes it to become reduced (Katzen *et al.*, 2002). It is reoxidized by means of DsbB which itself is oxidized by quinones within the cytoplasmic membrane (Chung *et al.*, 2000). Within this highly oxidized environment certain enzymes must be maintained in a reduced form in order to function. Thioredoxin reductase and cytoplasmic thioredoxin serve as an electron source with electrons transferred to DsbD which is responsible for the reduction of the disulfide isomerases DsbC and DsbG (Chung *et al.*, 2000). Missiakas and colleagues conducted a detailed analysis on DsbD activity in *E. coli* and found that non-functional mutants were defective in sulfide bond formation and caused the isomerases to accumulate in an oxidized form. Hence, they were able to deduce that this enzyme acts as a reductase and is important in maintaining a balance of oxidized and reduced substrates.

This is not the first study to link a reductase involved in another role to azo dye degradation. Mugerfeld *et al.* (2009) linked a putative azoreductase to heavy metal resistance in *Shewanella* species. Crystallography studies verified the presence of a NAD(P)H binding pocket in *E. coli* AzoR, *P. aeruginosa* paAzoR1 and *E. faecalis* AzoA (Punj and John, 2009). This is found to be a frequent feature amongst azoreductases identified thus far. No NAD(P)H, FAD or FMN binding sites were found to occur in DsbD, however since the electrons are received from an external source for the purpose of reduction, the presene of these sites is not necessary.

From the phylogenetic tree it was evident that DsbD was not closely related to other sequences within the database. Of the environmental isolates tested eleven Streptomycetes were able to degrade the sulfonated diazo dye. Yet on the tree, the closest enzyme matches from *Streptomyces* species were clustered separately from the *A. orientalis* enzyme. It is possible that this group possesses another gene for amido black biodegradation. This was further evidenced since no gene with a highly similar sequence was found in the fully sequenced genome of *S. coelicolor*, also an amido black decolorizer.

Optimal temperature of the enzyme was 37^{o}C which corresponds to many studies in the literature, however the pH showed a slight deviation with optimal activity at 6.5 rather than 7.0, which is commonly reported. *Gracibacillus* spp., *B. cereus* and *P.aeruginosa* enzyme activity were all optimal at pH 7.0 (Uddin *et al.*, 2007; Pricelius *et al*., 2007; Nachiyar and Rajakumar, 2005). Glucose, followed closely by maltose proved to be the most efficient carbon sources tested. Logically, sucrose was the least efficient since *S. lividans* is incapable of utilizing this due to lack of sucrase or invertase activity (Santamaria *et al.*, 2002). The addition of excess nitrogen, in the form of yeast extract combined with peptone negatively influenced dye removal. Liu *et al.* (2009) showed that a combination of yeast extract and glucose led to 70 % decolorization in less than 2 hours and took longer when these components were added individually.

The range of decolorization by pAM1 in the Streptomycete host was limited to amido black. This was further verified when transformed into *R. erythropolis* SQ1. The dyes tested which fall into the same class as amido black are congo red and biebrich scarlet. It can only be hypothesized why these dyes were not reduced. It is probable that the presence of the two benzene rings in biebrich scarlet and two naphthalene rings in congo red prevented their decolorization. Nigam and coworkers (1996) found that azo dyes with a hydroxy or amino group, such as amido black are degraded more easily than those carrying a methyl, methoxy, sulfo or nitro groups.

Useful dye degrading isolates should be capable of completely breaking down the dye to non-toxic components. Decolorization is only an indication of the conversion of the chromophore, thus the monitoring of toxicity reduction is important. By testing the rate of growth of *E. coli* in decolorized supernatant it was established that only partial detoxification occurred. Unfortunately, no literature exists on the biodegradation of amido black, thus no enzymes have been identified nor the biodegradative pathway uncovered. For these reasons it was not possible to determine what toxic end-product is being produced.

He *et al.* (2004) compared the results between immobilized and free cells and a found 99 % color removal in 6 hours for immobilized cells whereas 90 % decolorization was achieved after 24 hours with free cells. Cells are normally immobilized on polyvinyl alcohol beads. For employment of bacteria for use in bioreactors it is often

beneficial to immobilize them on a solid substrate. Cell immobilization was mimicked by spotting SlivAM1 bacteria onto agar pellets and incubating them in amido black. In comparison to freely suspended cells the immobilized cells took longer to degrade the azo dye (data not shown). It is possible that since only part of the cells were exposed to the dye (since the substrate mycelia were buried in the agar pellet) that this hampered the release of the enzyme.

Robinson *et al.* (2001) suggested that the best strategy would be to first adsorb the dyes onto a substrate in order to concentrate them and afterwards treat them microbially. The decision was made to check whether this would prove to be a useful strategy by adsorbing the dyes onto dead *S. coelicolor* cells and subsequently treating them with strain *A. orientalis* SY6. The live *S. coelicolor* and *A. orientalis* consortium led to the added degradation of amaranth and orange II, which neither had the ability to break down individually. The addition of dead *S. coelicolor* cells did not assist in the removal of the dye from the media by means of bioabsorption. The presence of the dead biomass did allow for the added degradation of biebrich scarlet, however it is unclear how this was possible since no adherence of the dye to the cell wall was witnessed.

4.1 Concluding remarks

A broad characterization of six dye subclasses decolorized by forty-three isolates was conducted. It was found that additional carbon supplementations were essential for the break down of the majority of azo dyes. Furthermore, the addition of surfactants to increase enzyme production has interesting implications that should be further analyzed. A gene with a reductive mechanism of activity was linked to amido black decolorization in *A. orientalis*. A basic characterization revealed that the enzyme worked optimally within a restrictive temperature and pH range of 37^{o}C and 6.5 respectively, not a suitable candidate for the treatment of effluent which is usually an alkaline pH. Enzymatic activity of the dye degrading enzyme tended to be very specific. Moreover, this enzyme has not been linked to azo dye biodegradation prior to this. This study was expanded upon in the next chapter by also screening for the genes allowing this isolate to break down the triphenylmethane dye, crystal violet.

Identification and characterization of genetic elements from *Amycolatopsis* species contributing to triphenylmethane decolorization

Chapter II abstract

Focus was placed on an *Amycolatopsis* species isolate found to breakdown two structurally distinct classes of dye, one of which is crystal violet. This species has never before been implicated with this ability, further encouraging focus on this strain. This study aimed to partially characterize the enzymes capable of dye biodegradation and identify the gene/s involved. A library was constructed in order to isolate genetic elements contributing to crystal violet decolorization. Three genes were isolated and characterized; a 3-deoxy-7-phosphoheptulonate synthase, N5, N10-methylene-tetrahydromethanopterin reductase and glucose/sorbosone dehydrogenase. The synergistic action of these genes led to crystal violet mineralization. The screening of gene expression was conducted in a closely related host species, namely *S. lividans*. Additionally, the activity of these genes was tested in two other strains, namely *Mycobacterium* spp. and *Rhodococcus* spp. It was found that the range of dye classes decolorized was extended in both species, showing that these genes adopted novel functional potentials in these hosts.

1. Introduction

1.1 Uses of triphenylmethane dyes

Crystal violet falls in the class of triphenylmethane dyes which are commonly used in the clothing industry to dye wool, silk and cotton (Kim *et al.*, 2005). It is well known as a biological stain, yet also possesses medicinal properties. It has been used in the treatment of pinworms and as a topical agent as well as being added to feed to prevent fungal growth (Azmi *et al.*, 1998). In addition, it is classified as a clastogen and has been linked to tumor development in fish (Chen *et al.*, 2007).

1. 2. Mechanism of triphenylmethane biodegradation

Bacterial triphenylmethane dye biodegradation has not generated as much interest as that of azo dyes. This is reflected strongly in the limited literature. While knowledge of the genes and enzymes involved is restricted, the mechanistic pathway of break down is well understood.

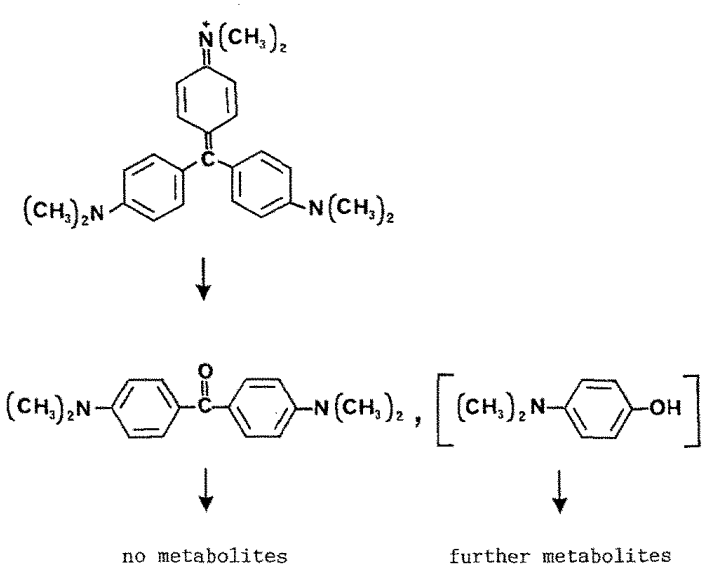

Fig. 1.1: Degradative pathway of crystal violet by *Nocardia corallina* (Yatome *et al.*, 1993).

Yatome and colleagues (1993) were the first to elucidate the degradation of crystal violet by *Nocardia* spp. Gas chromatography mass spectrometry allowed them to identify the main product as Michler's ketone which accumulated in the media and was not able to be metabolized further.

Utilizing high performance liquid chromatography Chen and coworkers (2007) were able to elucidate the biodegradation pathway of crystal violet by *Pseudomonas putida*. The identification of nine degradative products allowed them to conclude that the dye is broken down by means of demethylation, yielding mono-, di-, tri-, tetra-, penta- and hexa-demethylated end products. Notably, this pathway differs to that in *N. corallina* as illustrated in Fig. 1.2.

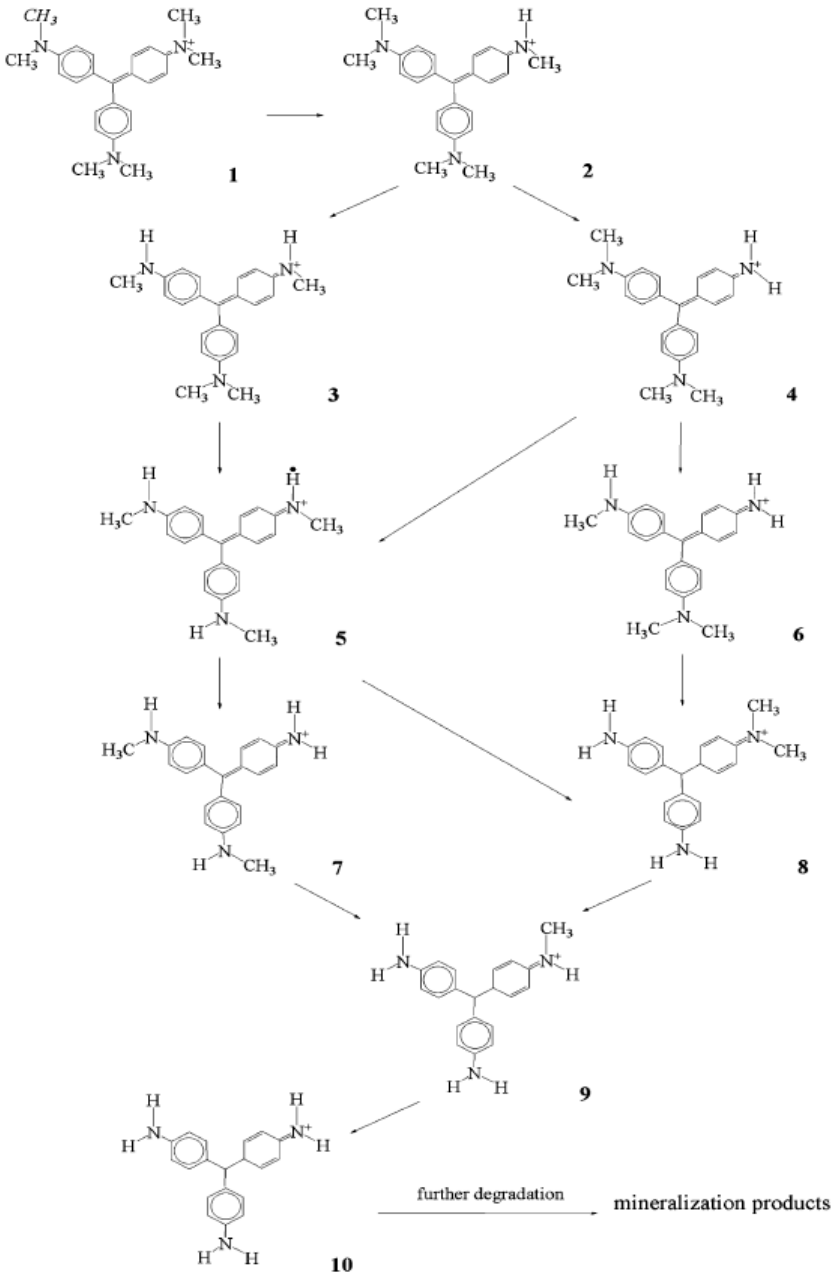

Fig. 1.2: Proposed crystal violet demethylation pathway in *P. putida*. 1 - N,N,N′,N′,N″,N″-hexamethyl pararosaniline, 2 - N,N-dimethyl-N′,N′-dimethyl-N″-methyl pararosaniline, 3 - N,N-dimethyl-N′-methyl-N″-methyl pararosaniline, 4 - N,N-dimethyl-N′N′-dimethyl pararosanilin, 5 - N-methyl-N′-methyl-N″-methyl pararosaniline, 6 - N,N-dimethyl-N′-methylpararosaniline, 7 - N-methyl-N′-methylpararosaniline, 8 - N,N-dimethylpararosaniline, 9 - N-methylpararosaniline, 10 – pararosaniline (Chen *et al.*, 2007)

In *Shewanella* spp. Chen and colleagues (2008) proposed a different degradative mechanism. They established that crystal violet was transformed into Michler's ketone and N,N-dimethylaminophenol. Unlike in the previous bacteria discussed, they identified several intermediates, namely; [N,N-dimethylaminophenyl] [N-methylaminophenyl] benzophenone, N,N-dimethylaminophenol, and N,N-dimethylaminobenzaldehyde [Fig. 1.3]. Again the main product formed was Michler's ketone which through reduction and demethylation split into derivative compounds.

Jang and colleages (2005) have discovered the only reductase definitively linked to triphenylmethane biodegradation; these researchers conducted in depth studies of the enzyme structure. Using site-directed mutagenesis the residues within the dinucleotide binding site were mutagenized, proving the region is essential for substrate interaction (Jang *et al.*, 2007). They went on to predict the mechanism of action of the reductase on malachite green through crystallization experiments linked to structure-function analysis studies. These researchers were able to work out which amino acids and atoms are involved at each stage of the decolorization process [Fig. 1.4 (left)]. In an oversimplified explanation, the dye interacts with the reductase via. hydrophobic interactions of leucine and histidine amino acids, among others. Its docking into the 'hydrophobic pocket' is such that the carboxyl dye group is in close contact with the carboxyl group of the NADPH cofactor forcing a break in the hydride bond, thus converting the dye into colorless leucomalachite green [Fig. 1.4 (right)].

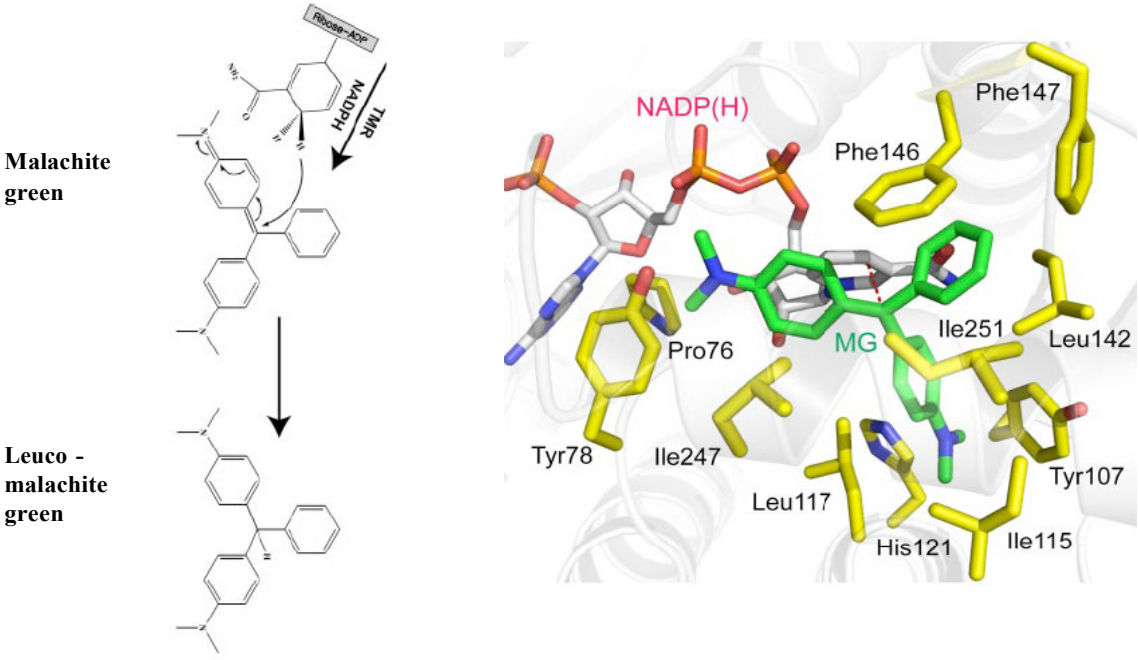

Fig. 1.3: Proposed decolorization mechanism of the triphenylmethane dye malachite green (left) and the substrate malachite green (represented in green) docked into the substrate binding site of the reductase-$NADP^+$ complex structure (NADP(H) represented in orange and red) (Kim *et al.*, 2008).

1.3. Decolorization and degradation of triphenylmethane dyes by fungi

While laboratory based studies have shown that white rot fungi are capable of triphenylmethane dye degradation, their applicability in the treatment of wastewaters is limited due to their low resilience to harsh environmental conditions (Chen *et al.*, 2008). The fungus *Cyathus bulleri* was capable of crystal violet decolorization; interesting features of this fungus included its biodegradation of the dye in the absence of a mediator and the lack of influence of nitrogen or pH on activity (Vasdev *et al.*, 1995). They found the laccase was able to work in a pH range of 2-10 and unlike other fungi did not work only under nitrogen limited conditions.

1.4 Genes and enzymes responsible for triphenylmethane decolorization

While a few triphenylmethane decolorizing bacteria have been isolated very little characterization work has been conducted on the enzymes involved. In the first study attempting to identify decolorizing genes, Kim and workers (2005) utilizing transposon mutagenesis isolated twenty-six crystal violet decolorizing defective mutants of *Citrobacter* species. The respective genes were identified and classified as potential decolorizing genes. Five of these were putative oxidoreductases, six were involved in the transport system and two were transcriptional regulators believed to control the expression of the pathway. A further eight clones were linked to hypothetical proteins. However, no definite gene was identified.

Jang and colleagues (2005) were the first to report on the cloning of a triphenylmethane reductase gene *(TMR)* associated with *Citrobacter* spp. KCTC 18061P (accession no. AY756172). Unlike many azoreductases, this enzyme showed maximal activity at an alkaline pH of 9.0 and relatively high temperature of 60^{o}C. The sequence did not show similarity to proteins of known functions. Thus, they proposed that this enzyme is a novel class of the short-chain dehydrogenase reductase family.

Similarly, only one study documenting a gene responsible for triphenylmethane dye mineralization in a Gram positive species was recently conducted. The *fbiC* gene from *M. smegmatis,* which encodes a 7,8-didemethyl-8-hydroxy-5-deazariboflavin (FO) synthase involved in the biosynthesis of electron carrier coenzyme F_{420} was linked to this activity (Guerra-Lopez *et al.*, 2007).

Table 1.1: Bacteria implicated in triphenylmethane dye decolorization

Strain	**Type of reductase/ oxidase**	**O_2 sensitive (S)/ O_2 in-sensitive (I)**	**Dye/s degraded**	**Enzyme class-ification**	**Reference**
Aeromonas hydrophila	Oxygenase	I	Crystal violet, basic fuchsin, brilliant green, malachite green, amaranth, great red GR, reactive red KE-3B, reactive brilliant blue K-GR	NAD(P)H oxygenase	Suizhou et al. (2006)
***Kurthia* spp.**	-	I	Magenta, crystal violet, pararosaniline, brilliant green, malachite green, ethyl violet and textile effluent	-	Sani and Banerjee (1999)
Citrobacter spp. MY-5	-	I	Crystal violet, gentian violet, malachite green, brilliant green, basic fuchsin, methyl red	-	An et al. (2002) and Kim et al. (2005)

Strain	**Type of reductase/ oxidase**	**O_2 sensitive (S)/ O_2 in-sensitive (I)**	**Dye/s degraded**	**Enzyme class-ification**	**Reference**
Citrobacter spp. KCTC 18061P	Reductase (TMR)	I	Crystal violet, malachite green, basic Fuchsin	NAD(P)H reductase	Jang et al. (2005)
Pseudomonas putida	-	I	Crystal violet	-	Chen et al. (2007)
Shewanella spp. NTOU1	-	S	Crystal violet	-	Chen et al. (2008)
***Mycobacterium smegmatis* mc^2**	Synthase (FO)	I	Malachite green, methyl violet	-	Guerra-Lopez et al. (2007)

Gram positive bacteria represented in bold print

1.6 Objectives

i. Establishment of maximum concentration of dye decolorizable by *A. orientalis* SY6

ii. Assessment of decolorization of the triphenylmethane dye by strain SY6 in the presence of carbon and nitrogen sources

iii. Assessment of combined dyes decolorized by strain SY6

iv. Establishment of the detoxification of crystal violet by strain SY6

v. Creation of genomic library and screening of clones on selective media

vi. Identification of crystal violet decolorizing DNA

vii. Cloning and sequencing of crystal violet decolorizing genes

viii. Characterization of optimal pH, temperature and carbon source utilization of clones

ix. Monitoring of the range of dyes decolorized when the identified genes are expressed in *S. lividans, R. erythropolis* and *M. smegmatis*

2. Materials and methods

Please refer to chapter I pages 27-46.

3. Results

3.1 Maximum concentration of dye decolorizable by SY6

Crystal violet was added to minimal media and monitored for color removal. Strain SY6 demonstrated an impressively potent decolorizing ability. Clearing of the dye was visible just five minutes after incubation. Visual observation of the decolorization over a period of time showed that the isolate struggled to mineralize the dye at a concentration of 30 µg/ml [Fig. 3.1].

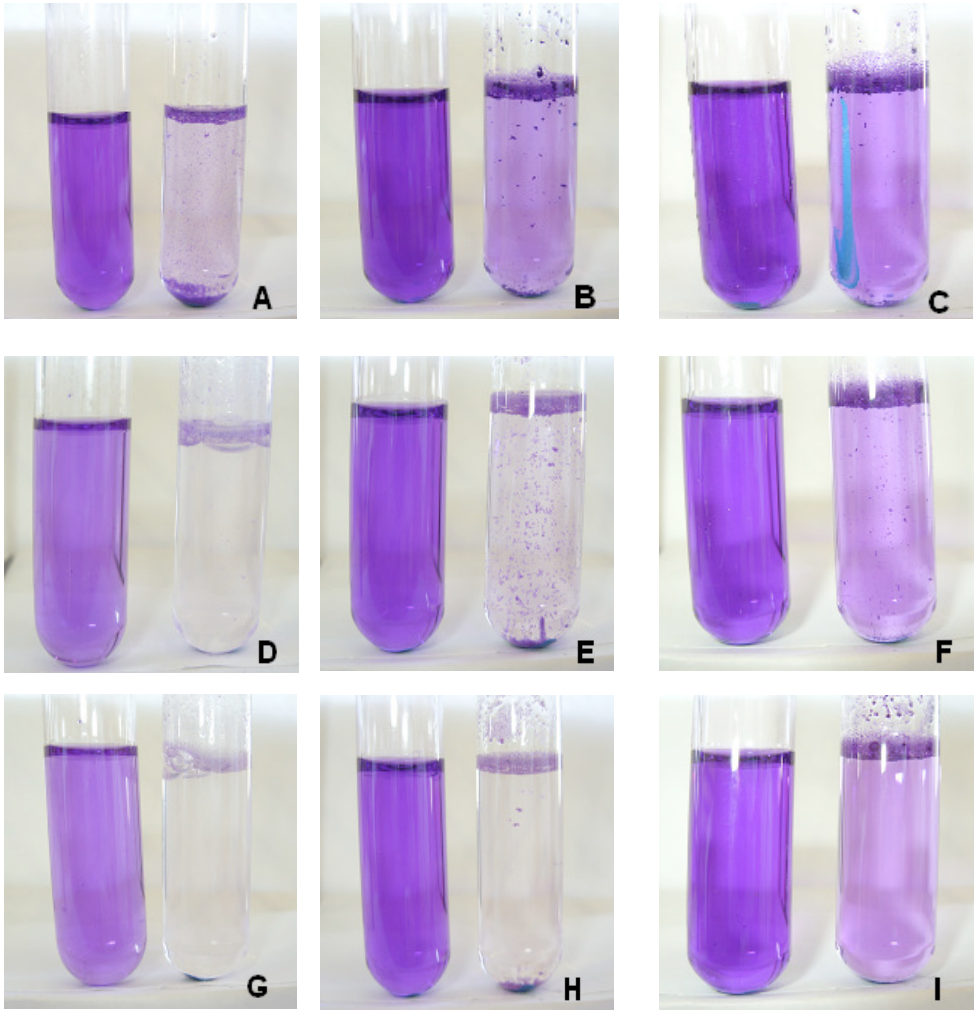

Fig. 3.1: Mineralization of crystal violet by strain SY6 at varying dye concentrations over 20 minute increments. (In each picture the tube on the left is the dye only control and the tube on the right is inoculated with strain SY6). 10 µg/ ml crystal violet at (A)

20 min., (D) 40 min. and (G) 60 min. 20 µg/ ml crystal violet at (B) 20 min., (E) 40 min. and (H) 60 min. 30 µg/ ml crystal violet at (C) 20 min. (F) 40 min. and (I) 60 min.

Acclimatization of SY6 showed that the strain could improve its decolorization capacity up to 30 µg/ml of the dye, however even prolonged incubation showed no ability to decolorize beyond this concentration.

These results were monitored on thin layer chromatography in 5, 10, 20, 30 and 60 min. intervals [Fig. 3.2]. At 5 min. a dramatic decrease in crystal violet intensity was already observed; its monitoring on thin layer chromatography against untreated crystal violet confirmed the extreme rate of degradation. Four main bands were observed from 5-20 min. The lowest band was no longer visible at 30 min. and both lower bands were not detected at 60 min.

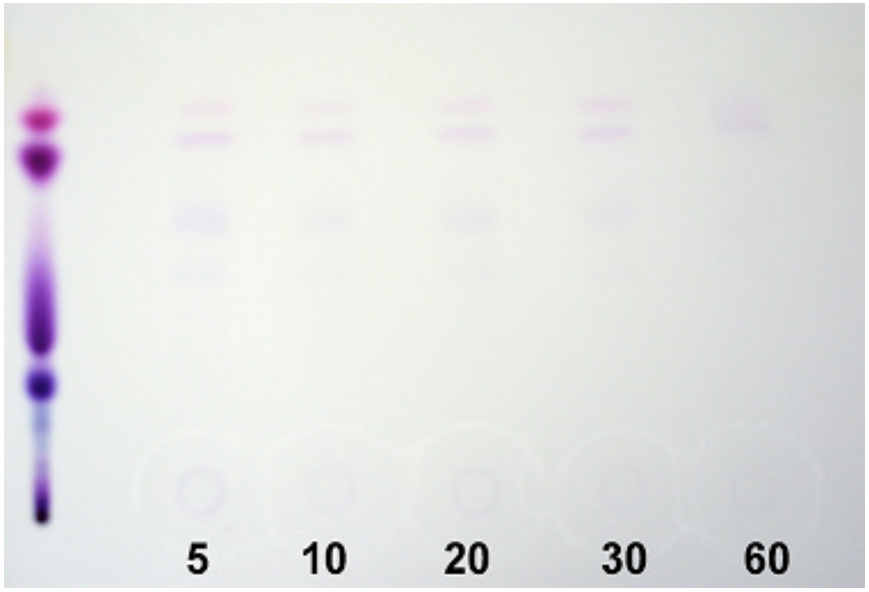

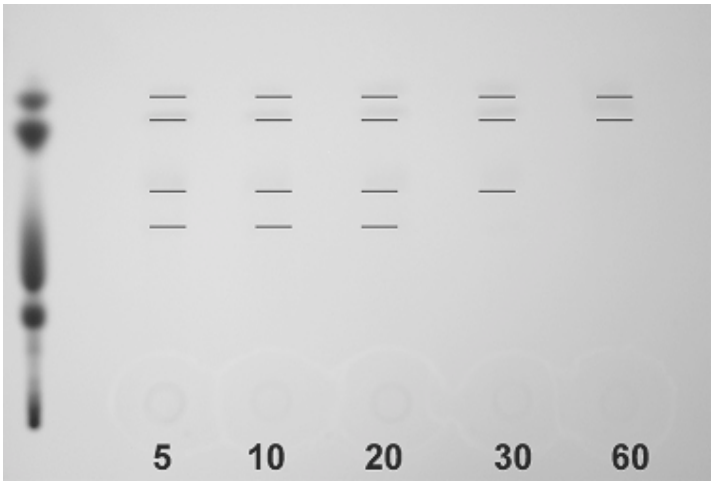

Fig. 3.2: Thin layer chromatography (TLC) of decolorized crystal violet (10 µg/ ml) supernatant harvested at 5 min., 10 min., 20 min., 30 min. and 60 min. Untreated crystal violet is on the extreme left. For clarity, bands visualized on TLC were underlined (above).

The possibility of extracellular enzymatic reduction was eliminated by adding dye and cofactor to the cell free extracellular supernatant and analyzing the decolorization percentage, an insignificant decrease was indicative of cellular related mineralization.

3.2 Decolorization of crystal violet by strain SY6 in the presence of nitrogen and carbon sources

Three carbon sources, namely glucose, starch and glycerol were tested, in addition to the nitrogen sources yeast extract and peptone. Yeast extract caused a slight reduction in decolorization (~ 3 %), while the other supplements were all equally effective with efficiencies greater than 69 % [Fig. 3.3].

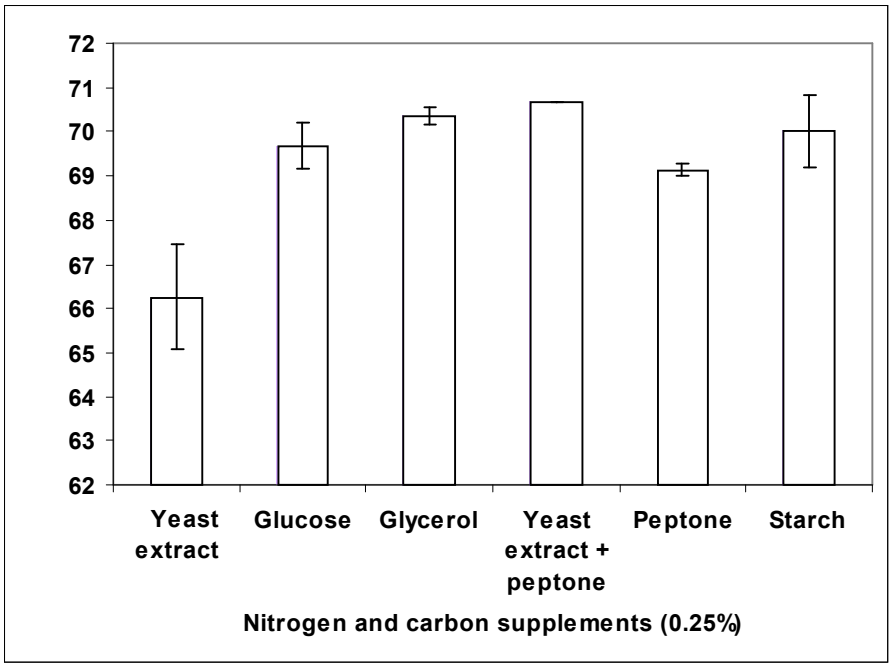

Fig. 3.3: Decolorization of crystal violet (10 µg/ml) in the presence of a range of carbon and nitrogen sources. Non-supplemented control showed 30 % decolorization (not shown).

3.3 Combined dyes decolorized by *A. orientalis* SY6

It was found that the range of decolorization by strain SY6 extended to several triphenylmethane dyes other than crystal violet such as brilliant green, basic fuchsin and malachite green. Since the isolate was capable of degrading these dyes individually, it was tested whether a combination of these dyes would also be easily decolorized [Fig. 3.4]. The isolate displayed a remarkable ability to decolorize the combined triphenylmethane dyes just as effectively as the decolorization of a single triphenylmethane dye. The addition of sulfonated azo dyes, amido black and janus green did not effect decolorization.

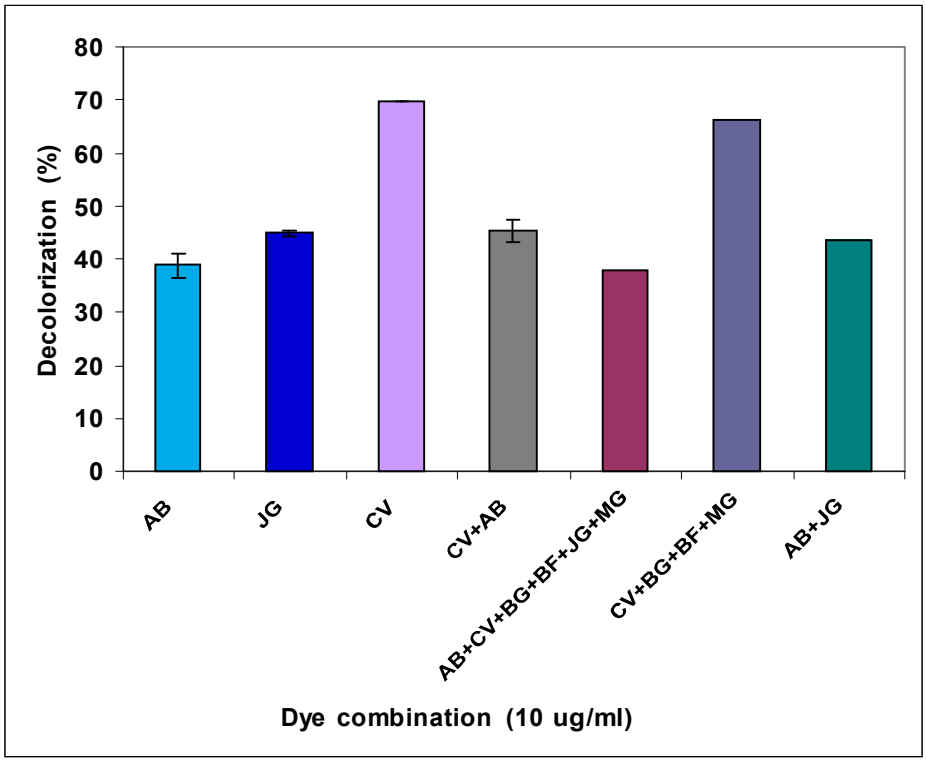

Fig. 3.4: Monitoring of the decolorization of multiple dyes (each dye was 10 µg/ml)

The combined triphenylmethane dyes were all easily decolorized, reflecting 66 % decolorization [Fig. 3.5].

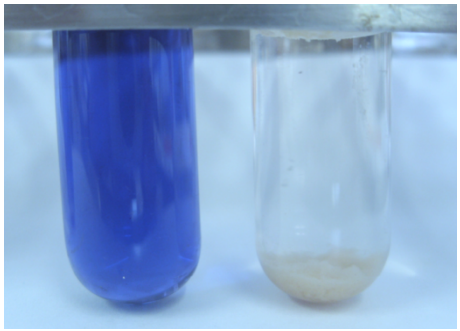

Fig. 3.5: Decolorization of combined triphenylmethane dyes (crystal violet + brilliant green + basic fuchsin + malachite green) by strain SY6. Combined dyes (left) and decolorization by *A. orientalis* SY6 (right).

3.4 Comparison of strain SY6 degradation to *R. erythropolis* and *M. smegmatis* strains

3.4.1 Thin layer chromatography

The rapid degradation of crystal violet by *Mycobacterium* spp. and *Rhodococcus* spp. closely matched that of strain SY6. The decolorized supernatant of both strains was run on TLC and the Rf values calculated for the observed bands [Fig. 3.6]. Similar banding patterns and correspondingly Rf values were obtained for all three strains [Table 3.1].

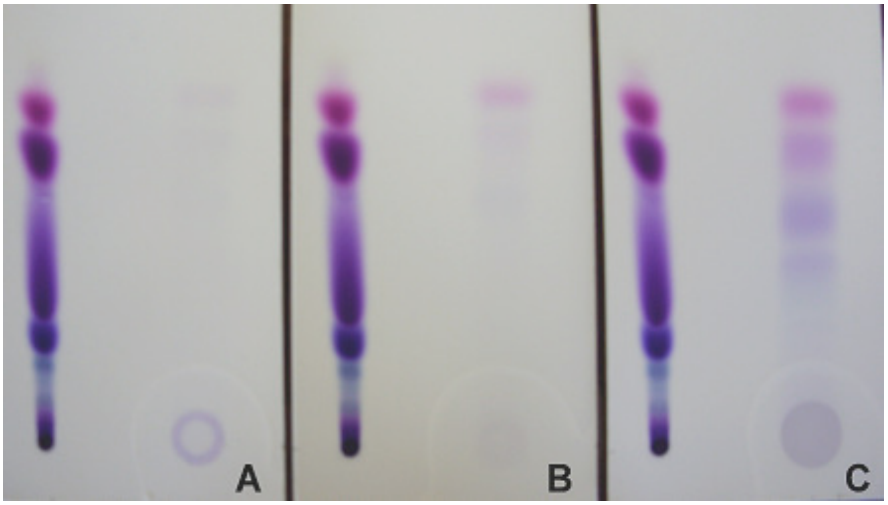

Fig. 3.6: Thin layer chromatography of crystal violet (10 µg/ml) decolorized supernatant harvested after 60 min. from (A) *R. erythropolis* SQ1, (B) *M. smegmatis* mc^2 155 and (C) *P. syringae* (non decolorizing control)

Table 3.1: Rf values calculated from TLC

Strain	**Rf values**
R. erythropolis SQ1	0.78 ; 0.66 ; 0.56
M. smegmatis mc^2 155	0.80 ; 0.67 ; 0.57
A. orientalis SY6	0.79 ; 0.68 ; 0.57

3.5 Detoxification of crystal violet by *A. orientalis* SY6

Strain SY6 decolorized the dye into a colorless derivative, however the toxicity of the by-products generated needed to be determined. This was done by monitoring the growth of an indicator strain, *E. coli* in the presence of the decolorized media. An inhibition of the strain was taken as a sign of toxicity. The colony forming units (CFU) per ml of the decolorized supernatant closely matched that of the media supplemented with a carbon source and was two times higher than non-supplemented media. This reflects no inhibition of the strain and thus complete detoxification.

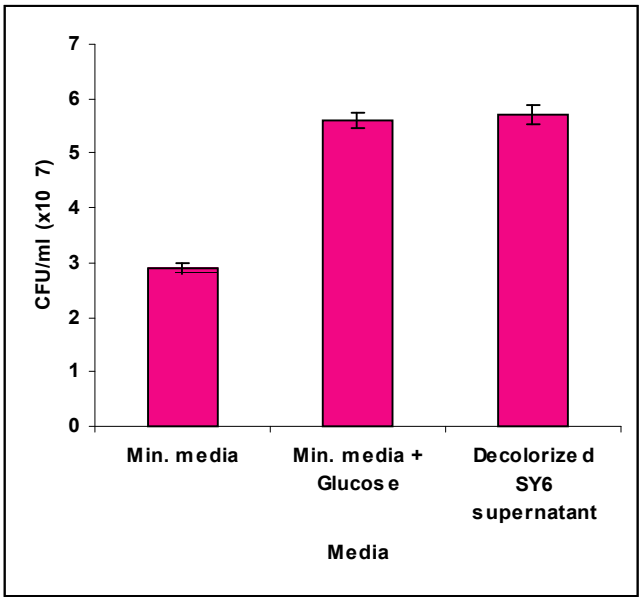

Fig. 3.7: CFU/ ml of indicator strain in minimal media, minimal media supplemented with glucose (0.25%) and decolorized crystal violet (10 µg/ml) supernatant of *A. orientalis* SY6

3.6 Creation of genomic library of strain SY6

See section 3.5 page 62 for details of library construction.

A positive selection library was created, meaning the transformable host *S. lividans* TK23 did not have the ability to grow on crystal violet at a low cell inoculum. Hence, any clones that were found to survive on the dye plates were screened. Following the

patching of approximately 5000 clones, ten colonies displaying a resistance to the triphenylmethane dye were isolated [Fig. 3.8].

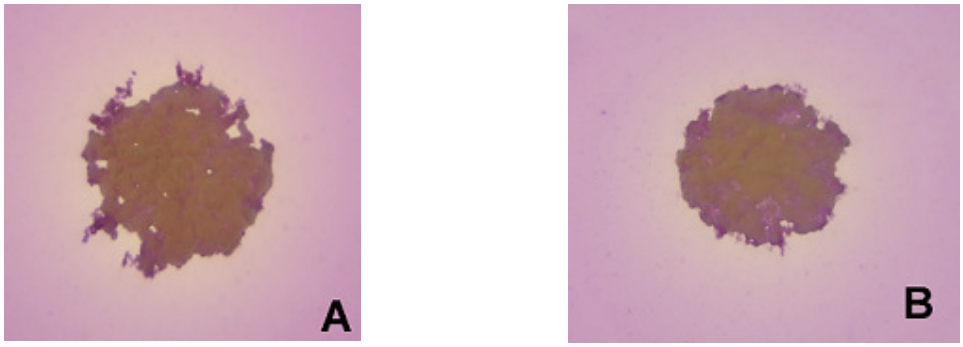

Fig. 3.8: Two of the *S. lividans* clones which survived on the crystal violet plates. A slight zone of clearing can be detected around the periphery of the colonies

3.7 Screening and isolation of clones capable of crystal violet decolorization

A plasmid DNA extraction was conducted on all ten clones, of which three carried inserts. These clones were named SlivCV2, SlivCV4 and SlivCV6 and the DNA carried referred to as pCV2, pCV4 and pCV6 respectively. Restriction analysis revealed that there was no commonality among the inserts. *S. lividans* clones CV2, CV4 and CV6 carried ~ 600 bp, > 2000 bp and > 2000 bp gene fragments respectively [Fig. 3.9].

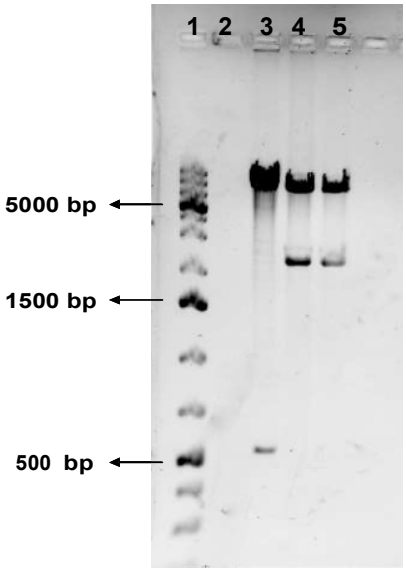

Fig. 3.9: Agarose gel showing the release of inserts of pCV DNA, lanes **1**: DNA ladder, **3**: pCV2 *Bgl*II, **4**: pCV4 *Bgl*II and **5**: pCV6 *Bgl*II

3.8 Characterization of optimal pH, temperature and carbon source utilization of clones SlivCV2, SlivCV4 and SlivCV6

3.8.1 *Liquid assay determining optimal temperature of SlivCV2, SlivCV4 and SlivCV6*

The optimal temperature profiles of the individual clones were analyzed. Clone SlivCV2 highest decolorization rate was 66 % at 20°C. This clone exhibited an atypical contour line, unlike the bell shaped curve commonly observed. Clones SlivCV4 and SlivCV6 showed optimal activity at 37°C with decolorization percentages of 67 % and 60 % respectively [Fig. 3.10].

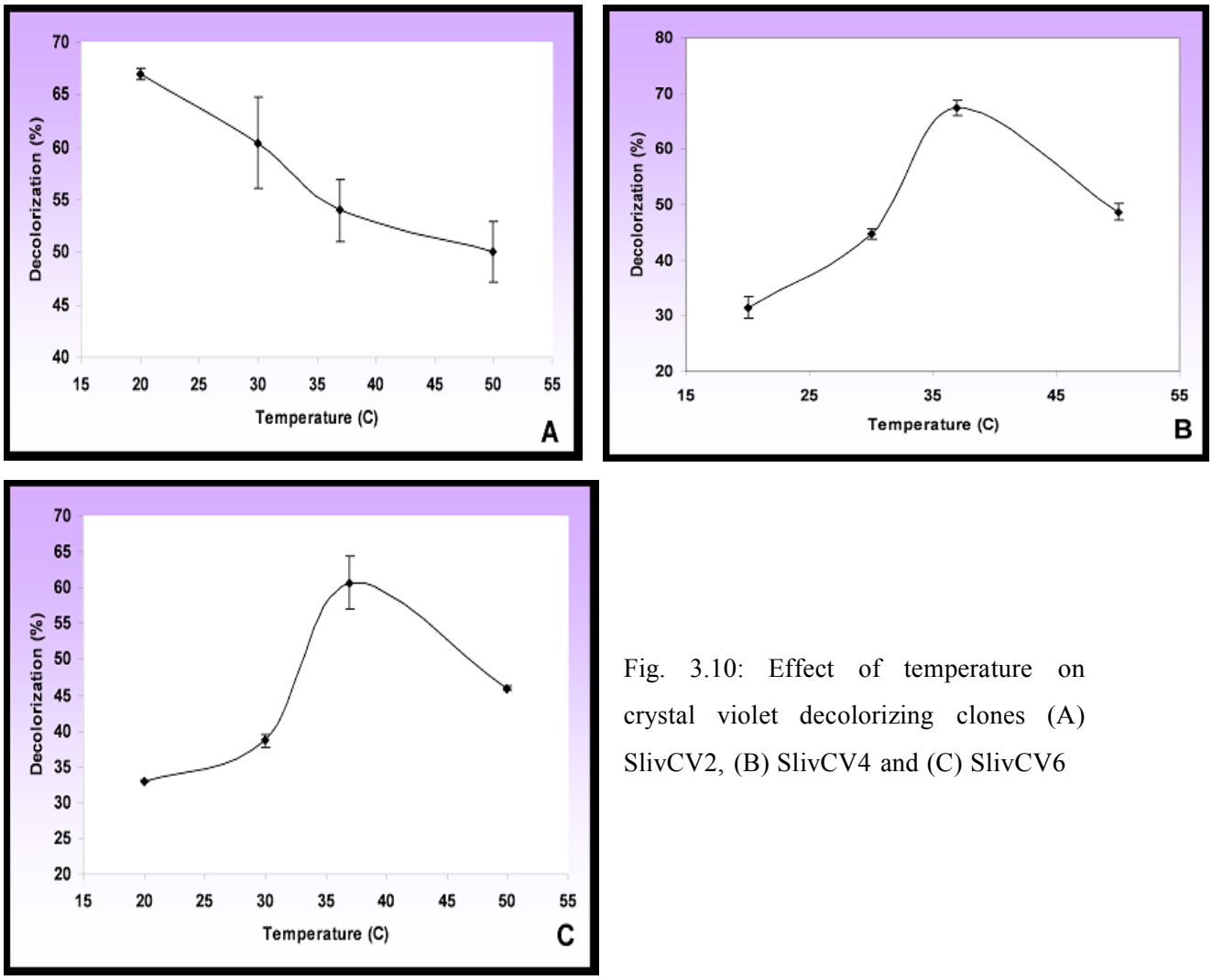

Fig. 3.10: Effect of temperature on crystal violet decolorizing clones (A) SlivCV2, (B) SlivCV4 and (C) SlivCV6

3.8.2 *Liquid assay determining optimal pH of SlivCV2, SlivCV4 and Sliv CV6*

The activity of the clones at a pH range of 6-8 was monitored [Fig. 3.11]. Clones SlivCV2 and SlivCV4 showed optimal activity at pH 7.5 and moderate activity at pH 8.0. SlivCV4 showed highest activity at pH 7.0 which decreased rapidly with either a 0.5 increase or decrease in the pH.

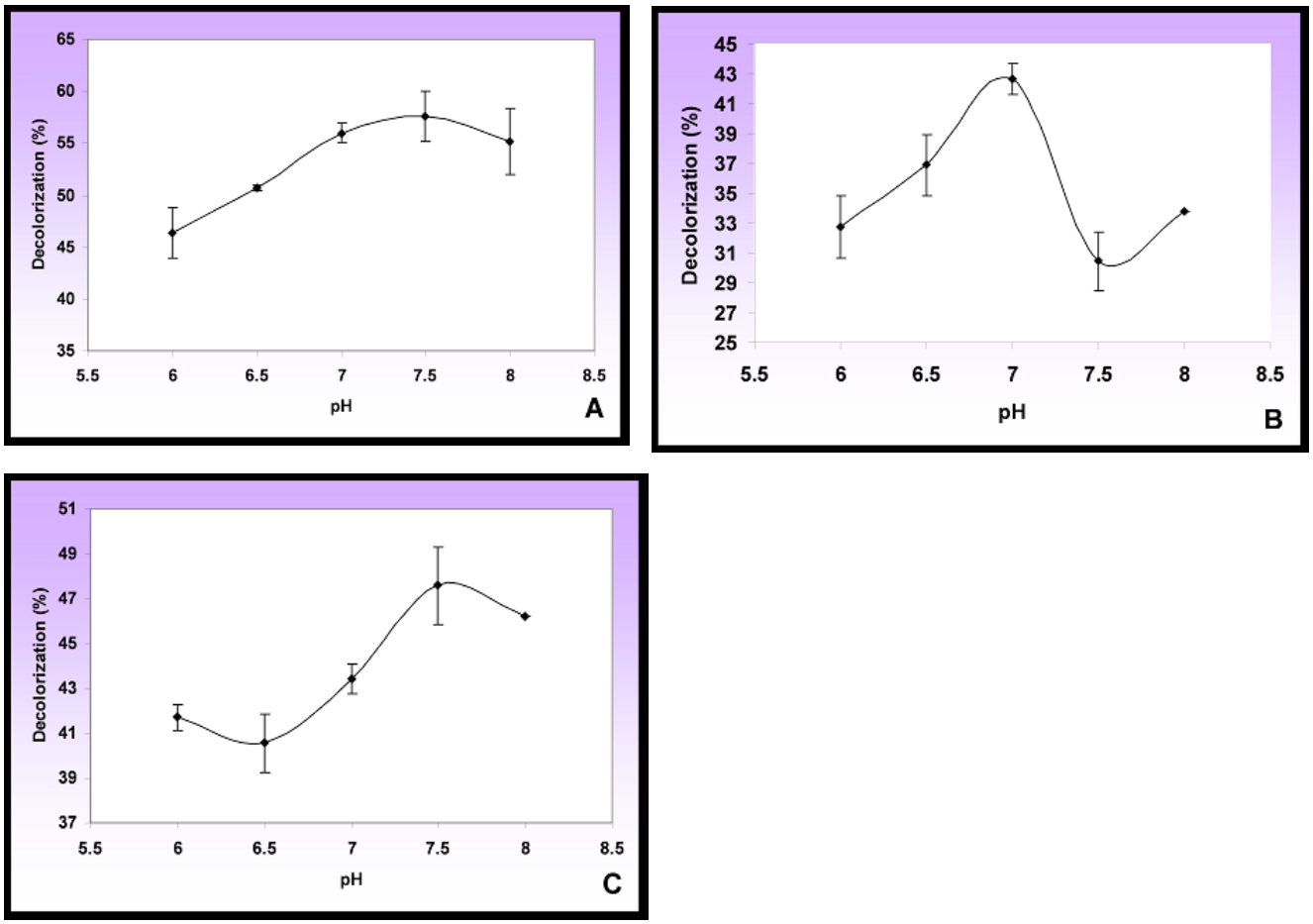

Fig. 3.11: Effect of pH on crystal violet decolorizing clones (A) SlivCV2, (B) SlivCV4 and (C) SlivCV6

3.8.3 *Liquid assay determining carbon source utilization of SlivCV2, SlivCV4 and SlivCV6*

Carbon sources were added to SlivCV clones and the decolorization monitored. The presence of fructose reduced decolorization in all cases by between 6 and 14 %. Overall, succinate seemed to be the most favorable substrate followed by inositol [Fig. 3.12].

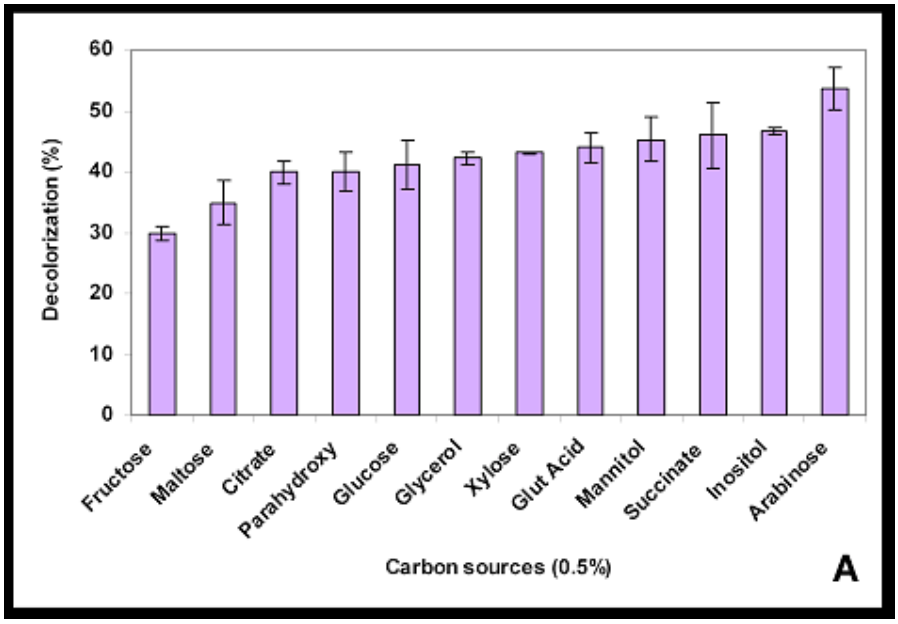

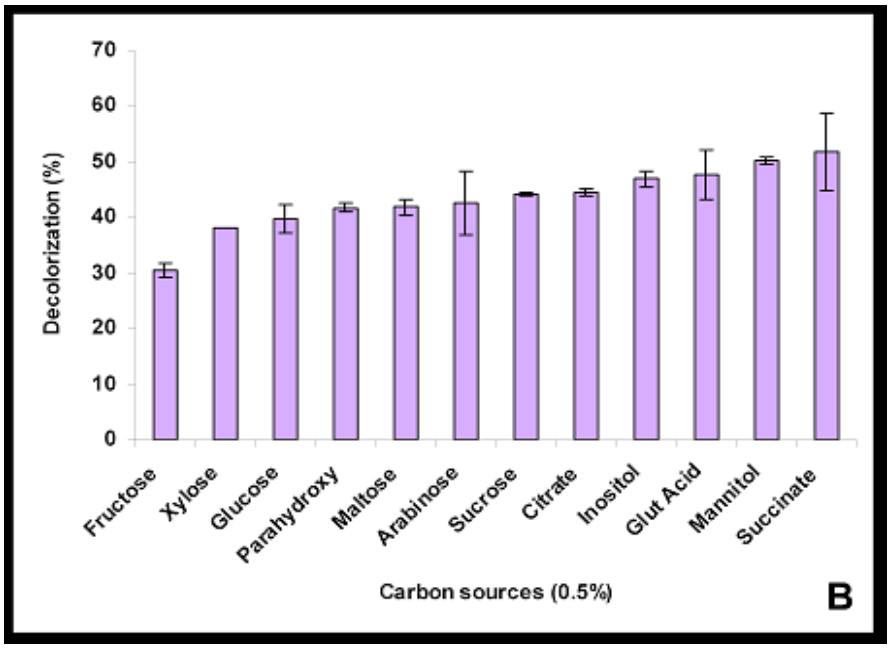

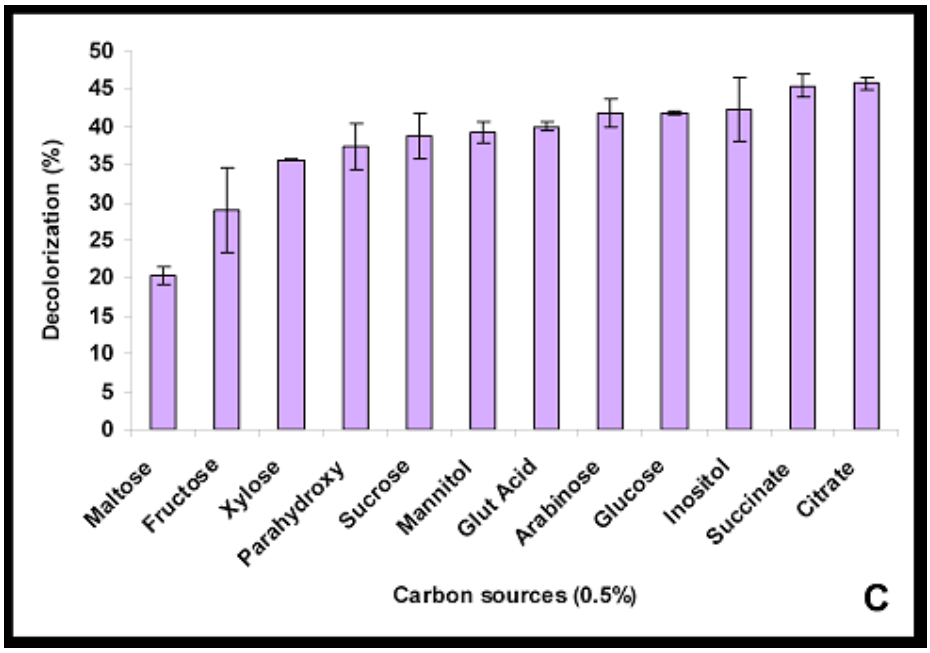

Fig. 3.12: Effect of carbon sources on crystal violet decolorizing clones (A) SlivCV2, (B) SlivCV4 and (C) SlivCV6

3.9 Decolorization of combined SlivCV clones

The individual incubation of CV clones in crystal violet showed evidence of partial decolorization [Fig. 3.13]. Noticeably, the dye was removed from the media, however it remained attached to the cell wall of the bacteria.

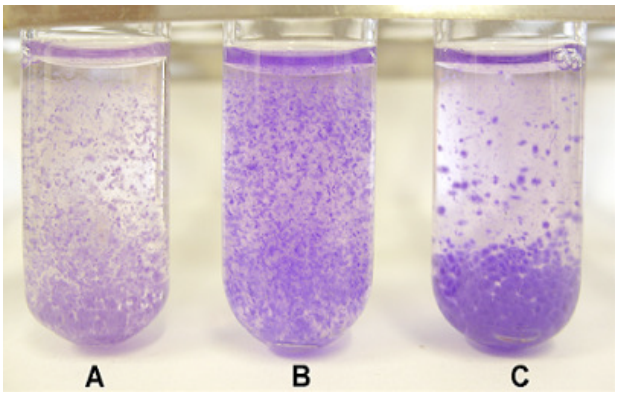

Fig. 3.13: Incubation of crystal violet (10 µg/ml) with clones (A) SlivCV2, (B) SlivCV4 and (C) SlivCV6

Unexpectedly, it was the combination of all three clones that led to the mineralization of the triphenylmethane dye [Fig. 3.14].

Fig. 3.14: Reduction of crystal violet (10 µg/ml) by combined CV clones at 37^{o}C at pH 7.0

Two clones were combined in various combinations in order to assess if the eliminated clone was required for mineralization. From the results below it was evident that all three clones were required. The elimination of any of the clones resulted in partial decolorization.

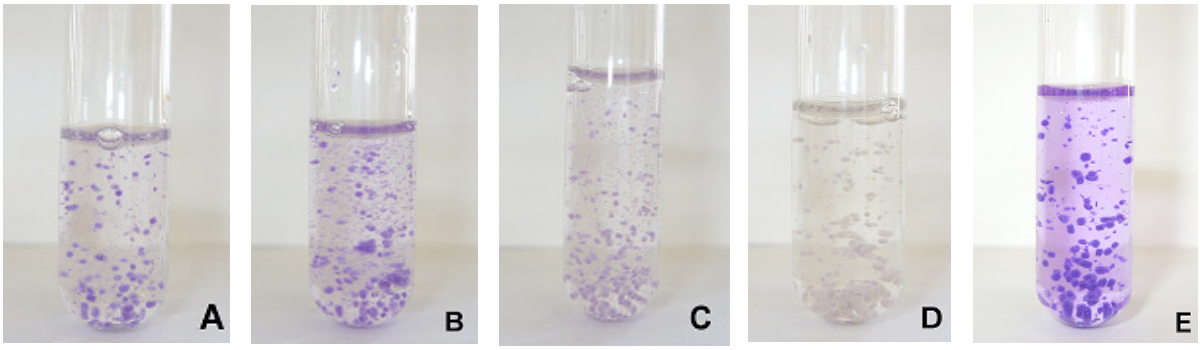

Fig. 3.15: Clones SlivCV4 + SlivCV6 (A), SlivCV2+SlivCV6 (B), SlivCV2+SlivCV4 (C), SlivCV2+SlivCV4+SlivCV6 (D), *S. lividans* TK23 (E), added to crystal violet (10 µg/ml) in minimal media and incubated for 3 days.

3.9.1 *Liquid assay determining optimal temperature and pH profile of combined CV clones*

The optimal parameters for the combined clones were determined. An optimal temperature of 35°C and pH of 6.8 was discerned.

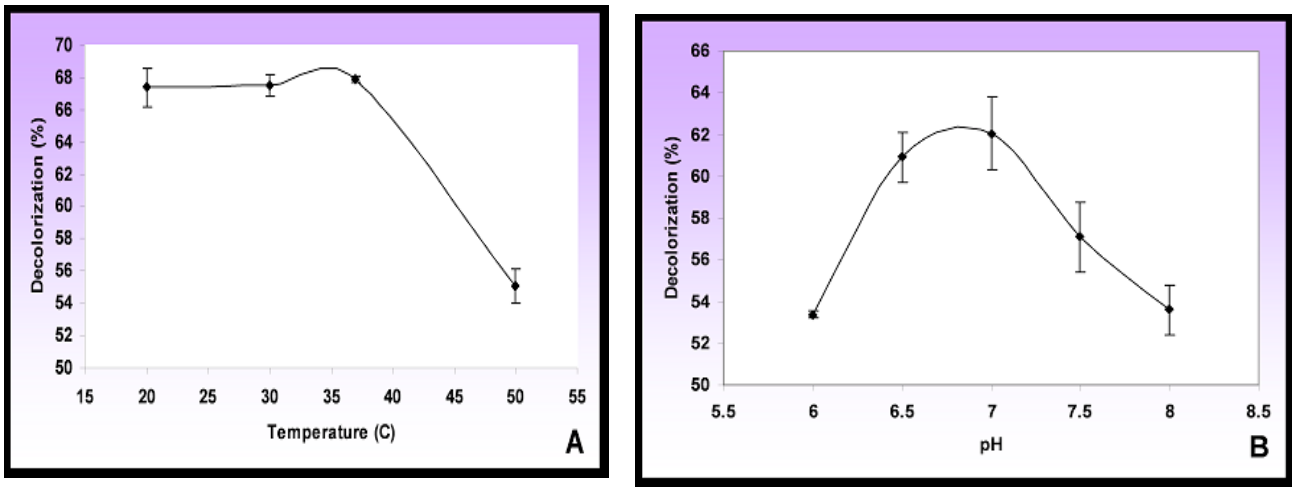

Fig. 3.16: The effect of (A) temperature and (B) pH on the decolorization percentage of all three SlivCV combined clones

3.10 Sequence identification of CV clones

The inserts were ligated into an appropriate vector and sent for sequencing. The resulting sequence data was compared against the NCBI PubMed database, revealing the following results:

Table 3.2: Closest protein matches to isolated sequences

Clone	Description	Species	Maximum identity (%)	E value
2	3-deoxy-7-phosphoheptulonate synthase (DAHP synthase)	*Amycolatopsis mediterranei* U32	95	1e-100
4	Methylmalonyl-CoA mutase and N5,N10-methylene-tetrahydromethanopterin reductase-related protein	*Amycolatopsis mediterranei* U32	85 ; 82	2e-86 ; 2e-56
6	LGFP repeat-containing protein	*Amycolatopsis mediterranei* U32	61	7e-54

Insert CV2 showed high sequence identity to a DAHP synthase. Insert CV4 carried two genes namely a methylmalonyl-CoA mutase and reductase related protein. Interestingly, the reductase related protein sequence was matched to just one protein in the entire database. Five LGFP repeats in insert CV6 occured at the C terminus end of the protein, at the N-terminal end was a glucose/sorbosone dehydrogenase and a polycystic kidney disease I (PKD) domain.

3.11 Determination of enzyme functionality

3.11.1 *Tertiary structure of encoded enzymes*

From the above results it was difficult to infer functions from the proposed enzymes. Thus these enzymes were analyzed on a tertiary level. The protein sequence was converted to a three dimensional structure and compared to 3D structure homologs available in the database [Table 3.3].

Table 3.3: Related tertiary structures matching identified proteins

Clone	**Protein**	**Related tertiary structure and organism**	**Related function**
2	DAHP synthase	DAHP synthase; *Mycobacterium tuberculosis*	Transferase
4	Methylmalonyl-CoA mutase	Methylmalonyl-CoA mutase; *Propionibacterium freudenreichii*	Isomerase
4	N5,N10-methylene-tetrahydromethanopterin reductase-related protein	1,6 Monooxygenase; *Pseudomonas putida*	Oxidoreductase
6	LGFP repeat-containing protein	No structure available	No structure available
6	Polycystic kidney disease I (PKD) domain	Collagenase; *Clostridium Histolyticum*	Hydrolase
6	Glucose/sorbosone dehydrogenase	Pqq-dependent sugar dehydrogenase; *Pyrobaculum aerophilum*	Oxidoreductase

The only relevant matches which provided information as to possible functions were the PKD I domain, reductase related protein and dehydrogenase which were linked to a hydrolytic and oxidoreductive activities respectively.

3.11.2 *Alignment of tertiary structures*

A 3D alignment of the query sequence with the most closely related structure is shown below [Fig. 3.17]. In general just a moderate level of structural similarity was found. This was not unexpected since the homologous structures available in the database are from phylogenetically distantly related bacteria. However, it did serve to show that structurally these proteins are similar and thus can be associated with the proposed functions.

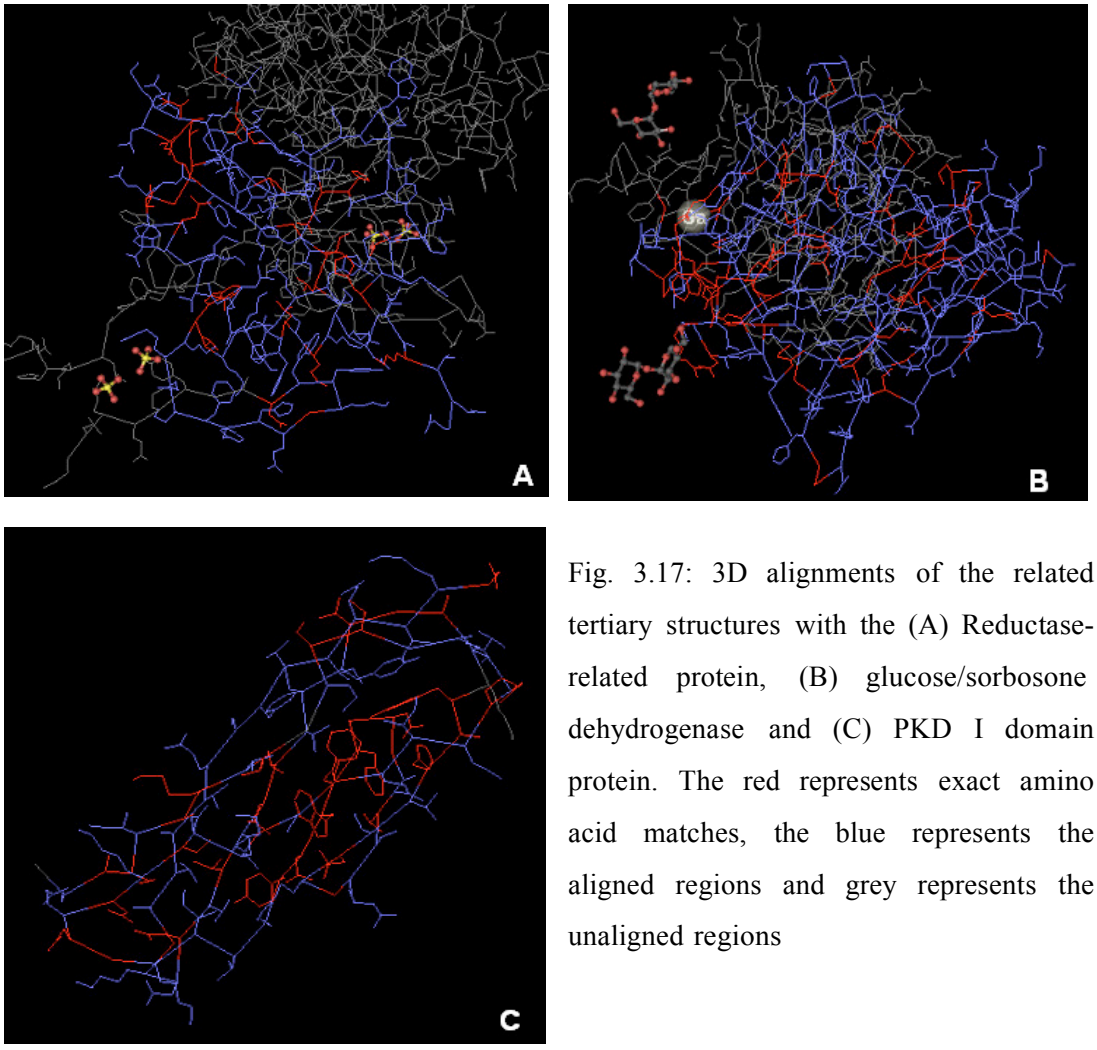

Fig. 3.17: 3D alignments of the related tertiary structures with the (A) Reductase-related protein, (B) glucose/sorbosone dehydrogenase and (C) PKD I domain protein. The red represents exact amino acid matches, the blue represents the aligned regions and grey represents the unaligned regions

3.12 Range of dyes decolorized by combined SlivCV clones

The decolorization activity of the clones was determined in the presence of other dyes. Other than crystal violet the clones were able to decolorize three sulfonated azo dyes, namely amaranth, ponceau S and biebrich scarlet [Table 3.4]. Although congo red and eriochrome T were removed from the media they remained tightly bound to the cell wall of the strains.

Table 3.4: Dyes decolorized by combined SlivCV clones

Dyes	***S. lividans* TK23**	**SlivCV2 + SlivCV4 + SlivCV6**
Brilliant green	+	+
Tartrazine	-	-
Basic fuchsin	-	-
Crystal violet	-	+
Amido black	+	+
Orange II	-	-
Janus green	+	+
Malachite green	+	+
Ponceau	-	+
Biebrich scarlet	-	+
Indigo	-	-
Bismarck brown	-	-
Congo red	-	- *
Eriochrome T	-	- *
Amaranth	-	+
Fast green	-	-

* - dye attached to cell wall

3.13 Range of dyes decolorized by combined CV DNA transformed into *R. erythropolis* SQ1

In the former experiment, discovery of the clones to additionally decolorize azo dyes led to the inquiry of what the result of the expression of these genes in other host species would be. Consequently, the pCV2, pCV4 and pCV6 recombinant vectors were transformed into a *Rhodococcus* spp. host and referred to as SQ1CV2, SQ1CV4 and SQ1CV6 respectively. The host strain into which the DNA was transformed possessed the ability to decolorize four of the five triphenylmethane dyes, as did the clones, hence it was not possible to evaluate whether any contribution was made by the expressed genes. Instead dyes which the original host could not decolorize were concentrated on.

Table 3.5: Dyes decolorized by combined SQ1CV clones

Dyes	***R. erythropolis* SQ1**	**SQ1CV2 + SQ1CV4 + SQ1CV6**
Brilliant green	+	+
Tartrazine	-	-
Basic fuchsin	+	+
Crystal violet	+	+
Amido black	-	+
Orange II	-	+
Janus green	+	+
Malachite green	+	+
Ponceau	-	-
Biebrich scarlet	-	+
Indigo	-	-
Bismarck brown	-	-
Congo red	-	- *
Eriochrome T	-	- *
Amaranth	-	-
Fast green	-	-
Crystal violet + brilliant green + malachite green + basic fuchsin + orange II + biebrich scarlet	-	+

* - dye attached to cell wall

The SQ1CV clones decolorized the sulfonated dyes amido black, orange II and biebrich scarlet [Table 3.5]. Notably, this was not similar to the pattern of decolorization when in the *S. lividans* host.

Below is a visual representation of some of the dyes decolorized by the SQ1CV combined clones. Impressively, the combination of six dyes led to complete biodegradation by the clones [Fig. 3.18].

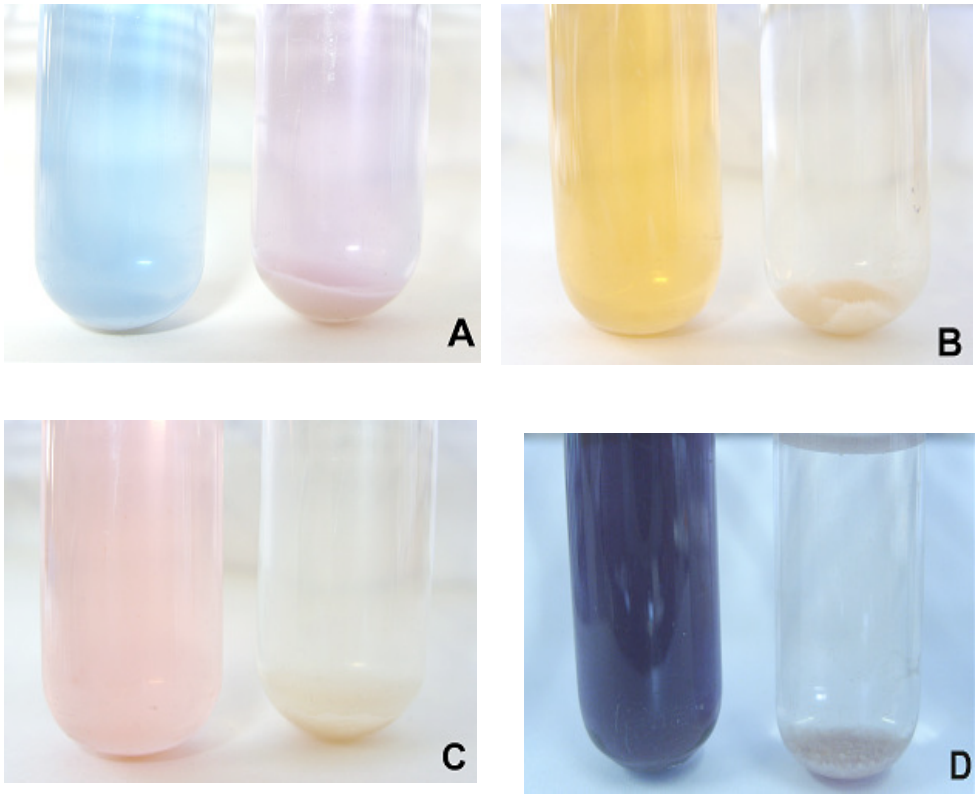

Fig 3.18: Decolorization of (A) amido black, (B) orange II, (C) biebrich scarlet and (D) combined dyes. On the left are inoculated controls with *R. erythropolis* SQ1 and on the right are the SQ1CV combined clones.

3.14 Range of dyes decolorized by combined CV DNA transformed into *M. smegmatis* mc^2 155

The variable expression of the genes in *Rhodococcus* spp. caused me to evaluate the expression of these genes in a *Mycobacterium* spp. host. The pCV2, pCV4 and pCV6 recombinant vectors were transformed into a *Mycobacterium* spp. host and referred to as 155CV2, 155CV4 and 155CV6 respectively. The combined 155CV clones were able to decolorize amido black, bismarck brown and janus green [Table 3.6]. Again this was slightly different to the expression of the genes in the latter and former strains.

Table 3.6: Dyes decolorized by 155CV clones

Dyes	***M. smegmatis* mc^2 155**	**155CV2 + 155CV4 + 155CV6**
Brilliant green	+	+
Tartrazine	-	-
Basic fuchsin	+	+
Crystal violet	+	+
Amido black	-	+
Orange II	-	-
Janus green	-	+
Malachite green	+	+
Ponceau	-	-
Biebrich scarlet	-	-
Indigo	-	-
Bismarck brown	-	+
Congo red	-	-*
Eriochrome T	-	-*
Amaranth	-	-
Fast green	-	-

* - dye attached to cell wall

4. Discussion

In the United States, three classes of dyes are classified as harmful, these include triphenylmethane, azo and anthraquinone dyes (Guerra-Lopez *et al.*, 2007). Having focused on the decolorization of azo dyes, focus was shifted to the triphenylmethane class of dyes.

Sixteen Streptomycete strains were screened for the ability to biodegrade crystal violet, however no strains capable of this were isolated. From the literature it was assumed that since just two Gram positive bacterial species were linked with the ability to degrade this dye that this was a rare trait. However, when screening known isolates from the laboratory Genetics culture collection it was surprising to find that this ability is in fact common among *Rhodococcus* spp.; *R. rhodochrous*, *R. erythropolis* and *R. opacus* all displayed a potent crystal violet mineralizing capacity. *Gordonia* spp. and *Mycobacterium* spp. were equally strong triphenylmethane degraders. From the environmental isolates tested just *A. orientalis* SY6 displayed this activity and again was chosen for supplementary genetic screening.

Strain SY6 was capable of rapid intracellular or membrane based biodegradation of crystal violet. A reduction in the decolorization of increasing crystal violet concentrations by this isolate could be attributed to increasing toxicity of the dye or a saturation of active sites on the enzyme. It has been reported that these dyes inhibit cell growth by interfering with nucleic acid synthesis thus decreasing protein synthesis (Azmi *et al.*, 1998). Additionally, the presence of sulfonic groups can inhibit bacteria by acting as detergents (Chen *et al.*, 2003).

In general, it was noticed that bacteria capable of degrading crystal violet were also able to mineralize other triphenylmethane dyes such as malachite green, brilliant green and basic fuchsin. Yet, our earlier study indicated that bacteria able to breakdown an azo dye from a particular class were not necessarily capable of degrading any other dyes within the same class. This allows for the speculation that either the enzymes responsible for triphenylmethane class degradation are more lenient in their substrate interactions or the dye structural differences are minor and

hence easier to accommodate. These results can be paralleled to those of the TMR (triphenylmethane reductase) enzyme isolated from *Citrobacter* species; malachite green was found to fit most favorably into the catalytic region of TMR, however the additional dimethylamino group in crystal violet produced a less favorable interaction while the positively charged amino groups in basic fuschin were problematic (Kim *et al.*, 2008). Additionally, research done on *P. pseudomallei* found that decolorization of triphenylmethane dyes was not linked to the molecular weight or permeability of the compound through the membrane (Azmi *et al.*, 1998).

The advantage of using a consortium for dealing with dye mixtures has been well established. Some studies have shown that bacteria which did not show an ability to breakdown certain dyes individually when combined with other strains were capable of dye decomposition (Moosvi *et al.*, 2007; Nigam *et al.*, 1996). These bacteria could cleave the molecule at different positions facilitating complete degradation or further catabolize the breakdown of dye products (Forgacs *et al.*, 2004). In general microbial consortiums have demonstrated an enhanced ability in anaerobic as opposed to aerobic treatment systems (Nigam *et al.*, 1996). Nevertheless, various strain combinations were tested in order to establish an 'optimal' aerobic consortium for a mixture of triphenylmethane dyes. *A. orientalis* SY6 was combined with either *G. rubripertincta*, *R. erythropolis* SQ1 or *M. smegmatis* and incubated in crystal violet media. Overall, all consortium combinations rapidly mineralized the triphenylmethane dye and no strain inhibition was detected from colony counts (data not shown).

Strain SY6 was able to decolorize amido black, janus green and several triphenylmethane dyes effectively. It was assessed whether this ability was retained when these dyes were combined. Results show that the combination of four triphenylmenthane dyes were efficiently decolorized to colorless derivatives. This suggests that the same enzyme/s might be involved in the reduction of all these dyes. The addition of the azo dyes, amido black and janus green did not affect the activity of the strain. Notably, the decolorization percentages represented on the graph [Fig. 3.4] give the false impression that the addition of the azo dyes reduced the overall decolorization. However, amido black and janus green are not reduced to colorless derivatives. Amido black is decolorized to a violet colored compound and janus green

is reduced to diethylsafranine which remains pink in suspension (Lazarow and Cooperstein, 1953). Since the decolorization percentage corresponds to that of the individually reduced azo dyes this shows that the multiple dyes were effectively decolorized. Similarly, Sani and Banerjee (1999) demonstrated the potent ability of *Kurthia* spp. to completely decolorize five triphenylmethane dyes (2µM) in just 30 minutes.

Nigam and coworkers (1996) reported on how the additional supplementation of yeast extract to the media in comparison to glucose led to a higher rate of decolorization, while Chen and fellow researchers (2003) showed that peptone and yeast extract effectively increased decolorization while glucose completely inhibited the reaction. It was also reported that the addition of starch led to 93% decolorization (Moosvi *et al.*, 2007). Likewise, an anlaysis was conducted on the effect of additional organic nitrogen and carbon supplementations on the reduction of the dye by *A. orientalis* SY6. Of particular interest were glucose and glycerol as these are low cost supplements. With the exception of yeast extract which decreased decolorization slightly, the other supplements all proved to increase decolorization equally well, being separated by less than 1.3 %. Although, it is believed that the high decolorization detected with a combination of peptone and yeast extract is due to the former compensating for the decreased activity caused by yeast extract. With fungal studies concerning dye degradation, additional nitrogen sources can either have a positive or adverse effect on decolorization. Investigators reported on the inhibition of indigo and congo red biodegradation by *Aspergillus* spp. at high nitrogen conditions (Khelifi *et al.*, 2009). They proposed that nitrogen suppressed the enzymatic system and found that a nitrogen limiting environment stimulates enzyme production. Although its clear that additional nitrogen reduces decolorization, we found no evidence to suggest that nitrogen limitation exerted a positive effect on activity.

The analysis of treated crystal violet by strains SY6, SQ1 and 155 on thin layer chromatography showed that similar band patterns occurred. Thus, it is probable that the same degradative pathway is present in all three strains. Unfortunately, since the exact pathway has not been uncovered in any of these strains it is difficult to determine what end products are being produced. It was noticed that following

prolonged incubation, the two upper bands remained in the supernatant. From the literature we can deduce the possibility of one of these products being Michler's ketone which researchers found can remain stably in the media for 100 hours and in some instances can not be catabolized further (Chen *et al.*, 2008 ; Yatome *et al.*, 1993). The other product is likely to be leucocrystal violet which was reported in *Citrobacter* spp. as being the first product into which the dye was rapidly reduced (Jang *et al.* 2005). The lower bands which are only present in the early stages are likely to be derivatives of both or one of these compounds formed through reductive splitting or demethylation; its disappearance reflecting its metabolism by the isolate (Chen *et al.*, 2008).

The screening of the positive selection library led to the identification of three clones harboring a resistance to crystal violet. SlivCV2 carried a DAHP synthase, SlivCV4 a methylmalonyl-CoA mutase and N5, N10 methylene-tetrahydromethanopterin reductase and SlivCV6 a LGFP repeat containing protein with an associated dehydrogenase and PKDI domain. These clones were tested in order to determine their optimal pH, temperature and carbon source utilization profiles. Clone SlivCV2 had an unusually low temperature optima at 20^{o}C, while SlivCV4 and SlivCV6 worked best at 37^{o}C. With regard to SlivCV2 a strong influence of temperature on decolorization was noticed; at 20^{o}C minor amounts of dye remained attached to the cell, yet with a steady temperature increase visibly more dye adsorbed onto the cell wall. This can be explained by the notion that temperature can influence enzyme conformations which in turn effects catalytic activity (Staub and Denes, 1969). More specifically, in many *Bacillus* species the feedback inhibition of this enzyme by prephenate is related to temperature (Jenson, 1970). I believe that at a low temperature DAHP synthase adopts a substrate conformation allowing it to interact with the substrates and initialize the pathway, while at a higher temperature it takes on an inhibitor binding conformation, preventing its expression (Staub and Denes, 1969; Jenson, 1970). Consequently, with this particular clone an inverse correlation between temperature and decolorization percentage was demonstrated. SlivCV2 showed good activity in the neutral to alkaline pH range but activity dropped rapidly in the acidic range. Murphy and Katz (1980) mentioned that DAHP synthase activity was inhibited at a pH below 7.0. SlivCV4 carrying the reductase related protein and methylmalonyl- CoA mutase was restrictive in its range of activity, not tolerating a shift from pH 7.0. Ma *et al.* (1990) reported similar findings when analyzing the reductase from *M. thermoautotrophicum*. SlivCV6 carrying the sorbosone dehydrogenase was also restrictive, with a pH change from

7.5 reflecting a decrease in activity. In contrast to these findings the characterization of this dehydogenase in *G. oxydans* worked optimally at an alkaline pH (Saito *et al.*, 1997). In general fructose and maltose supplements were linked to significant decreases in color removal. It is known that *S. lividans* possesses a fructose phosphotransferase system and a maltose regulator (Kieser *et al.*, 2000). It is probable that the strain preferentially utilizes these carbon sources impeding its utilization of the dye. Though it possesses the specialized gene *glk* and *gyl* operon which mediate glucose and glycerol catabolism respectively yet a reduction in decolorization efficacy was not noted in response to these supplements (Kieser *et al.*, 2000). Results suggest that the mineralized triphenylmethane dye was fully detoxified by strain SY6. Chen and coauthors (2008) tested the decolorized supernatant of *Shewanella* spp. and found that it was not completely detoxified. However, these researchers used cell cultures which are more sensitive than the testing of bacterial resistance (Scribner *et al.*, 1980).

Microbial decolorization can be attributed to either adsorption to the cell or biodegradation (Isik and Sponza, 2003). Investigation into the decolorization capacities of these individual strains in liquid media was disappointing. Noticeably, the dye adsorbed onto the cell wall, indicative of incomplete biodegradation. Kalme and coauthors (2007) measured the activities of several enzymes during the degradation of direct blue-6 by *Pseudomonas desmolyticum*. They found a significant increase in the oxidative enzymes, laccase and tyrosinase till complete decolorization at 96 hours, while reductase activities were only increased later after 48 hours. This inferred the synchronized working of collective genes involved in the decolorization process. This is in contrast to many publications which have identified a single gene involved in dye breakdown. The attainment of unfavorably low decolorization rates using individual clones made us evaluate the possibility of several gene products working together to break down the dye. Correspondingly, to establish whether this might be the possibility for strain SY6, the clones were combined and the extent of decolorization monitored. With the combined strains it was noticed that the dye was completely removed from the media and the cells retained their original color, indicative of mineralization.

A temperature profile of the combined strains reflected the strong influence of clone SlivCV2 at lower temperatures giving the graph an unusual high and consistent

decolorization from 20 – 37^{o}C and a steady decrease afterwards. The pH contour reflected an overall optimal activity near neutral. The decision was made to combine the clones in different combinations to establish the minimal number of clones required for mineralization. It was found that all three clones were required, however it was noticed that the contribution of each clone to the process of decolorization was unequal. A definite hierarchy was observed with regard to the crystal violet mineralizing clones; the absence of SlivCV2 was the most profound, this was followed by SlivCV4 and SlivCV6.

The sequencing of the inserts from the recombinant vectors led to the identification of a DAHP synthase, methylmalonyl-CoA mutase, N5, N10 methylene-tetrahydro-methanopterin reductase and a LGFP repeat containing protein with an associated dehydrogenase. Principally, all the literature thus far points towards genes with either a reductive, oxidative or oxidoreductive mechanism as being involved in dye decomposition. The gene isolated from *Citrobacter* spp. was a reductase and from *M. smegamatis* was responsible for the synthesis of an electron carrier (Kim *et al.*, 2008; Guerra-Lopez *et al.*, 2007). Hence, it was expected that these results would confer either an oxidoreductase, reductase, oxygenase or dehydrogenase. Correspondingly, the related reductase and dehydrogenase encoding genes made sense, however the involvement of the synthase was not immediately understandable.

With no immediate relevant functionality observed with regard to the DAHP synthase, the decision was made to shift focus to the pathway of the enzyme and search for an indirect mechanism of action resulting from the by-products or associated enzymes. DAHP synthases are divided into class Iα and Iβ, which are said to be '*E. coli*-like' homologues. The former class requires divalent metals for activity and the latter do not require additional elements (Subramanian *et al.*, 1998). The class II synthases are described as higher 'plant-like' homologues. Several plant-like DAHP synthases have been identified in actinomycetes. These have been linked to rifamycin production in *A. mediterranei*, chloramphenicol biosynthesis in *S. venezuelae* and ansatrienin and naphthomycin generation in *S. collinus* (Subramanian *et al.*, 1998).

The main involvement of DAHP synthase however is in the biosynthesis of phenylalanine, tyrosine and tryptophan through the shikimate pathway. This pathway is controlled by several enzymes with DAHP synthase catalyzing the first step through the condensation of D-erythrose 4-phosphate and phosphoenolpyruvate to form DAHP. Through seven metabolic steps this is converted to chorismate which acts as the precursor for phenylalanine, tyrosine and tryptophan as well as many other diverse compounds, which include cofactors, coenzymes, phenazines and siderophores (Dosselaere and Vanderleyden, 2001). Chorismate mutase converts chorismate to prephanate which leads to the production of phenylalanine and tyrosine, shifting the pathway away from tryptophan production (Qamra *et al.*, 2006). Looking at the variation in substrates that arise from a single pathway has caused researchers to speculate as to the evolution of this remarkable metabolic pathway. A comparative analysis of the chorismate utilizing enzymes revealed a complicated occurrence of the divergent evolution of some enzymes and convergent evolution of others all progressing towards a similar function (Dosselaere and Vanderleyden, 2001).

The DAHP synthase isolated in this study was most closely related to a class II DAHP synthase encoded by *aroF* in *A. mediterranei*. Hence, we looked closely at the reactions taking place along the pathway to the production of tyrosine and identified potential enzymes and biochemical reactions which could possibly interact or influence the dye substrate [Fig. 4.1]. Notably, the gene identified in *M. smegmatis* showed an indirect link due to an oxidative mechanism mediated by the synthase (Guerra-Lopez *et al.*, 2007). DAHP synthase substrate specificity is rigid, thus it is not likely that the synthase is reacting directly with the dye. The following are possible explanations for how these enzymes might contribute to dye decolorization. The 3-Hydroquinate synthase catalyzes an intramolecular oxidation-reduction reaction on DAHP (Herrmann, 1995). In *E. coli* the 3-hydroquinate synthase and dehydratase are expressed constitutively (Kramer *et al.*, 2003). Chorismate synthase is catalyzed by a reduced flavin nucleotide cofactor supplied by an associated reductase (Herrmann, 1995). Chorismate mutase possesses a prephenate dehydrogenase or dehydrolase activity (Qamra *et al.*, 2006). Dehydrogenase activity was identified in anaerobic bacteria and linked to the decolorization of azo dyes (Rafii and Cerniglia, 1995). A dehydrolase can possess an esterase activity (Akashi *et al.*, 2005). The relevance to this is that Bafana and Chakrabarti (2008) by computational methods

were able to identify acyl carrier protein phosphodiesterases as potential azoreductases. Furthermore, the conversion of chorismate to prephenate is a highly exergonic reaction (Kast *et al.*, 2000). We offer several possibilities of reactions in the shikimate pathway which might contribute to decolorization, however cannot state with certainty whether one or a combination of these are responsible.

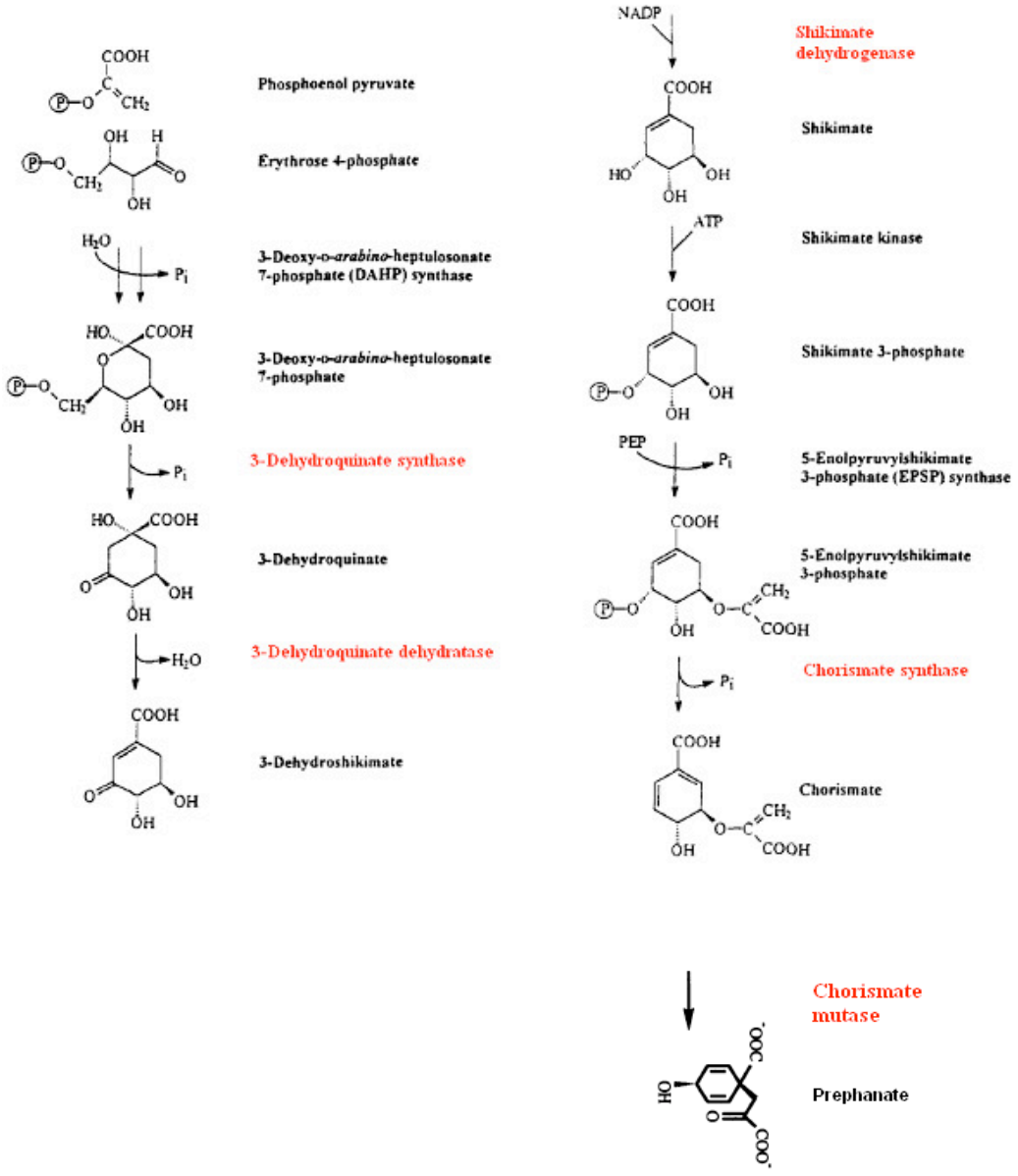

Fig. 4.1: The shikimate pathway. Enzymes in red represent reactions which could potentially lead to dye decolorization (Herrmann, 1995).

On an unrelated note, the shikimate pathway is maintained in plants, fungi and bacteria but absent in mammals. This makes the enzymes involved, particularly DAHP synthase which initiates the first step of this pathway a useful antimicrobial target (Rizzi *et al.*, 2005). An earlier study based on this concept has already shown promising results in *M. tuberculosis* in which disruption of one of the synthase encoded genes proved to be lethal (Rizzi *et al.*, 2005). Another interesting feature of this pathway is that shikimate is used as a key ingredient in Tamiflu® (Kramer *et al.*, 2003). This drug of course received worldwide recognition in the prevention of possible transmission of the H5N1 influenza strain. Kramer and coworkers (2003) describe various researchers work involving metabolic engineering in *E. coli* strains to produce shikimate. This is in response to the shortage of this drug due to global demand.

Even though a reductase was present on the pCV4 insert, the vitamin B_{12} dependent methylmalonyl CoA mutase could not immediately be eliminated as a suspect in the role of dye decomposition. Within this laboratory a potential vitamin B dependent gene was isolated from *R. equi* ATCC 14887 capable of decolorizing both amido black and orange II (Heiss and Dabbs, 1992). Recently, another vitamin B_{12} dependent gene isolated from a Gram negative *Duganella* spp. was found to be capable of decolorizing brilliant green (Beukes and Dabbs, 2010). With two potential vitamin B dependent genes from unrelated strains displaying decolorization of different dyes, this was aspect into which we were obligated to look into further.

Methylmalonyl CoA mutase has been identified in many animals and bacteria such as *E. coli, M. tuberculosis, S. cinnamonensis, C. elegans*, mice and man (Gruber and Kratky, 2001). The B_{12}- dependent methylmalonyl-CoA mutase (mcm) catalyzes the conversion of succinyl-CoA into methylmalonyl-CoA (Gruber and Kratky, 2001). This process is freely reversible, in favor of succinyl-CoA production. In *Streptomyces cinnamonensis* methylmalonyl-CoA is an essential component of polyketide antibiotics with the substrate incorporated into the polyketide backbone as a methyl branch (Birch *et al*, 1993). The illustration below depicts the reaction in which vitamin B_{12} acts as a 'radical reservoir' in the reaction, which proceeds as follows [Fig. 4.2]: (i) the homolytic cleavage of the carbon-Co bond of the 5' deoxyadenosine cobalamin (vitamin B_{12}) cofactor, generates a cob(II)alamin and

deoxyadenosyl radical, (ii) the radical abstracts hydrogen from the succinyl-CoA substrate which leads to a substrate derived radical (iii) an intermolecular transfer of hydrogen is followed by an intramolecular transfer of the organic group and, (iv) the substrate re-extracts hydrogen from the deoxyadenosine, hence the transfer of the radical regenerates the vitamin B_{12} cofactor (Banerjee and Vlasie, 2002; Dominique and Banerjee, 2006).

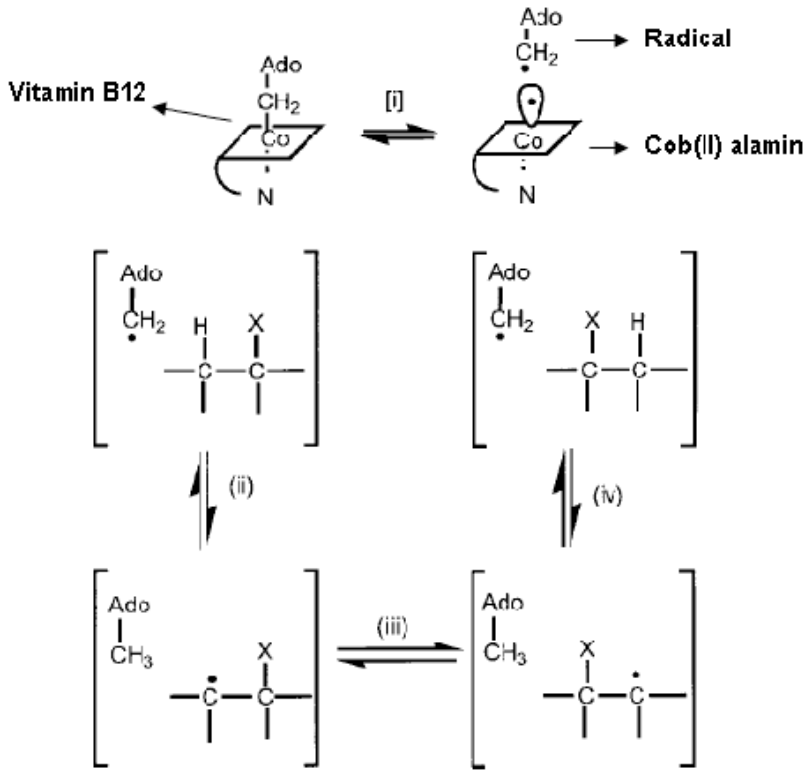

Fig. 4.2: Postulated general reaction mechanism for 5' deoxyadenosine cobalamin catalysed reaction. Ado represents the deoxyadenosyl radical (Banerjee and Vlasie, 2002).

Once again the comprehensively studied enzyme structure and pathway were looked at to determine relevant reactions that could influence dye break down. The crystal structure of mcm revealed the presence of a TIM barrel domain, which differs from conventional barrel domains that are hydrophobic and large (Gruber and Kratky, 2001). The mcm barrel domain is hydrophilic and small; offering just enough space for the coenzyme end of the substrate to bind along the axis. From this it was

conceded that the substrate specificity of mcm is rigid, therefore we propose no direct interaction of the mutase with crystal violet. Mechanistically, this enzyme works by means of a radical mechanism (as described above) and so we delved into the literature to establish the possibility of this radical being 'hijacked' by the dye substrate. Studies show that the interaction between the mutase and substrate induces a conformational change causing the enzyme to surround the substrate coenzyme tail, effectively sealing it off and initiating an internal electron transfer. With this reaction taking place within the enzyme cavity it is clear that radicals are prevented from taking part in other non-specific reactions (Gruber and Kratky, 2001). Since the gene was expressed on a high copy number vector (20-100 per cell) we looked into the probability of the mutase resulting in the generation of a low level of radicals (Hill *et al.*, 1989). Structural experiments have shown that in the absence of the substrate, the TIM barrel domain splits apart and is essentially inactive; upon substrate instigation the barrel encloses the substrate and initiates radical exchange, making this hypothesis improbable (Gruber and Kratky, 2001). Zhang and coworkers (1999) cloned the mcm gene from the rifamycin producing strain, *Amycolatopsis mediterranei* and expressed it in the monensin antibiotic producing strain, *Streptomyces cinnamonensis*. This led to a 32 % increase in antibiotic production in the Streptomycete strain. This brings a new complicated facet into determining what could contribute to dye degradation since this could mean having to take into account the extended pathway of methylmalonyl-CoA, which includes its incorporation into polyketide antibiotics. Since antibiotic biosynthesis is controlled by multiple enzyme complexes with complex interactions it would be difficult to pin point the exact reactions that could influence dye decolorization. Nonetheless, the literature surrounding this mutase only sought to establish how finely controlled and precise the mechanism of action of this enzyme is. Consequently, we were not able to show that this enzyme influences the decolorization of crystal violet and hypothesize that it is not involved in the reaction.

The N5, N10-methylene-tetrahydromethanopterin reductase (*mer*) was originally isolated from *Methanobacterium thermoautotrophicum* and *Methanopyrus kandleri.* This gene plays a role in the pathway conversion of carbon dioxide to methane and is a F_{420} dependent reductase. From this we can propose that the mer reductase is probably linked to crystal violet decolorization without assistance from the methylmalonyl-CoA mutase. This is further exemplified by the fact that a F_{420}

dependent enzyme was linked to malachite green mineralization in *M. smegmatis* (Guerra-Lopez *et al.*, 2007).

LGFP repeat containing proteins contain the conserved motif, L-G-x-P-x(7)-D-G (Adindla *et al.*, 2004). These repeats occur in cell surface proteins and have been identified in the genomes of *C. glutamicum, C. efficiens, M. tuberculosis, M.leprae, M. paratuberculosis* and *D. radiodurans* (Adindla *et al.*, 2004). Surface proteins can serve numerous functions linked to transportation, cell to cell communication and protection (Adindla *et al.*, 2004). These repeats are not well characterized, however one study suggests that they act as 'anchors' which attach the protein to the cell wall (Adindla *et al.*, 2004).

The presence of a glucose/sorbosone dehydrogenase was an encouraging result since it is functionally appropriate. L-sorbosone dehydrogenase converts D-sorbital to 2-keto-L-gulonate which is a precursor for L-ascorbic acid (vitamin C) (Saito *et al.*, 1997). Conventionally, vitamin C is synthesized by means of Reichsteins method in which glucose is converted to 2-keto-L-gulonic acid in a five step chemical process with a yield of around 50 % (Saito *et al.*, 1997). This is a long process which results in a low yield of the precursor. Saito and coworkers (1997) introduced the sorbose and sorbosone dehydrogenase encoding genes into *G. oxydans*. This resulted in high level production of 2-keto-L-gulonate (130mg /ml) directly from D-sorbitol by means of oxidation [Fig. 4.3]. From this we propose that the dye is able to act as an electron acceptor during these successive oxidative reactions, facilitating its reduction.

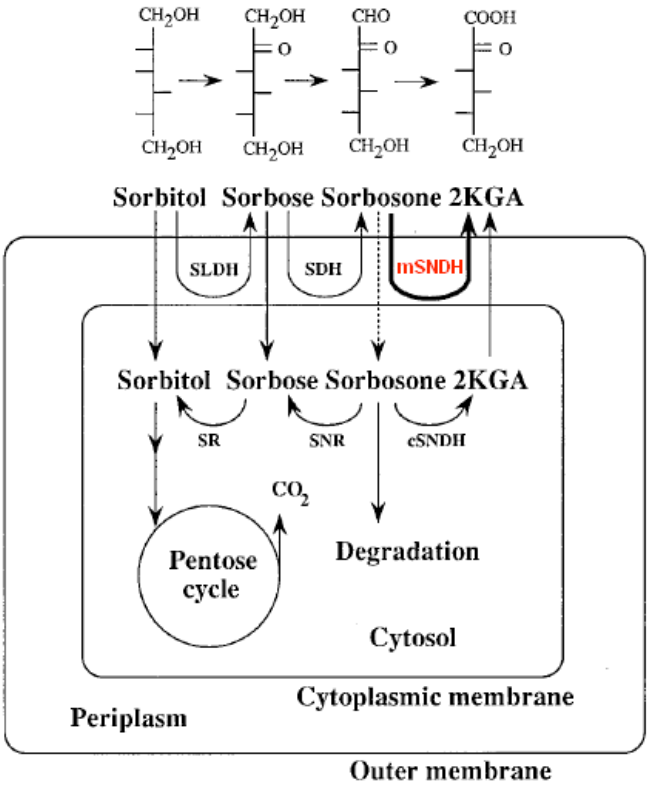

Fig 4.3: Mechanism of production of 2-keto-L-gulonate from D-sorbital and L-sorbosone in *G. oxydans*. SLDH- D-sorbitol dehydrogenase, SDH- L-sorbose dehydrogenase, SR- L sorbose reductase, SNR- L-sorbosone reductase, SNDH- L-sorbosone dehydrogenase, cSNDH- cytosolic SNDH, mSNDH-membrane bound SNDH. The thin lines show the metabolic pathway in *G. oxydans*; the thick line shows the catalytic reaction of the membrane-bound SNDH (shown in red), which was the target enzyme studied to improve the 2-keto-L-gulonate production yield in *G. oxydans* (Shinjoh *et al.*, 1995).

Analysis of the remaining sequence showed that a polycystic kidney disease I (PKD) domain was also present. Polycystic kidney disease in man is characterized by the development of cysts on the organ leading to a progressive loss of renal function (Bycroft *et al.*, 1999). Mutations in the PKD1 gene (which consists of sixteen copies of the PKD domain) and pKD2 genes have been linked to this disorder. Despite the name, this domain has also been identified in bacterial genomes in association with collagenases, chitinase and proteases. Through a set of elegant experiments it was

shown that the PKD domain was able to bind collagen and through an unknown mechanism caused it to swell, exposing the fibers consequently allowing it to be cleaved by a protease (Wang *et al.*, 2010). Orikoshi and coauthors (2005) set out to uncover the function of the PKD domain in relation to chitin degradation. Through site directed mutagenesis of key residues they were able to show that the PKD associated domain within the *chitinase A* gene directly participates in the hydrolysis of chitin. This was a key article showing that the domain plays a direct role in the biodegradation process and does not merely act as a binding domain for substrates. Correspondingly, we propose that the LGFP region allows for attachment to the cell wall, the PKD domain which occurs on the surface, binds to the substrate and via hydrolytic interaction with the dye is responsible for partial decolorization. Furthermore, the sorbosone dehydrogenase which can occur as a membrane bound or cytosolic protein also interacts with the dye via an oxidoreductive mechanism. While the influence of the dehydrogenase with the dye is highly probable the involvement of PKD is less so. However, this hypothesis is not completely implausible as lysozyme, which carries a hydrolytic function has been found to decolorize sulfonated azo dyes (Heiss and Dabbs, 1992). Taken altogether, these results reflect that there exists an oxidoreductive and hydrolytic mechanism of action in the presence of the combined crystal violet clones allowing for complete mineralization of the dye.

Following the realization that the combination of clones led to the decomposition of crystal violet, we decided to analyze the response of these clones in azo, sulfonated azo and other triphenylmethane dyes. It was interesting that the expression of these genes led to variable results, depending on the host strain into which it was introduced. I searched through the literature for homologues of the identified genes in *Rhodococcus* and *Mycobacterium* species in order to identify the functions that these genes would assume in these hosts. I was unable to find any investigations into the expression of DAHP synthase in *Rhodococcus* species, although this has been identified in the genomes of this species through the genome sequencing projects. Chorismate mutase is expressed constitutively with minor detection of feedback inhibition in *Mycobacterium* spp. (Schneider *et al.*, 2008). Since chorismate mutase posseses a dehydrogenase activity its overexpression due to the induction by DAHP synthase could influence the biodegradation of amido black, janus green and bismarck brown. A homolog of N5, N10-methylenetetra-hydromethanopterin reductase occurs

in *M. tuberculosis*, identified through the genome sequencing project, and through the KEGG pathway is hypothesized to play a role in 1,1,1-Trichloro-2,2-bis(4-chlorophenyl)ethane (DDT) degradation and limonene and pinene degradation (Kanehisa *et al.*, 2004). DDT is a highly toxic pesticide which was found to adversely affect humans and wildlife leading to its subsequent ban in the 1970's (Purnoma *et al.*, 2008). The gene is proposed to oxidize 4-chlorobenzaldehyde to 4-chlorobenzoate, the last step in the biodegradative pathway (Kanehisa *et al.*, 2004). Limonene is a hydrocarbon found in the rind of citrus fruit and pinene is present in the resin of conifers. The reductase catalyses the oxidation of myrtenal to myrtenic acid in the beginning stages of the biodegradative pathway (Kanehisa *et al.*, 2004). Within the abovementioned pathways oxidative reactions are the main commonality, thus it was hypothesized that this is responsible for the decolorization of amido black, bismarck brown and janus green. In a *Rhodococcus* spp., enzymes closely related to N5, N10-methylenetetra-hydromethanopterin reductase were responsible for the biodegradation of 2,4,6-trinitrophenol (commonly found in pesticides, dyes and explosives) (Heiss *et al.*, 2002). These enzymes took on the role of hydride transferases. Thus, it is possible that its function in the transferal of hydride ions allows this gene to contribute towards the decolorization of amido black, orange II and biebrich scarlet. Furthermore, within the human intestinal tract dehydrogenase activity was associated with azoreductases identified in *Clostridium* and *Eubacterium* species (Rafii and Cerniglia, 1995). This can be extended to the activity of the sorbosone dehydrogenase. Overall, the difference in metabolic activities and gene regulation means that there are many reasons why the expression of these genes induce different responses in different bacterial hosts.

Progressing from the above point the notion of heterologous expression is an interesting one. Depending on the genes being dealt with it seems customary to screen for expression in related strains. This is a trend which is deeply ingrained in Streptomycete genetics. The model strain for *Streptomyces* spp. gene expression is *S. lividans* and *S. coelicolor* A3(2) (Kieser *et al.*, 2000). Other strains such as *S. griseus*, *S. ambofaciens* and *S. rimosus* are also used although their use is not as wide as that of the previously mentioned strains and their derivatives. Genetic modifications made in the 1980's improved these strains making them highly transformable and the additional development of associated vectors made them indispensable very early on.

Ever since the isolation of *S. lividans* 66 and its derivatives as an effective transformation host for *Streptomcyes* spp., screening has been restrictively conducted in these strains. This study underscores that the expression of genes in other species can lead to a broader range of activity. Moreover, there is an added advantage of expressing the genes in for instance, *Rhodococcus* species. These resilient strains have been implicated in the biodegradation of many pollutants such as oil and pesticides and are commonly found in polluted wastewaters and toxic environments, making them a more practical choice for use when considering large scale bioremediation (Aoshima *et al.*, 2006; Shao and Behki, 1996).

4.1 Concluding remarks

Four species were identified with potent triphenylmethane degradative capacities. To our knowledge this is the first report of an *Amycolatopsis* spp. being implicated in crystal violet reduction and only the second report of the characterization of triphenylmethane decolorizing genes from a Gram positive bacterium. This isolate not only decolorized but detoxified the dye as well. This strains ability to rapidly breakdown a combination of triphenylmethane dyes within a short interval makes it a suitable candidate for further bioremediation work. Furthermore, these results indicate that it would be beneficial to start a trend in which genes are not only expressed in common species which are closely related but also tested in other species.

5. References

5.1 *References for Chapter I and II*

Abraham K.J. and John G.H., (2007). Development of a classification scheme using a secondary and tertiary amino acid analysis of azoreductase gene, Journal of Medical and Biological Sciences, **1** (2), 1-5

Adindla S., Inampudi K.K., Guruprasad K. and Guruprasad L., (2004). Identification and analysis of novel tandem repeats in the cell surface proteins of archael and bacterial genomes using computational tools, Comparitive and Functional Genomics, **5**, 2-16

Akashi T., Aoki T. and Ayabe S-I., (2005). Molecular and biochemical characterization of 2-hydroxyisoflavanone dehydratase. Involvement of carboxylesterase-like proteins in leguminous isoflavone biosynthesis, Plant Physiology, **127**, 882-891

Altschul, S.F., Gish, W., Miller, W., Myers, E.W. and Lipman, D.J. (1990). Basic local alignment search tool, Journal of Molecular Biology, **215**, 403-410

An S-Y., Min S-K., Cha I-H., Choi Y-L., Cho Y-S., Kim C-H. and Lee Y.C., (2002). Decolorization of triphenylmethane and azo dyes by *Citrobacter* sp. Biotechnology Letters, **24** (12), 1037-1040

Aoshima H., Hirase T., Tada T., Ichimura N., Yamaguchi H., Taguchi M. and Myoenzono T., (2006). Improvement of heavy oil degradation by *Rhodococcus erythropolis* C2, Journal of Environmental Biotechnology, **5** (2), 107-109

Azmi W., Sani R.K. and Banerjee U.C., (1998). Biodegradation of triphenylmethane dyes, Enzymes and Microbial Technology, **22** (3), 185-191

Bafana A. and Chakrabarti T., (2008). Lateral gene transfer in phylogeny of azoreductase system, Computational Biology and Chemistry, **32** (3), 191-197

Bafana A., Chakrabarti T. and Devi S.S., (2008). Azoreductase and dye detoxification activities of *Bacillus velezensis* strain AB, Applied Microbiology and Biotechnology, **77** (5), 1139-1144

Banerjee R. and Vlasie M., (2002). Controlling the reactivity of radical intermediates by coenzyme B_{12}-dependent methylmalonyl-CoA mutase, Biochemical Society Transactions, **30** (4), 621-624

Beukes G. and Dabbs E.R., (2010). Cloning of a *Duganella* sp. gene encoding for a synthase, whose activity is responsible for the degradation of the triphenylmethane dye, Brilliant green, Honours dissertation, University of Witwatersrand, 1-37

Biology software net, (2010). Bio-log plasm, China, (9 December 2010)

Birch A., Leiser A. and Robinson J.A., (1993). Cloning, sequencing, and expression of the gene encoding methylmalonyl-coenzyme A mutase from *Streptomyces cinnamonensis*,

Journal of Bacteriology, **175**, 11, 3511-3519

Blumel S., Knackmuss H-J. and Stolz A., (2002). Molecular cloning and characterization of the gene coding for the aerobic azoreductase from *Xenophilus azovorans* KF46F, Applied and Environmental Microbiology, **68** (8), 3948-3955

Bridges B.A. and Stannard M., (1982). A new pathway for repair of cross-linkable 8-methoxypsoralen monoadducts in Uvr⁻ strains of *Escherichia coli*, Mutation research/ Fundamental and molecular mechanisms of mutagenesis, **92** (1-2), 9-14

Bürger S. and Stolz A., (2010). Characterisation of the flavin-free oxygen-tolerant azoreductase from *Xenophilus azovorans* KF46F in comparison to falvin-containing azoreductases, Applied Microbiology and Biotechnology, **87**, 2067-2076

Bycroft M., Bateman A., Clarke J., Hamill S.J., Sandford R., Thomas R.L. and Chothia C., (1999). The structure of a PKD domain from polycystin-1: implications for polycystic disease, The EMBO Journal, **18** (2), 297-305

Chen C-C., Liao H-J., Cheng C-Y., Yen C-Y. and Chung Y-C., (2007). Biodegradation of crystal violet by *Pseudomonas putida*, Biotechnology letters, **29** (3), 391-396

Chen C-H., Chang C-F., Ho C-H., Tsai T-L. and Liu S-M., (2008). Biodegradation of crystal violet by *Shewanella*, Chemophere, **72** (11), 1712-1720

Chen K-C., Wu J-Y., Liou D-J. and Hwang S-C.J., (2003) Decolorization of the textile dyes by newly isolated bacterial strains, Journal of Biotechnology, **101** (1), 57-68

Chou D.K., Krishnamurthy R., Randolph T.W., Carpenter J.F. and Manning M.C., (2005). Effects of tween 20® and tween 80® on the stability of albutropin during agitation, Journal of Pharmaceutical Sciences, **94** (6), 1368-138

Chung J., Chen T. and Missiakas D., (2000). Transfer of electrons across the cytoplasmic membrane by DsbD, a membrane protein involved in thiol-disulfide exchange and protein folding in the bacterial periplasm, Molecular Microbiology, **35** (5), 1099-1109

Dabbs E.R., Gowan B.,Quan S. and Andersen S.J. (1995). Development of improved *Rhodococcus* plasmid vectors and their use in cloning genes of potential commercial and medical importance, Biotechnologia, **7** (8),129-135

Doble M. and Kumar A., (2005). Biotreatment of industrial effluents, Elsevier Butterworth-Heinemann, 111-132

Dominique P. and Banerjee R., (2006). Alternative pathways for radical dissipation in an active site mutant of B_{12}-dependent methylmalonyl-CoA mutase, Biochemistry, **45** (9), 2951-2959

Dosselaere F. and Vanderleyden J., (2001). A metabolic node in action: chorismate- utilizing enzymes in microorganisms - abstract, Critical reviews in Microbiolology, **27** (2), 75

Edublogs.org, (2010). The Egyptians, 1hollypark.edublogs.org/2009/04/28/the-egyptians/, 12 December 2010

Forgacs E., Cserhati T. and Oros G., (2004). Removal of synthetic dyes from wastewaters: a review, Environment International, **30** (70), 953-971

Goszczynski S., Paszczynski A., Pasti-Grigsby M.B., Crawford R.L. and Crawford D.L., (1994). New pathway for degradation of sulfonated azo dyes by microbial peroxidases of *Phanerochaete chrysosporium* and *Streptomyces chromofuscus*, **176** (5), 1339-1347

Grekova-Vasileva M., Popov I., Vassilev D. and Topalova Y., (2009). Isolation and characterisation of microbial strain AZO29 capable of azo dye decolourization, XI Anniversary Scientific Conference special edition on-line

Gruber K. and Kratky C., (2001). Methylmalonyl CoA mutase handbook of metalloproteins, John Wiley and Sons, Chichester, 995-1009

Guerra-Lopez D., Daniels L. and Rawat M., (2007). *Mycobacterium smegmatis* mc2 155 fbiC and MSMEG_2392 are involved in triphenylmethane dye decolorization and coenzyme F420 biosynthesis, Microbiology, **153**, 2724-2732

Gurung T.D., Sherpa C., Agrawal V.P. and Lekhak B., (2009). Isolation and characterization of antibacterial actinomycetes from soil samples of Kalapatthar, Mount Everest region, Nepal Journal of Science and Technology, **10**, 173-182

Harazono K. and Nakamura K., (2004). Decolorization of mixtures of different reactive textile dyes by the white-rot basidiomycete *Phanerochaete sordida* and inhibitory effect of polyvinyl alcohol, Chemosphere, **59** (1), 63-68

He F., Hu W. and Li Y., (2004). Biodegradation mechanisms and kinetics of azo dye 4BS by a microbial consortium, Chemosphere, **57** (4), 293-301

Heiss G.S. and Dabbs E.R., (1992). Characterization of the genes for enzymes involved in the degradation of azo dyes by nocardioforms, Masters dissertation, University of Witwatersrand, 1-187

Heiss G., Hofmann K.W., Trachtmann N., Walters D.M., Rouviere P., and Knackmuss H-J., (2002). Npd gene functions of *Rhodococcus (opacus) erythropolis* HL PM-1 in the initial steps of 2,4,6-trinitrophenol degradation, Microbiology, **148**, 799-806

Herrmann K.M., (1995). The shikimate pathway: early steps in the biosynthesis of aromatic compounds, The Plant Cell, **7**, 907-919

Isik M. and Sponza D.T., (2003). Effect of oxygen on decolorization of azo dyes by *Escherichia coli* and *Pseudomonas* sp. and fate of aromatic amines, Process Biochemistry, **38** (8), 1183-1192

Jang M-S., Lee Y-M., Kim C-H., Lee J-H., Kang D-W., Kim S-J. and Lee Y-C., (2005). Triphenylmethane reductase from *Citrobacter* sp. strain KCTC 18061P: Purification, characterization, gene cloning, and overexpression of a functional protein in *Escherichia coli*, Applied and Environmental Microbiology, **71** (12), 7955-7960

Jenson R.A., (1970). Taxonomic implications of temperature dependence of the

allosteric inhibition of 3-deoxy-D-*arabino*-heptulosonate 7-phosphate synthetase in *Bacillus*, Journal of Bacteriology, **102** (2), 489-497

Kalme S.D., Parshetti G.K., Jadhav S.U. and Govindwar S.P., (2006). Biodegradation of benzidine based dye direct-blue 6 by *Pseudomonas desmolyticum* NCIM 2112, Bioresource Technology, **98** (7), 1405-1410

Kanehisa M., Goto S., Kawashima S., Okuno Y. and Hattori M., (2004). The KEGG resource for deciphering the genome, Nucleic Acids Research, **32** (1), D277-D280

Kast P., Grisostomi C., Chen I.A., Li S., Krengel U., Xue Y. and Hilvert D., (2000). A strategically positioned cation is crucial for efficient catalysis by chorismate mutase, The Journal of Biological Chemistry, **275** (47), 36832

Katzen F., Deshmukh M., Daldal F. and Beckwith J., (2002). Evolutionary domain fusion expanded the substrate specificity of the transmembrane electron transporter DsbD, The EMBO Journal, **21** (15), 3960-3969

Kaushik P. and Malik P., (2008). Fungal dye decolourization: recent advances and future potential, Environment International, **35** (1), 127-141

Khehra M.S., Saini H.S., Sharma D.K., Chadha B.S. and Chimni S.S., (2005). Decolorization of various azo dyes by bacterial consortium, Dyes and Pigments, **67**, 55-61

Khelifi E., Ayed L., Bouallagui H., Touhami Y. and Hamdi M., (2009). Effect of nitrogen and carbon sources on Indigo and Congo red decolorization by *Aspergillus alliaceus* strain 121C, Journal of Hazourdous Materials, **163** (2-3), 1056-1062

Kieser T., Bibb M.J., Buttner M.J., Chater K.F. and Hopwood D.A., (2000). Practical *Streptomyces* genetics, The John Innes Foundation, 1-585

Kim J-Y., Lee Y-M., Jang M-S., Kang D-W., Kim S-J., Kim C-H., Lee Y-C., (2005). Identification of genes required for decolorization of crystal violet in *Citrobacter* sp. MY-5, The Journal of General and Applied Microbiology, **51** (3), 191-195

Kloosterman H., Hessels G.I., Vrijbloed J.W., Euverink G.J. and Dijkhuizen, (2003). (De)regulation of key enzyme steps in the shikimate pathway and phenylalanine-specific pathway of the actinomycete *Amycolatopsis methanolica*, Microbiology, **149**, 3321-3330

Kokol V., Doliska A., Eichlerova I., Baldrian P. and Nerud F., (2007). Decolorization of textile dyes by whole cultures of *Ischnoderma resinosum* and by purified laccase and Mn-peroxidase, Enzyme and Microbial Technology, **40** (7), 1673-1677

Kramer M., Bongaerts J., Bovenberg R., Kremer S., Muller U., Orf S., Wubbolts M. and Raeven L., (2003). Metabolic engineering for microbial production of shikimic acid, Metabolic Engineering, **5**, 277-283

Kudlich M., Keck A., Klein J. and Stolz A., (1997). Localization of the enzyme system involved in anaerobic reduction of azo dyes by *Sphingomonas* sp. strain BN6 and effect of

artificial redox mediators on the rate of azo dye reduction, Applied and Environmental Microbiology, **63** (9), 3691-3694

Lazarow A. and Cooperstein S.J., (1953). Studies on the enzymatic basis for the Janus green B staining reaction, Journal of Histochemistry and Cytochemistry, **1**, 234-241

Liu G., Zhou J., Wang J., Zhou M., Lu H. and Jin R., (2009). Acceleration of azo dye decolorization by using quinone reductase activity of azoreductase and quinone redox mediator, Bioresource Technology, **100**, 2791-2795

Ma K. and Thauer R.K., (1990). Purification and properties of N^5,N^{10}-methylenetetrahydromethanopterin reductase from *Methanobacterium thermoautotrophicum*, European Journal of Biochemistry, **191**, 187-193

Mancia S. and Evans P.R., (1998). Conformational changes on substrate binding to methymalonyl CoA mutase and new insights into the free radical mechanism, Structure, **6** (6), 711-720

McMullan G., Meehan C., ConneelyA., Kirby N., Robinson T., Nigam P., Banat I.M., Marchant R. and Smyth W.F., (2001). Microbial decolourisation and degradation of textile dyes, Applied Microbiology and Biotechnology, **56** (1-2), 81-87

Meehan C., Bjourson A.J. and McMullan G., (2001). *Paenibacillus azoreducens* sp. nov., a synthetic azo dye decolorizing bacterium from industrial wastewater, International Journal of Systematic and Evolutionary Microbiology, **51**, 1681-1685

Missiakas D., Schwager F. and Raina S., (1995). Identification and characterization of a new disulphide isomerase-like protein (DsbD) in *Escherichia coli*, The EMBO Journal, **14** (14), 3415-3424

Molina-Guijarro J.M., Perez J., Munoz-Dorado J., Guillen F., Moya R., Hernandez M. and Arias M.E., (2009). Detoxification of azo dyes by a novel pH-versatile, salt-resistant laccase from *Streptomyces ipomoea*, International Microbiology, **12** (1), 13-21

Moosvi S., Kher X. and Madamwar X., (2007). Isolation, characterization and decolorization of textile dyes by a mixed bacterial consortium JW-2, Dyes and Pigments, **74** (3), 723-729

Mugerfeld I., Law B.A., Wickham S.G. and Thompson D.K., (2009). A putative azoreductase gene is involved in the *Shewanella oneidensis* response to heavy metal stress, Applied Microbiology and Biotechnology, **82** (6), 1131-1141

Murphy M.F. and Katz E., (1980). Regulatory control of 3-deoxy-D-arabino- heptulosonic acid 7 –phosphate synthetase in *Streptomyces antibioticus* - abstract, Canadian Journal of Microbiology, **26** (8), 874

Nachiyar C.V., Suseela R., (2005). Degradation of a tannery and textile dye, Navitan fast blue S5R by *Pseudomonas aeruginosa,* World Journal of Microbiology and Biotechnology, **19** (6), 609-614

Nicholson P.T. and Shaw I., (2000). Ancient Egyptian materials and technology, Cambridge University Press, 278-280

Nigam P., Banat I.M., Singh D. and Marchant R., (1996). Microbial process for the decolorization of textile effluent containing azo, diazo and reactive dyes, Process Biochemistry, **31** (5), 435-442

Nishikawa M. and Ogawa K., (2002). Distribution of microbes producing antimicrobial ε-poly-L-lysine polymers in soil microflora determined by a novel method, Applied and Environmental Microbiology, **68** (7), 3575-3581

Nolling J., Pihl T.D. and Reeve J.N., (1995). Cloning, sequencing, and growth phase-dependent transcription of the coenzyme F_{420}-dependent N5, N10-methylenetetrahydromethanopterin reductase-encoding genes from *Methanobacterium thermoautotrophicum* ΔH and *Methanopyrus kandleri*, Journal of Bacteriology, **177** (24), 7238-7244

Orikoshi H., Nakayama S., Hanato C., Miyamoto K. and Tsujibo H., (2005). Role of the N-terminal polycystic kidney domain in chitin degradation by chitinase A from a marine bacterium, *Alteromonas* sp. Strain O-7, Journal of Applied Microbiology, **99**, 551-557

Pasti-Grigsby M.B., Paszczynski A., Goszczynski S., Crawford D.L. and Crawford R.L., (1992). Influence of aromatic substitution patterns on azo dye degradability by *Streptomyces* spp. and *Phanerochaete chrysosporium*, Applied and Environmental Microbiology, **58** (11), 3605-3613

Pickard M.A., Vandertol H., Roman R. and Vazquez-Duhalt R., (1999). High production of ligninolytic enzymes from white-rot fungi in cereal bran liquid medium, Canadian Journal of Microbiology, **45**, 627-631

Pricelius S., Held C., Murkovic M., Bozic M., Kokol V., Cavaco-Paulo A. and Guebitz G.M., (2007). Enzymatic reduction of azo and indigoid compounds, Applied Microbiology and Biotechnology, **77** (2), 321-327

Punj S. and John G.H., (2008). Purification and identification of an FMN-dependent NAD(P)H azoreductase from *Enterococcus faecalis*, Current Issues in Molecular Biology, 11, 59-66

Purnomo A.S., Kamei I. and Kondo R., (2008). Degradation of 1,1,1-Trichloro-2,2- Bis (4-chlorophenyl) ethane (DDT) by brown-rot fungi, Journal of Bioscience and Bioengineering, **105** (6), 614-621

Qamra R., Prakash P., Aruna B., Hasnain S.E. and Mande S.C., (2006). The 2.15 A crystal structure of *Mycobacterium tuberculosis* chorismate mutase reveals reveals an unexpected gene duplication and suggests a role in host-pathogen interactions, Biochemistry, **45** (23), 6997-7005

Rafii F., Franklin W. and Cerniglia C.E., (1990). Azoreductase activity of anaerobic bacteria isolated from human intestinal flora, Applied and Environmental Microbiology, **56** (7), 2146-2151

Rafii F. and Cerniglia C.E., (1995). Reduction of azo dyes and nitroaromatic

compounds by bacterial enzymes from the human intestinal tract, Environmental Health Perspectives, **103**, 17-19

Rajaguru P., Kalaiselvi K., Palanivel M. and Subburam V., (2000). Biodegradation of azo dyes in a sequential anerobic-aerobic system, Applied Microbiology and Biotechnology, **54**, 268-273

Rani C., Jana A.K. and Bansal A., (2009). Studies on the biodegradation of azo dyes by white rot fungi *Phlebia radiata*, Proceedings of International Conference on Energy and Environment, 203-207

Reese E.T. and Maguire A., (1969). Surfactants as stimulants of enzyme production by microorganisms, Applied Microbiology, **17** (2), 242-245

Rizzi C., Frazzon J., Ely F., Weber P.G., da Fonseca I.O., Gallas M., Oliveira J.S., Mendes M.A., de Souza B.M., Palma M.S., Santos D.S. and Basso L.A., (2005). DAHP synthase from *Mycobacterium tuberculosis* H37Rv: cloning, expression, and purification of functional enzyme, Protein Expression Purification, **40**, 23-30

Robinson T., McMullan G., Marchant R. and Nigam P., (2001). Remediation of dyes in textile effluent: a critical review on current treatment technologies with a proposed alternative, Bioresource Technology, **77** (3), 247-255

Roxon J.J., Ryan A.J. and Wright S.E., (1967). Enzymatic reduction of tartrazine by *Proteus vulgaris* from rats, Food and Cosmetics Toxicology, **5**, 645-656

Saito Y., Ishii Y., Hayashi H., Imao Y., Akashi T., Yoshikawa K., Noguchi Y., Soeda S., Yoshida M., Niwa M., Hoshoda J. and Shimomura K., (1997). Cloning of genes coding for L-sorbose and L-sorbosone dehydrogenases from *Gluconobacter oxydans* and microbial production of 2-keto-L-gulonate, a precursor of L-ascorbic acid, in a recombinant *G. oxydans* strain, Applied and Environmental Microbiology, **63** (2), 454-460

Sani R.K. and Banerjee U.C., (1999). Decolorization of triphenylmethane dyes and textile and dye-stuff effluent by *Kurthia* sp., Enzyme and Microbial Technology, **24** (7), 433-437

Santamaria R.I., Leal F., Fernandez –Abalos M.D.J.M., (2002). Morphological and physiological changes in *Streptomyces lividans* induced by different yeasts, Archives of Microbiology, **177** (3), 259-266

Schneider C.Z., Parish T., Basso L.A. and Santos D.S., (2008). The two chorismate mutases from both *Mycobacterium tuberculosis* and *Mycobacterium smegmatis*: Biochemical analysis and limited regulation of promoter activity by aromatic amino acids, Journal of Bacteriology, **190** (1), 122-134

Scribner J.D., Koponen G., Fisk S.R. and Woodworth B., (1980). Binding of the dye intermediates michler's ketone and methane base to rat liver nucleic acids and lack of mutagenicity in *Salmonella Typhimurium*, Cancer Letters, **9**, 117-121

Shao Z.Q. and Behki R., (1996). Characterization of the expression of the *thcB* gene, coding

for a pesticide-degrading cytochrome P-450 in *Rhodococcus* strains, Applied and Environmental Microbiology, **62** (2), 403-407

Shinjoh M., Tomiyama N., Asakura A. and Hoshino T., (1995). Cloning and nucleotide sequencing of the membrane-bound L-sorbosone dehydrogenase gene of *Acetobacter liquefaciens* IFO 12258 and its expression in *Gluconobacter oxydans*, Applied and Environmental Microbiology, **61** (2), 413-420

Staub M. and Denes G., (1969). Purification and properties of the 3-deoxy-D-arabino-heptulosonate -7-phosphate syntase (phenylalanine sensitive) of *Escherichia coli* K12, Biochimica et Biophysica Acta, **178**, 588-598

Stolz A., (2001). Basic and applied aspects in the microbial degradation of azo dyes, Applied Microbiology and Biotechnolgy, **56** (1-2), 69-80

Subramaniam P.S., Xie G., Xia T. and Jensen R.A., (1998). Substrate ambiguity of 3- Deoxy-D-manno-Octulosonate 8-Phosphate synthase from *Neisseria gonorrhoeae* in the context of its membership in a protein family containing a subset of 3-Deoxy-D- arabino-Heptulosonate 7-Phosphate synthases, Journal of Bacteriology, **180** (1), 119-
127

Sugiura W., Yoda T., Matsuba T., Tanaka Y. and Suzuki Y., (2006). Expression and characterization of the genes encoding azoreductases from *Bacillus subtilis* and *Geobacillus stearothermophilus*, BioScience, Biochemistry and Biotechnology, 70 (7), 1655-1665

Suizhou R., Guo J., Zeng G. and Sun G., (2006). Decolorization of triphenylmethane, azo and anthraquinone dyes by a newly isolated *Aeromonas hydrophila* strain, Applied Microbiology and Biotechnology, **72** (6), 1316-1321

Suzuki Y., Yoda T., Ruhul A. and Sugiura W., (2001). Molecular cloning and characterization of the gene coding for azoreductase from *Bacillus* sp. OY1-2 isolated from soil, The Journal of Biological Chemistry, **276** (12), 9059-9065

Svobodova K., Erbanova P., Sklenar J. and Novotny C., (2006). The role of Mn-dependent peroxidase in dye decolorization by static and agitated cultures of *Irpex lacteus*, Folia Microbiologica, **51** (6), 573-578

Swamy J. and Ramsay J.A., (1999). The evaluation of white rot fungi in the decoloration of textile dyes, Enzyme and Microbial Technology, **24**, 130-137

Tan G.Y.A., Ward A.C. and Goodfellow M., (2006). Exploration of *Amycolatopsis* diversity in soil using genus-specific primers and novel selective media, Systematic and Applied Microbiology, **29**, 557-569

Tavcar M., Svbodova K., Kuplenk J., Novotny C. and Pavko A., (2006). Biodegradation of azo dye R016 in different reactors by immobilized *Irpex lacteus*, Acta Chimica Slovenica, **53**, 338-343

Telke A.A., Kalyani D.C., Dawker V.V. and Govindwar P., (2009). Influence of organic and inorganic compounds on oxidoreductive decolorization of sulfonated azo dye C.I. reactive orange 16, Journal of Hazourdous Materials, **172** (1), 298-309

Tyagi O.D and Yadav M., (2001). A textbook of synthetic dyes, Anmol Publications PVT Ltd., 1-304

Uddin M.S., Zhou J., Qu Y., Guo J., Wang P. and Zhao L-h., (2007). Biodecolorization of azo dye acid red B under high salinity condition, Bulletin of Environmental Contamination and Toxicology, **79** (94), 440-444

Vijaykumar M.H., Vaishampayan P.A., Shouche Y.S. and Karegouda T.B., (2007). Decolourization of naphthalene-containing sulfonated azo dyes by *Kerstersia* sp. strain VKY1, Enzyme and Microbial Technology, **40** (2), 204-211

Vasdev K., Kuhad R.C. and Saxena R.K., (1995). Decolorization of triphenylmethane dyes by the bird's nest fungus *Cyathus bulleri*, Current Microbiology, **30** (5), 269-272

Wang Y-K., Zhao G-Y., Li Y., Chen X-L., Xie B-B., Su H-N., Lv Y-H., He H-L., Liu H., Hu J., Zhou B-C. and Zhang Y-Z., (2010). Mechanistic insight into the function of the c-terminal PKD domain of the collagenolytic serine protease deseasin MCP-01 from deep sea *Pseudoalteromonas* sp. SM9913, The Journal of Biological Chemistry, **285** (19), 14285-14291

Yatome C., Yamada S., Ogawa T. and Matsui M., (1993). Degradation of crystal violet by *Nocardia corallina*, Applied Microbiology and Biotechnology, **38**, 565-569

Zhang W., Yang L., Jiang W., Zhao G., Yang Y. and Chiao J., (1999). Molecular analysis and heterologous expression of the gene encoding methylmalonyl-coenzyme A mutase from rifamycin SV-producing strain *Amycolatopsis mediterranei*, Applied Biochemistry and Biotechnology, **82**, 209-225